DESIGN OF DYNAMIC NONLINEAR CONTROL TECHNIQUES FOR FLEXIBLE-LINK MANIPULATORS

Victor Gavriloiu

A Thesis

in

The Department

of

Electrical and Computer Engineering

Presented in Partial Fulfillment of the Requirements

for the Degree of Master of Applied Science at

Concordia University

Montreal, Quebec, Canada

April 2005

Your file Votre référence
ISBN: 0-494-04370-9
Our file Notre référence
ISBN: 0-494-04370-9

ABSTRACT

Design of Dynamic Nonlinear Control Techniques for Flexible-Link Manipulators

Victor Gavriloiu

In the past several years, considerable research interest has been made in the literature to the problems of modelling and control of flexible-link manipulators. These manipulators have a number of potential advantages such as increased payload-to-arm mass ratio, faster motion capabilities, lower energy consumption, and smaller actuators. However, design of controllers for flexible manipulators is a challenging and a complicated task due to the highly nonlinear and coupled dynamics of the system. In addition, the non-minimum phase characteristic of a flexible manipulator makes the design of stable controllers that ensure stringent tracking requirements a highly nontrivial and challenging problem.

In this thesis, we develop robust dynamical controllers for addressing the problems of tracking and regulation of both rigid-link and flexible-link manipulators. The design of the dynamical controller is based on construction of a two-time scale dynamical motion of the closed-loop system. Furthermore, other conventional control methods such as the PD control, computed torque, and localization methods are investigated for comparison purposes. The main control objective is to achieve stability of the closed-loop system

while ensuring boundedness of all the control signals as well as sufficiently small tip-position tracking requirement. In order to achieve a minimum phase behaviour for utilizing output feedback control strategy, a new redefined output is proposed. Instead of using the joint angles as outputs in the rigid-link case, a new output is chosen for the flexible-link case which will provide and guarantee stability of the closed-loop flexible system. Simulations results are provided for both the rigid-link and flexible-link manipulators using the proposed control strategies. A comparative analysis is also included to demonstrate and illustrate the advantages and disadvantages of the considered control methodologies.

To my parents

and

to my wife

who have always supported me

ACKNOLEDGEMENTS

I wish to express my sincere gratitude and appreciation to my supervisors Dr. K. Khorasani and Dr. V.Yurkevich for their great insights, perspectives, and guidance. Their comments and suggestions on the theoretical developments proved to be most valuable towards the completion of this research.

I would like to thank to my wife for her support and understanding during my studies.

TABLE OF CONTENTS

TABLE OF FIGURES

LIST OF TABLES

Chapter 1 **Introduction**

"A reprogrammable, multifunctional manipulator designed to move material, parts, tools, or specialized devices through various programmed motions for the performance of a variety of tasks". This is the definition given in 1979 by the "Robot Institute of America". Even though the definition dates 26 years ago, it reflects the current status of robotics technologies [1]. Because of its programmability, an industrial robot is a part of an automated system. In the last decades, automation has been increased in industry, and one important link in this chain is represented by manipulators. The manipulator consists of a sequence of rigid or flexible links interconnected by means of joints. Another part could be the end-effector at the end of the last link. The motion of the links is provided by the actuators, and the status of the manipulator is given by measurements using sensors. The desired motion of the manipulator is achieved by using a control system which provides commands to the joint actuators depending on the implemented control methodology.

Conventional rigid-link manipulators have been widely used in industry. Their load-carrying capacity is only five to ten percent of their own weight. This restriction is due to the requirement of the rigidity. Other disadvantages are represented by the power consumption which is very high for these large-weight manipulators, and the speed of operation which is generally low. All of these problems could be avoided by using a lightweight flexible manipulator. At the same time, the number of applications of the manipulators has been increasing in the last decades. For example, space operations require the same lightweight manipulator which is characterized by flexibility of the links. Below are some benefits of using flexible manipulators:

- increased load-carrying capacity – the ratio of acceptable ratio payload weight to robot weight is increased
- energy consumption – the lightweight manipulators require smaller actuators, which means less energy consumptions
- cost – flexible robots require fewer materials and smaller actuators
- movement – flexible links can handle higher accelerations
- safer operations - the low inertia of the flexible manipulator reduces the possible damages resulting from physical interaction between the manipulator and the working environment.

However, there are some disadvantages using the flexible manipulators. There are stronger nonlinear effects due to the joint friction, backslash in the control system, nonlinear interaction and couplings. These along with the known flexibility of the link could decrease the performance of the manipulator in terms of accuracy, vibrations, and/or interaction with the working environment.

In order to minimize the effects of flexibility of the link, and to exploit maximum advantages provided by the flexible manipulators, it is required to have realistic, accurate and complete dynamic models to use for control. A suitable model is very useful in the development of control methodologies for the manipulator as well as for simulations purposes.

1.1 Literature review

The rigid and, especially, the flexible multi-body structures have been extensively analysed in the recent years [2], [3], [4]. One reason is the increasing demand coming from the industry regarding the use of manipulators. Research has been conducted in the literature both on modelling and controlling the manipulators. This chapter presents a literature review of the research in the area of modelling and controlling of flexible manipulators.

1.1.1 Modelling the flexible-link manipulators

Flexible manipulators are continuous systems characterized by infinite number of degrees of freedom, and are governed by nonlinear partial differential equations. The dynamic equations of motion of a manipulator can be derived using different methods such as Newton-Euler equations, Lagrangian equations, Hamilton's canonical equations etc. Within these methods, the Lagrangian method is the most applied because of its scalar nature even though the Newton-Euler method is more efficient in terms of computation factors.

As a first step in modelling the flexible manipulators, one could consider a one-flexible link manipulator. Wang and Vidyasagar [5] investigate the transfer function between the torque input and the net tip deflection. It is shown that by increasing the number of modes, the relative degree of the system becomes ill-defined. An alternate solution is provided by using an output defined as the rigid body deformation minus the elastic deformation. In this case, the resulting transfer matrix has a well-defined relative degree

even though the number of modes approaches infinity. Using three or four modes makes the task of control of a flexible link manipulator easier.

Hasting and Book [6] provide a linear state-space model for a flexible link manipulator arm. This method uses a separable formulation of assumed modes to represent the transverse displacements due to bending. The kinetic and potential energies for the system are obtained using the Lagrangian formulation. Subsequently, the dynamic equations are organized into a state-space model which can be investigated using linear control system design procedures. It was shown that the proposed model agrees with the experimental measurements using only two assumed flexible modes.

Canon and Schmitz [7] provide a detailed dynamic analysis of a single flexible-link. The dynamic analysis was done using Euler-Bernoulli beam theory, Hamilton principle and Lagrangian approach. The assumption of small deflection was used. The results are in form of infinite ordinary equations in decoupled form, but only a finite number was applied.

Extensive research was conducted in the literature for modelling one flexible-link manipulators [8], [9], [10]. The results are very important in order to better understand the nonlinear interactions between the rigid and flexible components of arm dynamics. Furthermore, various methods have been proposed for dynamic modelling of multilink manipulators [11] [12].

Book [13] uses a four by four transformation matrix to represent the joint and deflection motion. The link deflection is assumed small so that the link transformation is represented in terms of summation of modal shapes. The equations are free from assumptions of a nominal motion and do not ignore the interaction of angular rates and

deflections. It was shown that the computational complexity and time is reduced by using proper choice of mode shapes. This method uses recursive formulation for calculation of different coefficients and transformation matrices.

A dynamic model for multilink manipulators is described in [2] by Alessandro de Luca and Bruno Siciliano. The kinematic model describes both rigid rotation and flexible displacement under small deflection assumption. The dynamic model of the manipulator is derived using the Lagrangian approach. The links are modeled as Euler-Bernoulli beams with clamped-mass boundary conditions. In order to obtain a finite-dimensional model, the assumed modes method is used. The equations of motion are detailed for a two-link manipulator assuming two modes of vibration for each link.

Another class of multilink manipulators is represented by the manipulators having only the last link flexible. Wang and Vidyasagar [3] provide a modelling for an entire class of multilink manipulators with the last link flexible such as: the five bar linkage manipulator, the elbow manipulator, the cylindrical manipulator, or the spherical manipulator. The studied manipulator is the five-bar-linkage manipulator with the last link flexible while the others are assumed rigid. In order to obtain a simplified model some assumptions are considered: the dimensions of the last link are assumed to have a cross-section where the height is greater than the width so that the link will flex horizontally but not vertically. In addition, it is assumed that there is no payload or a small payload. This method neglects the small elements of the inertia matrix to simplify the dynamic equations. If this manipulator is used for "pick-and-place" operations, a rigid controller can be used for "pick" and "place" operations while for "move" any other controller designed for flexible link could be employed.

1.1.2 Control of flexible-link manipulators

In the past several years a considerable interest has been focused on the modelling and control of flexible-link manipulators. This was necessary due to the increased demand of energy efficient lightweight robot manipulators in industry. These manipulators have a lot of potential advantages such as: an increased payload-to-arm mass ratio, faster motions, lower energy consumption, and small actuators. Along with these advantages, some disadvantages arise due to flexibility of the links. Designing controllers for flexible manipulators becomes a complicated task because of the highly nonlinear, coupled dynamics of the system. The flexible motion is approximated by using finite dimensional system, and a large number of flexible modes is required to accurately model the dynamics. The rigid body dynamics and the flexible dynamics results in large system dimensions which can cause computational problems in the controller design. Another problem is represented by the non-minimum phase characteristic of the flexible manipulators.

In the last decades, a variety of methods have been investigated including linear control, adaptive control, frequency domain techniques, singular perturbation, and neural networks based approach. Initial experimentation on flexible robots began with single-link manipulators. One of the first complete work in this area was reported by Cannon and Schmitz [7]. They applied a linear quadratic Gaussian (LQC) control by designing an optimal controller that assumes the availability of all of the states of the system. Due to the unavailability of the states, they should be reconstructed from the available input, which is the applied torque at the hub and from the output, namely the hub velocity and the tip position. An optimal estimator was used to reconstruct the states by assuming that

the measurement errors and disturbances have Gaussian probability density functions. In [14] Sakawa et al. used a linear quadratic control (LQ) to dampen the flexible modes while tracking the hub reference trajectory by assuming that all of the states are available for measurement.

Luca and Siciliano [15] proposed a simple controller for the regulation problem of flexible manipulators under gravity with or without internal damping of link vibrations. The control law does not require any feedback from the deflection variables, and it consists of a linear term plus a nominal feedforward term. This is a joint PD feedback plus a constant feedforward term. The link stiffness K and the gravity term should be known for defining the steady-state deformation. Global asymptotic stability of the reference equilibrium state is provided. Asymptotic stability of joint PD controller for planar manipulator without gravity has been shown in [16], and for the case without internal damping has been considered in [17]. Full state asymptotic stabilization of flexible manipulators using strain measurements was described in [18].

In [19] Arteaga and Siciliano presents a controller for solving the tracking problem of flexible robot arms. In order to achieve this goal, the desired trajectory for the link (flexible) coordinates is computed from the dynamic model of the robot arm and is guaranteed to be bounded, and the desired trajectory for the joint (rigid) coordinates can be assigned arbitrarily. The case of no internal damping is also considered, and a robust control technique is used to enhance the damping of the system.

A widely used control method is the inverse dynamics control [20]. This approach consists of transforming the nonlinear system dynamics of the flexible manipulator into a linear one, where then linear control techniques could be employed. Because of the non-

minimum phase characteristic of the flexible manipulators, one could use a re-defined output instead of the direct tip position.

Wang and Vidyasagar [21] have shown that the nonlinear flexible-link manipulator is not in general input-state linearizable, but it is locally input-output linearizable. If the tip position is considered the output of the system, for the associated zero-dynamics are unstable. The output redefinition approach was used to overcome the non-minimum characteristic of the system. The same authors have proposed in [5] the redefined output as the reflected-tip position in order to achieve stable zero dynamics. De Luca and Lanari [22] have studied the regions of sensor and actuator locations for achieving the minimum phase property.

Kwon and Book [4] decomposed the inverse dynamics of the flexible link manipulator into a causal system, which was integrated forward in time, and an anti-causal system which was integrated backward in time by using coordinate transformations. Bayo [23] has proposed a non-causal controller by integrating the end-point acceleration profile that acts before the tip starts to move and after the tip stops to move. Both of these two approaches require substantial amount of computation, and are under assumptions of linear approximation model of flexible-link manipulator.

An inverse dynamics control strategy for tip position tracking of flexible multilink manipulators is presented in [24]. The control objective is to achieve small tracking errors for a class of multilink manipulators. The redefined output is used, and the control inputs are augmented by terms which ensure stable operation of the closed-loop system under specific conditions. This approach requires measurements of rates of change of flexible modes with time which is difficult to measure. This problem is solved by using an

observer-based inverse dynamics control strategy [25]. In [26] the authors present an inverse dynamics sliding control of flexible link manipulators. To achieve minimum phase characteristic the redefined output and inversion techniques are employed. The robustness of the system is given by two main factors: the resulting input-output linearization scheme tends to approximately decouple the dynamics, and the sliding control component forces the off-manifold trajectories to be attracted to the surface.

Command shaping methods have also been applied to the control of flexible multi-link robots. Hillsley and Yurkovich [27] use input shaping for gross slewing motion based on the natural frequency for an intermediate configuration. A feedback controller with link acceleration feedback is used to damp out the unavoidable residual vibrations caused by the nonlinearities. Later, Tzes and Yurkovich [28] developed an adaptive approach combining a frequency domain identification and a scheme for adjusting the necessary control impulses.

The transmission zero assignment for linear system was presented by Patel and Misra [29]. Based on this approach, Geniele et al. [30] applied this method to a single-link flexible manipulator to achieve tip position tracking control. The model was linearized about an operating point. The control strategy consists of an inner control loop that incorporates a feedthrough term to assign the system's transmission zeros at desired locations in the complex plane, and a feedback term to move the system's poles to appropriate positions in the left-half plane. In addition, a feedback servo loop is used to allow tracking of the desired trajectory.

The singular perturbation theory has been addressed by many researchers. This method is feasible due to the two-time-scale nature of the system dynamics. Khorasani and Spong

[31] has provided a singular perturbation model for the case of flexible-joint manipulators. The control strategy was based on stabilizing the fast dynamics and tracking the joint trajectories. Siciliano and Book [32] proposed a similar approach in terms of modelling for the case of multilink manipulators. The same approach was used in [33], [34], [35]. Aoustin et al.[36], experimentally has provided a comparison between some of these methods. In general, the joint position has been taken as output to avoid the non-minimum phase problem. The drawback could be large tip position, especially when the singular perturbation parameter is not small enough. To overcome this limitation, several researchers have used the integral manifold approach provided in [37, 38] to control flexible link manipulators [39] [40, 41].

Apart from the conventional control techniques, recently, intelligent-based control techniques have been investigated. Fuzzy logic and neural networks based approaches have been proposed. Khorasani [42] presents an intelligent-based control methodology for tip position tracking control of a single-link flexible manipulator. Based on the inverse dynamics method, two neural networks are proposed to learn the nonlinearities of the flexible arm associated with the inverse dynamics controller. In order to achieve the minimum phase property the redefined output approach is used. No *a priori* knowledge about the nonlinearities of the system is needed and the payload mass is also assumed to be unknown. It has been shown that by utilizing a neural network having the structure of a typical inverse dynamics controller, the limitations of the inverse dynamics scheme may be relaxed significantly.

Kubica and Wang [43] have proposed a fuzzy control strategy to control the rigid body and the first flexural mode of vibration in a single link robotic arm. They have shown by

simulation and experimentally that the rigid and flexible modes can be adequately controlled with the proposed technique.

1.2 Outline of the Thesis

Because of the large use and future potentials of the manipulators, researchers are trying to improve the control methodologies for such systems. One direction is the control of rigid link manipulators which have been widely used in industry. Because of the new demands from the industry, the lightweight manipulators are used in a number of applications. This is the reason that researchers have been trying to develop and improve new control methodologies.

The thesis outline is presented below:

Chapter 2 is devoted to the modeling of the rigid and flexible manipulators. In the first part of the chapter the rigid manipulators are presented. Kinematics is considered in terms of direct kinematics, inverse kinematics, and velocity kinematics. Using the Lagrange formulation the equations of motion of a manipulator in the joint space are derived. In the second part of the chapter, the flexible manipulators are presented. The assumed modes approach and the Euler-Bernoulli beam theory are used to derive the dynamic model for a flexible link manipulator. Using the recursive Lagrange approach, the dynamic equations for multi-link flexible manipulator are derived.

In Chapter 3, we present different control methods for comparative purposes for rigid link manipulators. Simulations are performed using different scenarios (different sets of initial conditions, different sets of gains, and in the presence or absence of a disturbance).

Chapter 4 is devoted to the control of flexible-link manipulators. First, some concepts such as output redefinition, input-output linearization, and zero-dynamics are presented.

Afterwards, the computed torque and the dynamic control methods are used for controlling a flexible link manipulator and a two-link manipulator for which the first link is rigid and the second link is flexible. Finally, a comparison between the rigid and flexible link manipulators is presented.

Chapter 5 presents the conclusions and suggestions for future work.

Chapter 2 **Mathematical Models for Rigid and Flexible Manipulators**

2.1 Modelling of rigid-link manipulators

A robotic manipulator can be modeled as a chain of rigid bodies called links. The links are interconnected to one another by means of joints. One end of the chain of links is fixed while the other end is free to move. In general, the mobile end of the manipulator has a tool or end-effector attached to it.

The objective is to control the position of the end-effector in the two-dimensional space. In order to control the end-effector, we have to formulate the relationships between the joint variables and the position of the tool through kinematics. Differential kinematics or velocity kinematics describes the analytical relationships between the joint motion and the end-effector motion in terms of velocities.

In order to analyse the structure of the manipulator and to design the control algorithms we need the dynamical model of the manipulator. There are two methods for derivation of the equations of motion of a rigid manipulator: the first method is based on Lagrange formulation and the second method is based on the Newton-Euler formulation.

2.1.1 **Kinematics of rigid link manipulators**

Direct kinematics

Let consider a two-link rigid manipulator as shown in figure 2.1. The manipulator consists of two rigid links of weight m_1 and m_2 and length l_1 and l_2, respectively. The joint angles are denoted by q_1 and q_2.

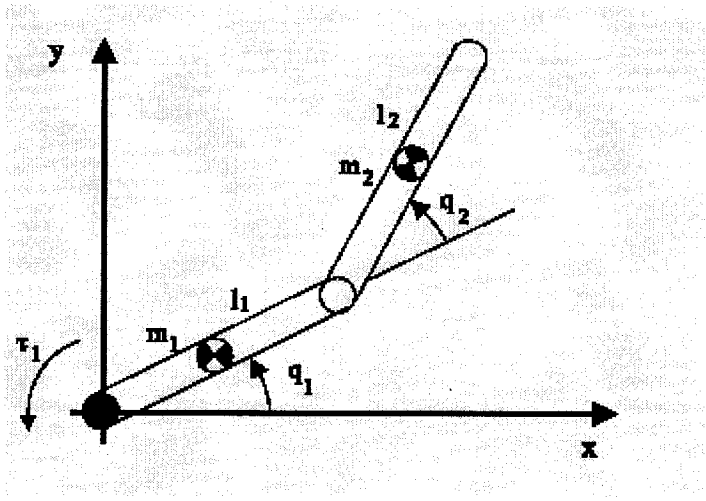

Figure 2-1 Two-link rigid manipulator

Direct kinematics problem may be stated as follows: given the joint angles q_1, q_2, determine the end-effector's position (coordinates) and orientation with respect to a coordinate frame attached to the robot base. Using this method we can express the position of the tip in terms of the joints angles as follows:

$$\begin{cases} x = l_1 \cos q_1 + l_2 \cos(q_1 + q_2) \\ y = l_1 \sin q_1 + l_2 \sin(q_1 + q_2) \end{cases} \tag{2.1}$$

where the orientation of the tool frame is given by:

$$\begin{cases} i_2 i_0 = \cos(q_1 + q_2) \\ j_2 i_0 = \sin(q_1 + q_2) \end{cases}$$

$$\begin{cases} i_2 j_0 = -\sin(q_1 + q_2) \\ j_2 j_0 = \cos(q_1 + q_2) \end{cases} \tag{2.2}$$

$$\begin{bmatrix} i_2 i_0 & j_2 i_0 \\ i_2 j_0 & j_2 j_0 \end{bmatrix} = \begin{bmatrix} \cos(q_1 + q_2) & -\sin(q_1 + q_2) \\ \sin(q_1 + q_2) & \cos(q_1 + q_2) \end{bmatrix}$$

Inverse kinematics

The inverse kinematics problem may be stated as follows: given a desired position and orientation for the end-effector of the manipulator, determine a set of joint angles that achieve desired position and orientation. The solution to the inverse kinematics problem is very important in order to transform the motion specifications of the end effector which are given in the operational space into the corresponding joint space motion.

Due to the structure of the equations the solution may not be unique. If we have a given (x, y), we can find two different solutions, named elbow-up and elbow-down.

That is we can write:

$$\cos q_2 = \frac{x^2 + y^2 - l_1^2 - l_2^2}{2 l_1 l_2} := D \tag{2.3}$$

This implies:

$$q_2 = \cos^{-1}(D)$$

We will find the solution $q_2 = \tan^{-1}(\pm \frac{\sqrt{1 - D^2}}{D})$. The sign $\pm$ implies that we have two different solutions.

Now, we can calculate:

$$q_1 = \tan^{-1}(\frac{y}{x}) - \tan^{-1}(\frac{l_2 \sin q_2}{l_1 + l_2 \cos q_2})$$

The two solutions of the inverse dynamics are given by:

$$\begin{cases} q_1 = \tan^{-1}(\frac{y}{x}) - \tan^{-1}(\frac{l_2 \sin q_2}{l_1 + l_2 \cos q_2}) \\ q_2 = \tan^{-1}(\pm\frac{\sqrt{1-D^2}}{D}) \end{cases} \tag{2.4}$$

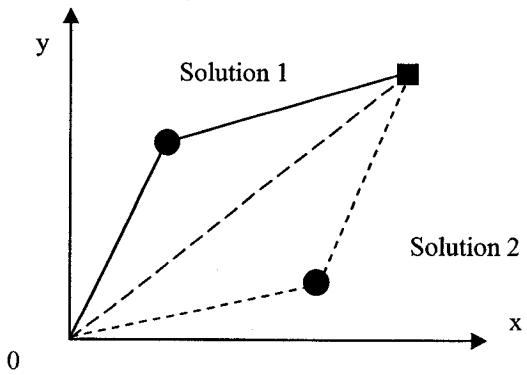

Figure 2-2 Multiple manipulator solutions for the inverse kinematics problem

Referring to figure 2.2 we can distinguish the two different solutions namely solution 1 which is named elbow-up, and solution 2 which is named elbow-up.

Velocity kinematics

The velocity kinematics problem determines the relationships between the joint velocities and the end-effector linear or angular velocity. The direct kinematics equations define a function between the space of Cartesian positions and orientations and the space of joint positions. The velocity kinematics uses the Jacobian of this function, namely:

$$\begin{cases} \dot{x} = -l_1 \sin q_1 \dot{q}_1 - l_2 \sin(q_1 + q_2)(\dot{q}_1 + \dot{q}_2) \\ \dot{y} = -l_1 \cos q_1 \cos \dot{q}_1 + l_2 \cos(q_1 + q_2)(\dot{q}_1 + \dot{q}_2) \end{cases} \tag{2.5}$$

Let us denote:

$$X = \begin{bmatrix} x \\ y \end{bmatrix} \text{ and } q = \begin{bmatrix} q_1 \\ q_2 \end{bmatrix}$$

Now, we can rewrite the equation (2.5) in the following form:

$$\dot{X} = \begin{bmatrix} -l_1 \sin q_1 - l_2 \sin(q_1 + q_2) & -l_2 \sin(q_1 + q_2) \\ l_1 \cos q_1 + l_2 \cos(q_1 + q_2) & l_2 \cos(q_1 + q_2) \end{bmatrix} \dot{q} \tag{2.6}$$

or:

$$\dot{X} = J\dot{q} \tag{2.7}$$

The matrix J is called the Jacobian of the manipulator and it represents the contributions of each joint velocity to the linear and angular end-effector velocities. The Jacobian matrix is a function of the manipulator configuration. The cases when the Jacobian matrix is singular are named kinematics singularities, and the manipulator is said to be in a singular configuration.

Another form of the equation (2.6) is given below:

$$\begin{bmatrix} \dot{q}_1 \\ \dot{q}_2 \end{bmatrix} = \frac{1}{l_1 l_2} \sin q_2 \begin{bmatrix} l_2 \cos(q_1 + q_2) & l_2 \sin(q_1 + q_2) \\ -l_1 \cos q_1 - l_2 \cos(q_1 + q_2) & -l_1 \sin q_1 - l_2 \sin(q_1 + q_2) \end{bmatrix} \begin{bmatrix} \dot{x} \\ \dot{y} \end{bmatrix} \tag{2.8}$$

or

$\dot{q} = J^{-1}\dot{X}$, where J^{-1} is the inverse of the Jacobian matrix assuming that it is well-defined.

2.1.2 **Dynamic modelling of rigid link manipulators**

The dynamic model of the manipulator has a very important role for analysing the manipulator's behaviour, for designing control methodologies, and for simulation of motion. Simulation of robot motions could help one in developing improvements to the

control strategies without having an experimental manipulator. The control of the manipulator is improved if complex control strategies are used. In order to develop them, we need very precise dynamical models.

The dynamic behaviour of a manipulator is described in terms of the time rate of change of the arm configuration in relation to the joint torques. This relationship can be expressed by a set of differential equations, called equations of motion that govern the dynamic response of the manipulator to input torques. There are two methods for derivation of the equations of motion of a manipulator in the joint space: the Newton-Euler formulation and the Lagrange formulation. The following section presents only the Lagrange formulation. The details for Newton-Euler formulation are omitted for brevity.

2.1.1.1 Analytical model - Lagrange formulation

In this method, the system's behaviour is described in terms of work and energy using generalized coordinates. The resulting equations are generally compact and provide a closed-form expression in terms of joint torques and joint displacements.

Let consider the manipulator shown in figure 2.1 with the vector of generalized coordinates $q = [q_1 \quad q_2]^T$. Let l_{c1} and l_{c2} be the distances of the centers of mass of the two links from the respective joint axes. Let m_1 and m_2 be the masses of the two links. Let I_1 and I_2 be the moments of inertia relative to the centers of mass of the two links.

Using the inverse kinematics we can write:

$$\begin{cases} v_{c1} = J_{v_{c1}} \dot{q} \\ v_{c2} = J_{v_{c2}} \dot{q} \end{cases} \tag{2.9}$$

where:

$$J_{v_{c1}} = \begin{bmatrix} -l_{c1}\sin q_1 & 0 \\ l_{c1}\cos q_1 & 0 \\ 0 & 0 \end{bmatrix}$$

$$J_{v_{c2}} = \begin{bmatrix} -l_1\sin q_1 - l_{c2}\sin(q_1+q_2) & -l_{c2}\sin(q_1+q_2) \\ -l_1\cos q_1 - l_{c2}\cos(q_1+q_2) & l_{c2}\cos(q_1+q_2) \\ 0 & 0 \end{bmatrix}$$

Let us assume that the following conditions are provided: kinetic energy is a quadratic function of $\dot{q}$ and the potential energy is function of q, that is kinetic energy is given by:

$$K = \frac{1}{2}\sum_{i,j}^{2} d_{ij}(q)\dot{q}_i\dot{q}_j = \frac{1}{2}\dot{q}^T D(q)\dot{q} \tag{2.10}$$

where D is a symmetric and positive matrix for each $q \in R^2$.

We can derive the Euler-Lagrange equations by defining the Lagrangian as

$$L = K - V = \frac{1}{2}\sum_{i,j}^{2} d_{ij}(q)\dot{q}_i\dot{q}_j - V(q) \tag{2.11}$$

where $V(q)$ is the potential energy.

We have:

$$\frac{\partial L}{\partial \dot{q}_k} = \sum_j d_{kj}(q)\dot{q}_j \tag{2.12}$$

and

$$\frac{d}{dt}\frac{\partial L}{\partial \dot{q}_k} = \sum_j d_{kj}(q)\ddot{q}_j + \sum_j \frac{d}{dt}d_{kj}(q)\dot{q}_j = \sum_j d_{kj}(q)\ddot{q}_j + \sum_{i,j}\frac{\partial d_{kj}}{dq_i}\dot{q}_i\dot{q}_j \tag{2.13}$$

Also,

$$\frac{\partial L}{\partial q_k} = \frac{1}{2}\sum\frac{\partial d_{ij}}{dq_k}\dot{q}_i\dot{q}_j - \frac{\partial V}{\partial q_k} \tag{2.14}$$

Thus, we can write:

$$\sum_j d_{kj}(q)\ddot{q} + \sum \{\frac{\partial d_{kj}}{dq_i} - \frac{1}{2}\frac{\partial d_{ij}}{\partial q_k}\}\dot{q}_i\dot{q}_j - \frac{\partial V}{\partial q_k} = \tau_k, \qquad k = 1,..,n \tag{2.15}$$

where τ_k, $k = 1,..,n$ is the torque input applied to each joint.

By interchanging the order of summation and taking into consideration the symmetry, we can show that:

$$\sum \{\frac{\partial d_{kj}}{dq_i}\} q_i q_j = \sum_{i,j} \{\frac{\partial d_{kj}}{dq_i} + \frac{\partial d_{ki}}{dq_i}\}\dot{q}_i\dot{q}_j \tag{2.16}$$

Hence,

$$\sum_{i,j} \{\frac{\partial d_{kj}}{dq_i} - \frac{1}{2}\frac{\partial d_{ij}}{\partial q_k}\}\dot{q}_i\dot{q}_j = \sum_{i,j} \frac{1}{2}\{\frac{\partial d_{kj}}{dq_i} + \frac{\partial d_{ki}}{\partial q_j} - \frac{\partial d_{ij}}{\partial q_k}\}\dot{q}_i\dot{q}_j \tag{2.17}$$

Let us denote $c_{ijk} = \frac{\partial d_{kj}}{dq_i} + \frac{\partial d_{ki}}{\partial q_j} - \frac{\partial d_{ij}}{\partial q_k}$ → Christoffel symbols. For a fixed k we have:

$c_{ijk} = c_{jik}$. Let us denote

$$g_k = \frac{\partial V}{\partial q_k} \tag{2.18}$$

We can rewrite:

$$\sum_j d_{kj}(q)\ddot{q}_j + \sum_{i,j} c_{ijk}(q)q_i q_j + g_k(q) = \tau_k \tag{2.19}$$

In the matrix form, we have:

$$D(q)\ddot{q} + C(q,\dot{q})\dot{q} + g(q) = \tau \tag{2.20}$$

Let us derive the mathematical model for the two rigid-link manipulator.

The translational part of the kinetic energy is:

$$\frac{1}{2}m_1 v_{c1}^T v_{c1} + \frac{1}{2}m_2 v_{c2}^T v_{c2} = \frac{1}{2}\dot{q}\{m_1 Jv_{c1}^T Jv_{c1} + m_2 Jv_{c2}^T Jv_{c2}\}\dot{q} \tag{2.21}$$

The rotational kinetic energy is:

$$\frac{1}{2}\dot{q}^T \{I_1\begin{bmatrix}1 & 0\\ 0 & 0\end{bmatrix} + I_2\begin{bmatrix}1 & 1\\ 1 & 1\end{bmatrix}\}\dot{q} \tag{2.22}$$

From (2.10), (2.21), and (2.22), the inertia matrix is given by:

$$D(q) = m_1 Jv_{c1}^T Jv_{c1} + m_2 Jv_{c2}^T Jv_{c2} + \begin{bmatrix}I_1 + I_2 & I_2\\ I_2 & I_2\end{bmatrix} \tag{2.23}$$

where:

$$d_{11} = m_1 l_{c1}^2 + m_2(l_1^2 + l_{c2}^2 + 2l_1 l_{c2}\cos(q_2)) + I_1 + I_2$$

$$d_{21} = d_{12} = m_2(l_{c2}^2 + l_1 l_{c2}\cos q_2) + I_2$$

$$d_{22} = m_2 l_{c2}^2 + I_2$$

The Christoffel symbols are now explicitly given as:

$$c_{111} = \frac{1}{2}\frac{\partial d_{11}}{\partial q_1} = 0$$

$$c_{121} = c_{211} = \frac{1}{2}\frac{\partial d_{11}}{\partial q_2} = -m_1 l_1 l_{c2}\sin q_2 := h \tag{2.24}$$

$$c_{221} = \frac{1}{2}\frac{\partial d_{12}}{\partial q_2} - \frac{1}{2}\frac{\partial d_{22}}{\partial q_1} = h$$

$$c_{112} = \frac{1}{2}\frac{\partial d_{21}}{\partial q_1} - \frac{1}{2}\frac{\partial d_{11}}{\partial q_2} = -h$$

$$c_{122} = c_{212} = \frac{1}{2}\frac{\partial d_{22}}{\partial q_1} = 0$$

$$c_{222} = \frac{1}{2}\frac{\partial d_{22}}{\partial q_2} = 0$$

The potential energy of the manipulator is simply the sum of those of the two links:

$$V_1 = m_1 G l_{c1} \sin q_1$$

$$V_2 = m_2 G(l_1 \sin q_1 + l_{c2} \sin(q_1 + q_2)) \tag{2.25}$$

That implies:

$$V = m_1 G l_{c1} \sin q_1 + m_2 G l_1 \sin q_1 + m_2 G l_{c2} \sin(q_1 + q_2)$$

$$g_1 = \frac{\partial V}{\partial q_1} = (m_1 l_{c1} + m_2 l_1) G \cos q_1 + m_2 l_{c2} G \cos(q_1 + q_2) \tag{2.26}$$

$$g_2 = \frac{\partial V}{\partial q_2} = m_2 l_{c2} G \cos(q_1 + q_2)$$

Explicitly, the mathematical governing equation can be written as:

$$\begin{bmatrix} d_{11} & d_{12} \\ d_{21} & d_{22} \end{bmatrix} \begin{bmatrix} \ddot{q}_1 \\ \ddot{q}_2 \end{bmatrix} + \begin{bmatrix} h\dot{q}_2 & h(\dot{q}_1 + \dot{q}_2) \\ -h\dot{q}_1 & 0 \end{bmatrix} \begin{bmatrix} \dot{q}_1 \\ \dot{q}_2 \end{bmatrix} + \begin{bmatrix} g_1 \\ g_2 \end{bmatrix} = \begin{bmatrix} \tau_1 \\ \tau_2 \end{bmatrix} \tag{2.27}$$

We can rewrite equation (2.27) as follows:

$$D(q)\ddot{q} + C(q,\dot{q})\dot{q} + g(q) = \tau \tag{2.28}$$

where:

$D(q)$ is the inertia matrix (2x2 symmetric positive definite matrix), $C(q,\dot{q})$ is the term due to Coriolis, and centrifugal forces, q is the 2x1 vector of joint variables, $g(q)$ is the term due to gravity, τ is 2x1 vector of input torques.

As discussed previously for direct and inverse kinematics, for the behaviour of the system there are two dynamics problems: direct and inverse dynamics. The direct dynamics problem is concerned with computing the joint trajectory $q(t)$ given the applied torque $\tau(t)$, whereas the inverse dynamics problem computes the applied torque profile

$\tau(t)$ which corresponds to a given joint trajectory $q(t)$. The inverse dynamics is very useful in some control techniques based on the detailed model of the manipulator.

2.1.1.2 Properties of the dynamical model

Let us consider a planar, two-link, articulated manipulator. The dynamics of this two-rigid link manipulator can be written in the general form as

$$D(q)\ddot{q} + C(q,\dot{q})\dot{q} + g(q) = \tau \tag{2.29}$$

Properties of the inertia matrix

As discussed earlier the matrix D is symmetric and positive definite. Another important property of the inertia matrix is that is it is bounded above and below [44]. The inertia matrix is only function of q through sin and cos functions which are bounded by [-1 1], so that we can write:

$$\mu_1 I \le D(q) \le \mu_2 I, \tag{2.30}$$

with μ_1, μ_2 computable scalars. Similarly, the inverse of the inertia matrix has the same property:

$$\frac{1}{\mu_2} I \le D^{-1}(q) \le \frac{1}{\mu_1} I \tag{2.31}$$

Properties of the Coriolis and centrifugal term [45]

Define the matrix $N(q,\dot{q}) = \dot{D}(q) - 2C(q,\dot{q})$. Then $N(q,\dot{q})$ is skew symmetric, that is, the components n_{jk} of N satisfy $n_{jk} = -n_{kj}$.

Properties of the gravitational term

As discussed above, the gravitational term is defined as:

$$g_1 = \frac{\partial V}{\partial q_1} = (m_1 l_{c1} + m_2 l_1) G \cos q_1 + m_2 l_{c2} G \cos(q_1 + q_2) \tag{2.32}$$

$$g_2 = \frac{\partial V}{\partial q_2} = m_2 l_{c2} G \cos(q_1 + q_2)$$

The gravitational term is function of q through sin and cos functions, therefore they are bounded [44], that is

$$\|G(q)\| \leq g_b \tag{2.33}$$

2.2 Modelling of flexible-link manipulators

This section is devoted to modelling of a flexible link manipulator. The manipulator considered consists of a flexible beam attached directly to a motor and is driven by a torque. One end of the beam is fixed (hub), while the other one is free (end-effector). The end effector could have a small mass attached as a payload. In order to design a better control method for this type of manipulators an accurate dynamical model should be used. The dynamical model is derived using the Euler-Bernoulli beam theory in order to obtain a partial differential equations with the corresponding appropriate boundary conditions. Furthermore, using the Lagrangian formulation approach and the assumed modes method we can obtain the state-space representation of the manipulator.

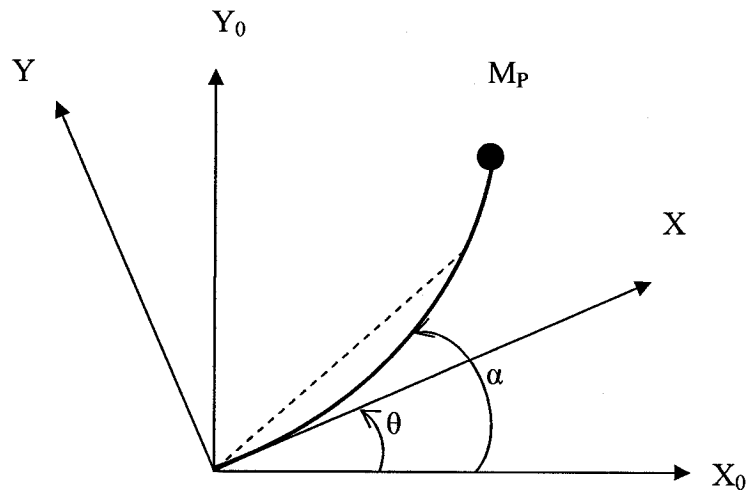

Figure 2-3 Schematic of a flexible link

2.2.1 Euler-Bernoulli beam equations

Consider a flexible link as shown in figure 2.3 moving in the planar field. The arm is clamped at the base and is driven by an actuator. The reference frame X0-Y0 is fixed, while the origin of the frame X-Y is attached to the actuator. In order to derive a mathematical model, we should take into consideration the following assumptions [46].

Assumption 2.1 The arm is a slender beam with uniform geometric characteristics and homogenous mass distribution.

Assumption 2.2 The arm is flexible in the lateral direction, being stiff with respect to axial forces, torsion, and bending forces due to gravity; furthermore, only elastic deformations are present.

Assumption 2.3 Nonlinear deformations as well as internal friction or other external disturbances are negligible.

The deflection of any point on the beam is given by the Euler-Bernoulli equation [47]:

$$EI\frac{\partial^4 w(\varepsilon,t)}{\partial \varepsilon^4} - \rho A_b L^4 \frac{\partial^2 w(\varepsilon,t)}{\partial t^2} = 0 \tag{3.34}$$

where $\varepsilon = x/L$ is the normalized position along the link of length L and area A_B, E is the Young's modulus of elasticity, I is the inertia of the cross-section of the beam, and ρ is its density.

Let us assume that the separability in time domain and space domain is satisfied:

$$w(x,t) = \sum \Phi_i(x)\Psi_i(t) \text{ for } i = 1,2...n \tag{3.35}$$

In this case, the flexible deflections are described by two functions, one function is a function of time while the second function is function of a spatial variable. This yields:

$$EI\frac{\partial^4 \Phi(\varepsilon)}{\partial \varepsilon^4}\Psi(t) - \rho A_b L^4 \Phi(\varepsilon)\frac{\partial^2 \Psi(t)}{\partial t^2} = 0 \tag{3.36}$$

Let us assume that $\Psi(t) = e^{j\omega t}$. This implies that

$$EI\left[\frac{d^4\Phi(\varepsilon)}{\partial \varepsilon^4} - \rho A_b L^4 \Phi(\varepsilon)\omega^2\right]\Psi(t) = 0 \tag{3.37}$$

This equation should be satisfied for each t which means that the term within the brackets should be equal to zero:

$$\frac{d^4\Phi(\varepsilon)}{\partial \varepsilon^4} - \beta^4 \Phi(\varepsilon) = 0$$

where $\beta = \frac{\rho A_b}{EI} L^4 \omega^2$

The solution to the above equation could be written as:

$$\Phi_i(\varepsilon) = A\sin(\beta\xi) + B\cos(\beta\xi) + C\sinh(\beta\xi) + D\cosh(\beta\xi) \tag{3.38}$$

Boundary conditions

In order to find the solution $\Phi_i(\varepsilon)$, we need four boundary conditions which are given by:

$$\Phi(\xi) = 0 \text{ for } \xi = 0$$

$$\frac{d\Phi(\xi)}{d\xi} = 0 \text{ for } \xi = 0$$

$$\frac{d^2\Phi(\xi)}{d\xi^2} = 0 \text{ for } \xi = 1 \tag{3.38}$$

$$\frac{d^3\Phi(\xi)}{d\xi^3} = -\frac{M_p\beta^4}{\rho A_0 L^3}\Phi(\xi) \text{ for } \xi = 1$$

The conditions at the joints yield:

$$B = -D \text{ and } A = -C$$

The third condition yields:

$$B = \frac{\sin\beta + \sinh\beta}{\cos\beta + \cosh\beta} A$$

The mass conditions at the end-point lead to $Q(\beta)\begin{bmatrix} A \\ B \end{bmatrix} = 0$.

By setting the determinant of matrix $Q(\beta)$ to zero, a frequency equation could be obtained as follows:

$$1 + \cosh(\beta)\cos(\beta) + \frac{M_p}{\rho A_0 L^3}\beta(\sinh(\beta)\cos(\beta) - \cosh(\beta)\sin(\beta)) = 0 \tag{3.39}$$

The natural frequencies of vibration are obtained from:

$$\omega_i = \beta^2\sqrt{\frac{EI}{\rho A_0 L^4}} \tag{3.40}$$

Substituting the boundary conditions in the form of the mode shapes, we can write:

$$\Phi_i(\varepsilon) = B_i(\sin(\beta_i\xi) - \sinh(\beta_i\xi) - \frac{\sin(\beta_i\xi) + \sinh(\beta_i\xi)}{\cos(\beta_i\xi) + \cosh(\beta_i\xi)}[\cos(\beta_i\xi) - \cosh(\beta_i\xi)]) \quad (3.41)$$

The coefficients B_i are chosen by normalizing the mode shape functions $\Phi_i(\xi)$:

$\int_0^1 \Phi_i^2(\xi)d\xi = 1$, $i = 1,...,m$.

Each natural frequency ω_i yields a specific mode shape function $\Phi_i(\xi)$ and specific amplitude $\Psi_i(t)$. A single solution to the deflection problem is now given by:

$$w_i(x,t) = \Phi_i(x)\Psi_i(t) \quad (3.42)$$

The single solution $w_i(x,t)$ will not usually satisfy the initial conditions for position and velocity. Since the equation (3.34) is linear and homogenous, the principle of superposition holds and the sum of the infinitely many solutions $w_i(x,t)$ is a solution of equation (3.34), that is

$$W(x,t) = \sum_{i=1}^{\infty} \Phi_i(x)\Psi_i(t) \quad (3.43)$$

2.2.2 **The assumed modes method**

The solution of equation (3.43) requires an infinite number of modes. Instead, an approximated solution could be used using only a finite number of modes, that is.

$$W(x,t) = \sum_{i=1}^{n} \varphi_i(x)\Psi_i(t) \quad (3.44)$$

where φ_i is any function satisfying the boundary conditions. If the functions φ_i are selected as polynomials in x, the resulting frequencies of vibration are approximations to the natural frequencies of the system. If the functions φ_i are selected as the

eigenfunctions $\Phi_i(x)$, the resulting frequencies of vibration equal the natural frequencies of the system.

In conclusion, the deflection of the cantilever beam can be approximated by:

$$W(x,t) = \sum_{i=1}^{n} \Phi_i(x)\Psi_i(t) \tag{3.45}$$

2.2.3 **Dynamical equations of a single flexible-link manipulator**

Taking into consideration a finite number of modes, the dynamic equations can be derived using the recursive Lagrange approach [13]. The dynamic equations for a planar single link manipulator are given by:

$$M\begin{bmatrix} \ddot{q} \\ \ddot{\delta} \end{bmatrix} + \begin{bmatrix} f_1(q,\dot{q}) + g_1(q,\dot{q},\delta,\dot{\delta}) + E_1\dot{q} \\ f_2(q,\dot{q}) + g_2(q,\dot{q},\delta,\dot{\delta}) + E_2\dot{\delta} + K\delta \end{bmatrix} = \begin{bmatrix} \tau \\ 0 \end{bmatrix} \tag{3.46}$$

The inertia matrix M is given by:

$$m_{11} = J_0 + J_L + M_L L_0^{\,2} + I_0 + M_L(\Phi_e^T\delta)^2$$

$$m_{1j} = M_L L_0 \Phi_{j-1,e} + J_L \Phi'_{j-1,e} + \sigma_{j-1} \qquad \text{for } j = 2,\ldots,m+1$$

$$m_{ii} = m_b + M_L \Phi^2{}_{i-1,e} + J_L \Phi'^2_{j-1,e} \qquad \text{for } i = 2,\ldots,m+1$$

$$m_{ij} = M_L \Phi_{i-1,e}\Phi_{j-1,e} + J_L \Phi'_{i-1,e}\Phi'_{j-1,e} \qquad \text{for } i = 2,\ldots,m+1 \text{ and } j \neq i$$

with:

$$\Phi_e^T = \Phi^T\big|_{\xi=1} = \left[\Phi_1 \quad \ldots \quad \Phi_m\right]_{\xi=1},\ \Phi_{ie} = \Phi_i(\xi)\big|_{\xi=1}$$

$$\Phi_e'^T = \left[\Phi'_{1e} \quad \ldots \quad \Phi'_{me}\right]_{\xi=1},\ \Phi'_{ie} = \frac{d\Phi_i(\xi)}{d\xi}\Big|_{\xi=1}$$

$$\sigma_i = \rho L_0^2 \int_0^1 \Phi_i(\xi)\xi d\xi \quad \text{for} \quad i = 2,...,m$$

The nonlinear terms f_1, f_2 representing the Coriolis and centrifugal forces are calculated by differentiation of the inertia matrix:

$$f_1 = 2M_L \dot{q}(\varphi_e{}^T \delta)(\varphi_e{}^T \dot{\delta})$$
$$f_2 = -M_L \dot{q}^2 (\varphi_e \varphi_e{}^T \delta)$$
- Coriolis and centrifugal forces

The matrices K, E_2 are given by:

$$K = diag\{k_1,...,k_m\} \qquad \text{where} \qquad k_i = \frac{EI}{L_0{}^3} \int_0^1 \left[\frac{d^2\Phi_i(\xi)}{d\xi^2}\right] d\xi$$

$$E_2 = diag\{f_{s1},...,f_{sm}\} \qquad \text{where} \qquad f_{si} = 0.2\sqrt{k_i}$$

2.2.4 **Dynamics of a multi-link flexible manipulator**

Using the same recursive Lagrangian approach, the dynamics for multi-link flexible manipulator can be derived as:

$$M\begin{bmatrix} \ddot{q} \\ \ddot{\delta} \end{bmatrix} + \begin{bmatrix} f_1(q,\dot{q}) + g_1(q,\dot{q},\delta,\dot{\delta}) + E_1\dot{q} \\ f_2(q,\dot{q}) + g_2(q,\dot{q},\delta,\dot{\delta}) + E_2\dot{\delta} + K\delta \end{bmatrix} = \begin{bmatrix} \tau \\ 0 \end{bmatrix} \tag{3.47}$$

where q is the $nx1$ vector of joint variables, δ is the $mx1$ vector of deflection variables, f_1, g_1, f_2, g_2 are the terms due to gravity, Coriolis, and centripetal forces, E_2 is the structural damping matrix, K is the stiffness matrix, E_1 is the hub damping, and τ is the vector of joint control torques.

If the number of flexible modes taken into consideration for each link is m_i, then

$\delta = [\delta_1 \quad ... \quad \delta_n]^T$ and $\delta_i = [\delta_{i1} \quad ... \quad \delta_{im_i}]^T$ for $i = 1,..,n$ and $m = \sum_{i=1}^{n} m_i$.

As it can be seen from the dynamical model of the flexible manipulator, the number of mechanical degrees of freedom is greater that the number of control inputs. That means that the flexible manipulator is an under-actuated system. This limitation makes the control of this type of manipulators more difficult than the ones designed for rigid manipulators where the number of degrees of freedom equal to the number of control inputs.

2.3 Conclusions

In this chapter the mathematical models for rigid and flexible-link manipulators are presented. The first part is devoted to rigid link manipulators. The kinematics and dynamics of this type of manipulators are discussed. Some important properties of the dynamic model are presented. In the second part of this chapter, the flexible link manipulators are considered. Basic assumptions for the validity of the model are stated [46], leading to the Euler-Bernoulli beam equations of motion. Furthermore, using the assumed modes method, the dynamical equations of a single flexible link manipulator are obtained. Taking into consideration a finite number of modes and using the recursive Lagrange approach, the dynamic equations for a multi-link flexible manipulator are derived.

Chapter 3 **Control of Rigid Manipulators**

The control problem for manipulators is to determine the joint inputs required to cause the end-effector execute a commanded motion [45]. The objective of the control can be divided into two different categories: regulation and tracking. Regulation problem or the point-to-point control is when the desired trajectory of the end-effector is chosen to be constant by specifying the final point. Tracking problem consists of following a time-varying joint reference trajectory. In this case, we have to take into consideration the manipulator's capacity in terms of maximum velocity and acceleration which should cover the corresponding values imposed by the desired trajectory. One could say that the regulation problem is a particular case of tracking problem where the desired velocity and desired acceleration are set to zero.

This chapter will presents four different control methods for rigid link manipulators, namely, PD control, computed torque, localisation, and dynamical control methods. For each method different scenarios are used with different sets of initial conditions and using different sets of control gains.

3.1 PD control method

We have shown in previous Chapter that the equations of motion of a rigid manipulator are described by:

$$D(q)\ddot{q}+C(q,\dot{q})\dot{q}+g(q)=\tau \tag{3.1}$$

The objective of the control is to determine the n components of the torques for the revolute joints that permit the end-effector move to a given final position $q_d = \begin{bmatrix} q_{d1} \\ q_{d2} \end{bmatrix}$.

In order to achieve the desired position, we can use a proportional-derivative (PD) controller. The control law is based on the local measurements of the position errors $\tilde{q}_j = q_j - q_{dj}$ and joint velocities $\dot{q}_i$.

First, we consider the case when $g(q)=0$ (that is, no gravitational forces). The control law is given by:

$$\tau_j = -k_{p_j}\tilde{q}_i - k_{d_j}\dot{q} \tag{3.2}$$

where k_{p_j}, k_{D_j} are strictly positive constants. To show that the above control law is stable and achieves zero steady state error, consider the Lyapunov function candidate:

$$V = \frac{1}{2}[\dot{q}^T D(q)\dot{q} + \tilde{q}^T k_p \tilde{q}] \tag{3.3}$$

We can rewrite the conservation of energy in the following form:

$$\frac{1}{2}\frac{d}{dt}[\dot{q}^T D\dot{q}] = \dot{q}\tau \tag{3.4}$$

The right term represents the power input from the actuators, and the left term represents the derivative of the robot's kinetic energy. We have:

$$\tau_j = -k_{p_j}\tilde{q}_i - k_{d_j}\dot{q} \tag{3.5}$$

where k_p, k_d are constant symmetric positive definite matrices (usually diagonal matrices).

We can write the time derivative of V as:

$$\dot{V} = \dot{q}^T [\tau + k_p \tilde{q}] \tag{3.6}$$

Using $\tau_j = -k_{p_j} \tilde{q}_i - k_{d_j} \dot{q}$, it implies that:

$$\dot{V} = -\dot{q}^T k_D \dot{q} \leq 0 \tag{3.7}$$

Let us consider $\dot{V} = 0$. This implies that

$$\dot{q} = 0 \Rightarrow \ddot{q} = 0 \Rightarrow \ddot{q} = D^{-1} k_P \tilde{q} \Rightarrow \tilde{q} = 0 \tag{3.8}$$

In this case, the system trajectories converge to the desired state. Now, let us assume that $g(q) \neq 0$. In this case, we can write the control law in the following form:

$$\tau_j = -k_{p_j} \tilde{q}_i - k_{d_j} \dot{q} + g(q) \tag{3.9}$$

In this case, the control law cancels the effects of the gravitational terms. This control law requires the calculus of $g(q)$ at each instant from the Lagrangian equations.

3.1.1 **Simulation results**

We present the results of the PD control method for two rigid links manipulator. In these simulations the following parameters are used: the masse of each link is $m = 1kg$ and the length of each link is: $l = 1m$.

The simulations are run using three different sets of initial conditions for the manipulator: the equilibrium point, near the equilibrium point, and away from the equilibrium point. Also, we can consider two different cases regarding the manipulator:

1. $g(q) = 0$ - in the absence of gravitational force

2. $g(q)=0$ and $\begin{cases}\tau_{d1}=10Nm\\ \tau_{d2}=0\end{cases}$ - in the absence of the gravitational force, and in the presence of the external torque disturbance τ_{d1} at joint 1.

The simulations results are shown in figures 3.1-3.4. The same simulations are conducted again but in the presence of a disturbance $\begin{cases}\tau_{d1}=10\\ \tau_{d2}=0\end{cases}$. The results are shown in figures 3.5-3.8. These simulations are run using the following scenario: the initial conditions are $\begin{cases}q_{i1}=-\pi/2\\ q_{i2}=0\end{cases}$, and the desired final position is set to $\begin{cases}q_{d1}=-\pi\\ q_{d2}=\pi/2\end{cases}$, and the gains used are $\begin{cases}k_D=100\\ k_P=100\end{cases}$.

For the tracking case, the results are shown in figures 3.9-1.12 and in figures 3.13-3.16 in the presence of a disturbance $\begin{cases}\tau_{d1}=10\\ \tau_{d2}=0\end{cases}$. For the tracking case, the trajectories to be followed are given by $y_{d1}=A\sin(\omega t)$, and $y_{d2}=A\sin(\omega t)$ where $A=1$ and $\omega=1$. The gains selected are $\begin{cases}k_D=100\\ k_P=100\end{cases}$.

The simulations results are summarized in Tables 3.1-3.3. The three sets of initial conditions are given below.

I. Initial conditions are:

$$\begin{cases} q_{i1} = -\pi/2 \\ q_{i2} = 0 \end{cases} \qquad \begin{cases} q_{d1} = -\pi \\ q_{d2} = \pi/2 \end{cases} \qquad \begin{cases} \tau_{d1} = 10 \\ \tau_{d2} = 0 \end{cases}$$

PD Gain	Disturbances	t_s	er_1	er_2	$\lvert\tau_1\rvert_{max}$	$\lvert\tau_2\rvert_{max}$
$k_P = 25$ $k_D = 10$	$\tau_d = 0$	2	-1.28e-8	1.36e-5	40	40
	$\tau_d = 10$	3	-0.4	1.59e-5	40	40
$k_P = 100$ $k_D = 20$	$\tau_d = 0$	2	-9e-6	4e-5	160	160
	$\tau_d = 10$	2	-0.1	2e-5	160	160
$k_P = 400$ $k_D = 40$	$\tau_d = 0$	0.5	8e-6	-1.9e-5	600	600
	$\tau_d = 10$	0.5	-0.0249	-1.4 e-5	600	600
$k_P = 900$ $k_D = 60$	$\tau_d = 0$	0.4	-6e-6	3 e-5	1500	1500
	$\tau_d = 10$	0.4	-0.011	7 e-5	1500	1500

Table 3-1 Summary of the results using the first set of initial conditions

II. Initial conditions are:

$$\begin{cases} q_{i1} = -\pi/2 + \pi/18 \\ q_{i2} = \pi/18 \end{cases} \qquad \begin{cases} q_{d1} = -\pi \\ q_{d2} = \pi/2 \end{cases} \qquad \begin{cases} \tau_{d1} = 10 \\ \tau_{d2} = 0 \end{cases}$$

PD Gain	Disturbances	t_s	er_1	er_2	$\lvert\tau_1\rvert_{max}$	$\lvert\tau_2\rvert_{max}$
$k_P = 25$ $k_D = 10$	$\tau_d = 0$	2	6e-6	2e-5	40	40
	$\tau_d = 10$	3	-0.4	-4e-5	40	40
$k_P = 100$ $k_D = 20$	$\tau_d = 0$	1	4e-6	1e-5	150	180
	$\tau_d = 10$	2.3	-0.1	0.0002	150	180
$k_P = 400$ $k_D = 40$	$\tau_d = 0$	0.6	6e-5	0.0002	600	700
	$\tau_d = 10$	2	-0.025	0.0003	600	700
$k_P = 900$ $k_D = 60$	$\tau_d = 0$	0.5	4e-5	0.0001	1500	1500
	$\tau_d = 10$	0.5	-0.011	4e-6	1500	1500

Table 3-2 Summary of the results using the second set of initial conditions

III. Initial conditions are:

$$\begin{cases} q_{i1} = 0 \\ q_{i2} = 0 \end{cases} \qquad \begin{cases} q_{d1} = -\pi \\ q_{d2} = \pi/2 \end{cases} \qquad \begin{cases} \tau_{d1} = 10 \\ \tau_{d2} = 0 \end{cases}$$

PD Gain	Disturbances	t_s	er_1	er_2	$\lvert\tau_1\rvert_{max}$	$\lvert\tau_2\rvert_{max}$
$k_P = 25$ $k_D = 10$	$\tau_d = 0$	2	-3.8e-5	3.36e-5	80	40
	$\tau_d = 10$	3	-0.4	-6.2e-5	80	40
$k_P = 100$ $k_D = 20$	$\tau_d = 0$	1	2e-6	-5e-6	300	150
	$\tau_d = 10$	2	-0.099	-3.8e-5	300	150
$k_P = 400$ $k_D = 40$	$\tau_d = 0$	0.5	7e-5	-0.0003	1300	600
	$\tau_d = 10$	0.5	-0.024	-5e-5	1300	600
$k_P = 900$ $k_D = 60$	$\tau_d = 0$	0.4	3.5e-6	-1.9e-5	2900	1500
	$\tau_d = 10$	0.4	-0.011	-3.9e-5	2900	1500

Table 3-3 Summary of the results using the third set of initial conditions

3.1.2 Conclusions

In order to decrease the error we can use higher gains K_p and K_D. Another effect of using higher gains is the decrease of the settling time. For gains $\begin{cases} k_P = 900 \\ k_D = 60 \end{cases}$, we can achieve a settling time of 0.4 seconds in all of the three sets of initial conditions. The effects of the torque disturbance are reduced by using higher gains. The most important disadvantage of using higher gains is that it could lead the system to the neighbourhood of large oscillations and transients.

In all of the cases, there is a large initial value for the control signal. Because of the mechanical restrictions imposed by the manipulators, a saturation function after the controller can be employed. For example, a threshold logic having as minimum and maximum values of +/- 50Nm could be used.

In the case of tracking results, the error is increased, but the system can generally track the desired sinusoidal trajectory. The steady state error could be removed by using a PID controller instead of a PD controller. This controller is locally stable, and can solve the regulation problem, but at the same time, cannot achieve uniformity of the transient behaviour [46].

In the cases presented above, gravity is not taken into consideration. In order to avoid the static error due to gravity for a manipulator operating in a gravitation field (that is not in a horizontal plane), a PD controller that takes into consideration the gravity term can be used. In this case, the controller requires exact knowledge of the gravity term in order to calculate the control signals.

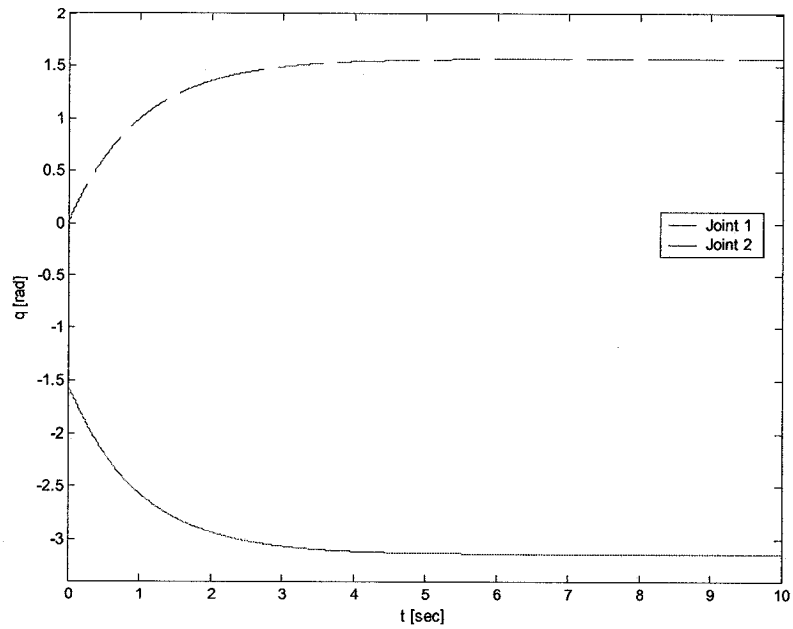

Figure 3-1 PD control scheme - joint angles

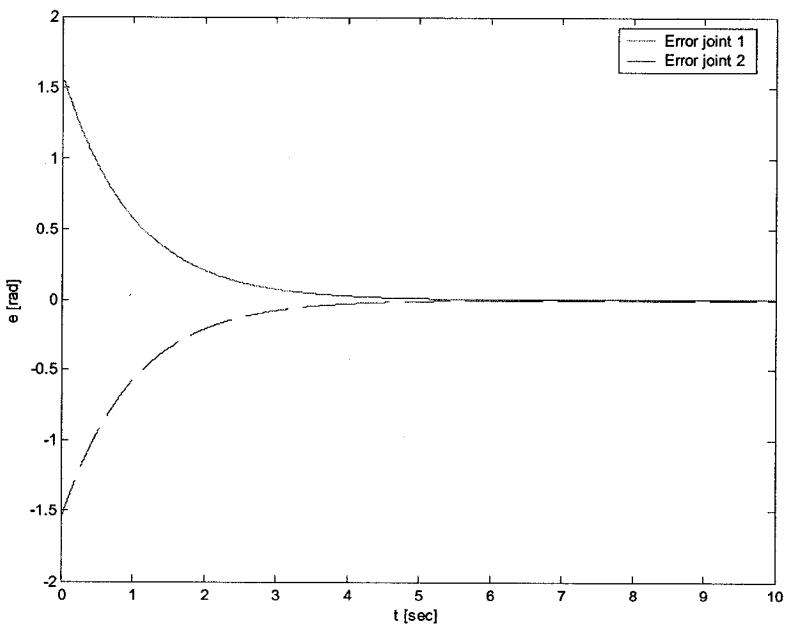

Figure 3-2 PD control scheme - joint angles error

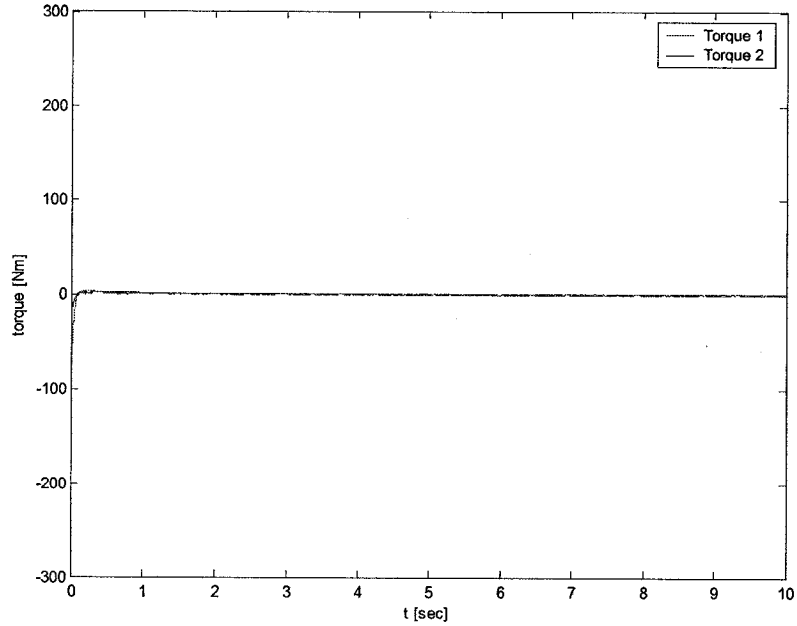

Figure 3-3 PD control scheme - joint torques command

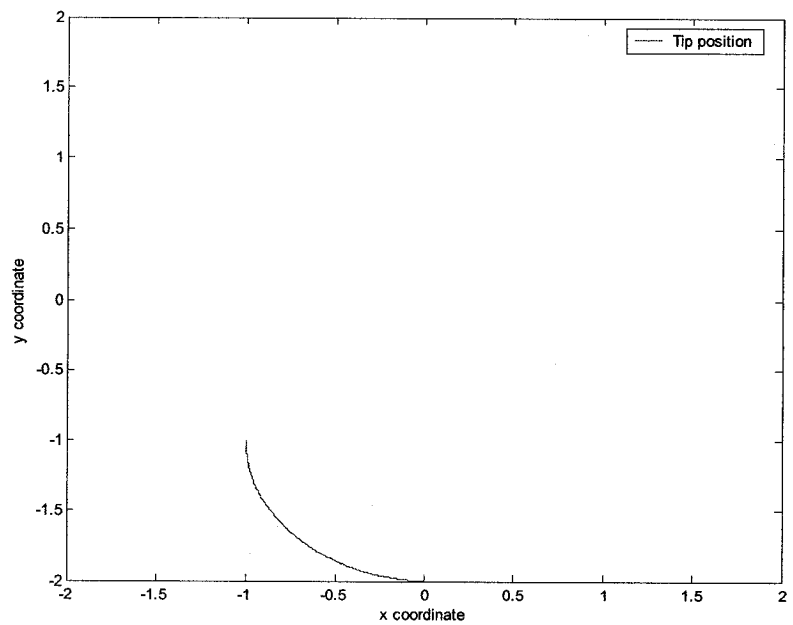

Figure 3-4 PD control scheme - end-effector position

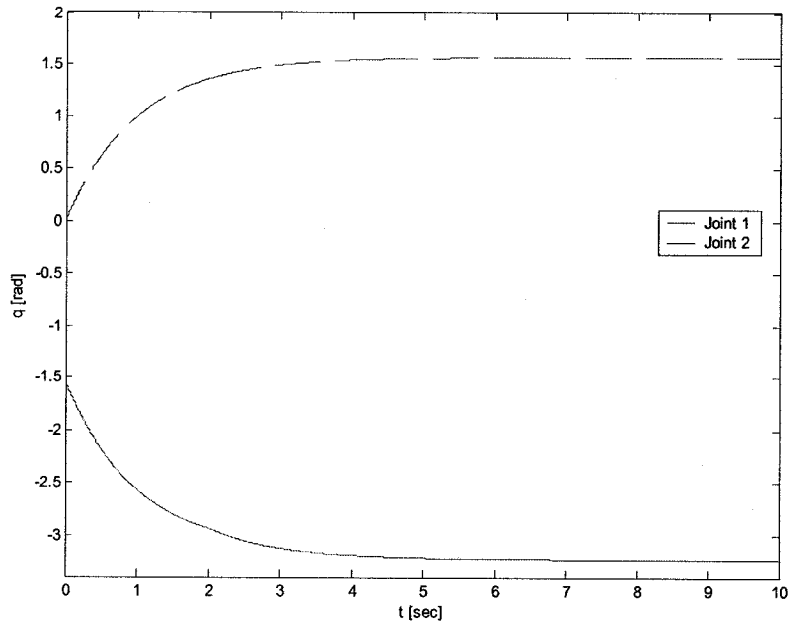

Figure 3-5 PD control scheme - joint angles

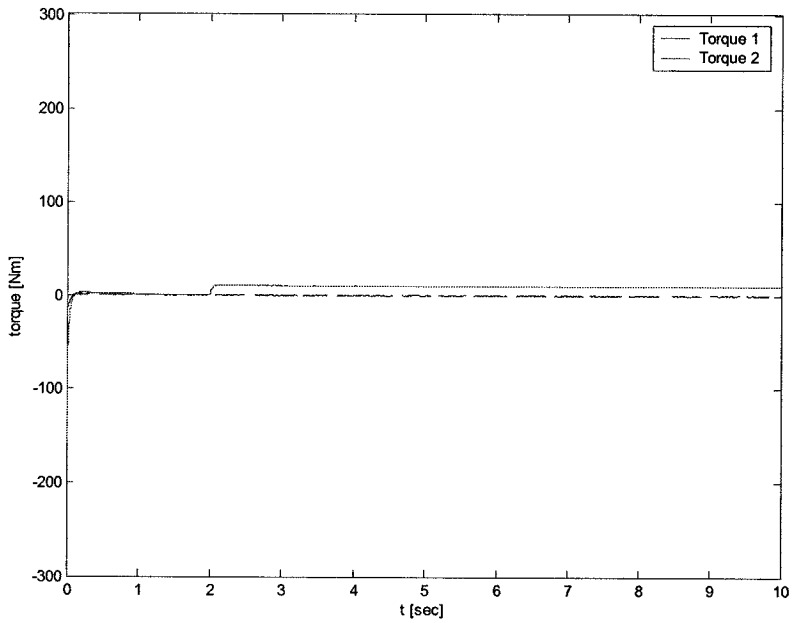

Figure 3-6 PD control scheme - joint torques command

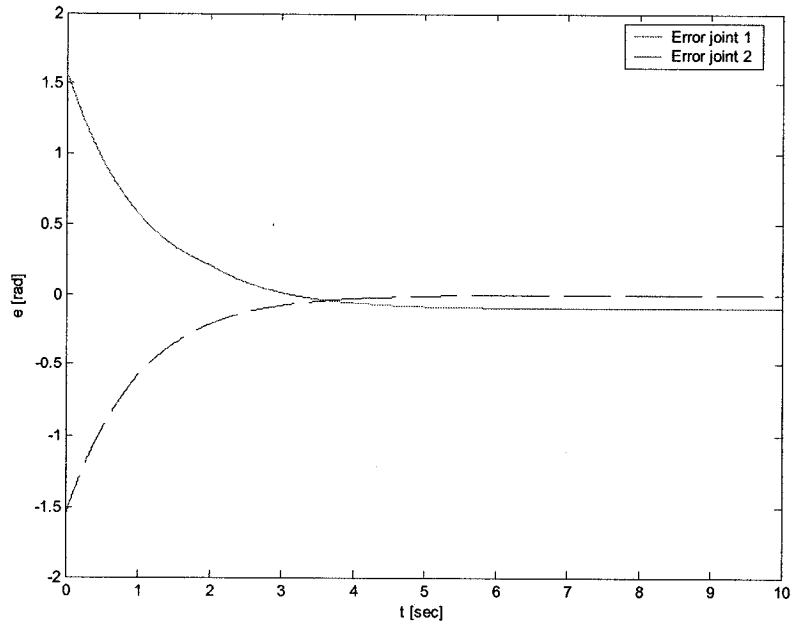

Figure 3-7 PD control scheme - joint angles error

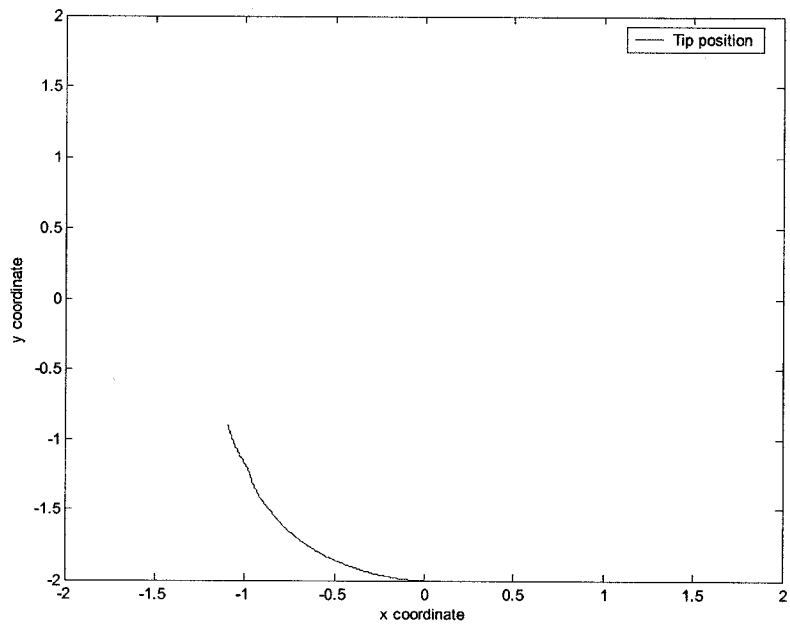

Figure 3-8 PD control scheme - end-effector position

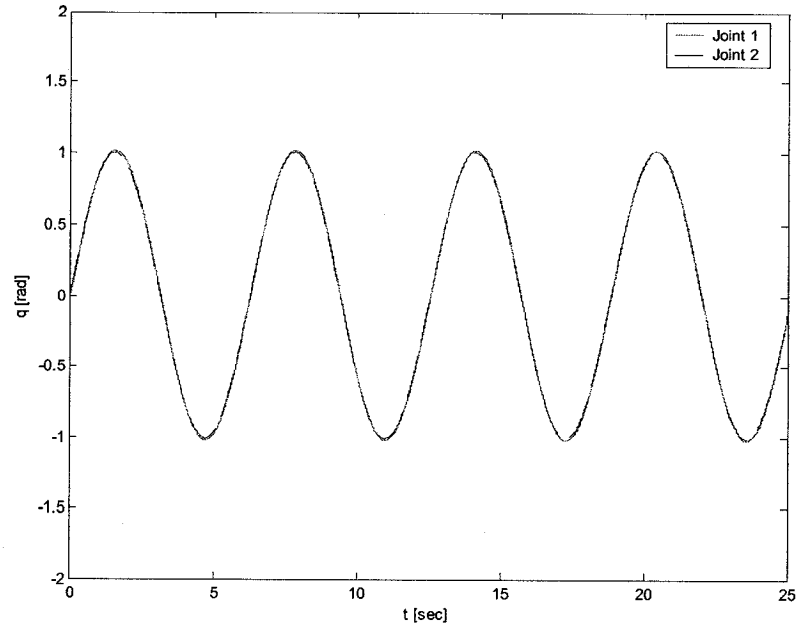

Figure 3-9 PD control scheme - tracking case - joint angles

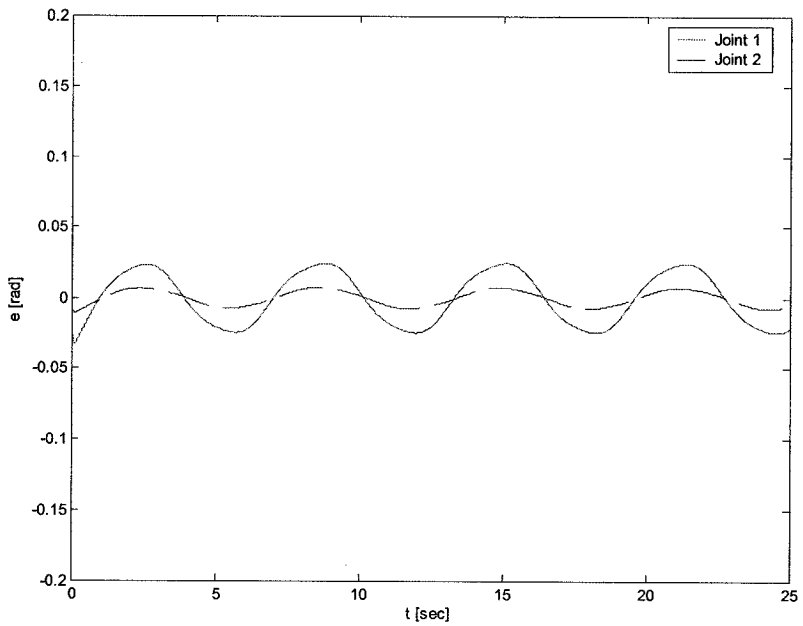

Figure 3-10 PD control scheme - tracking case - joint angles error

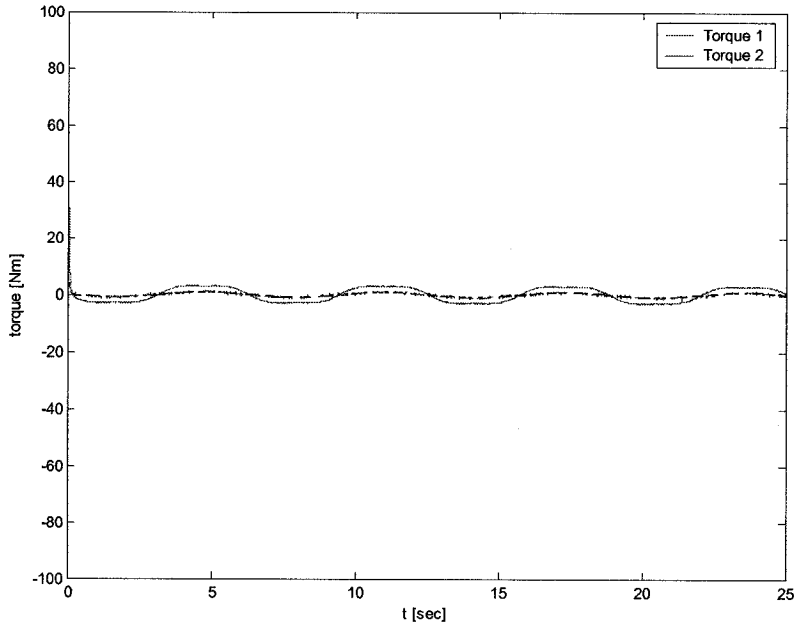

Figure 3-11 PD control scheme - tracking case - joint torques command

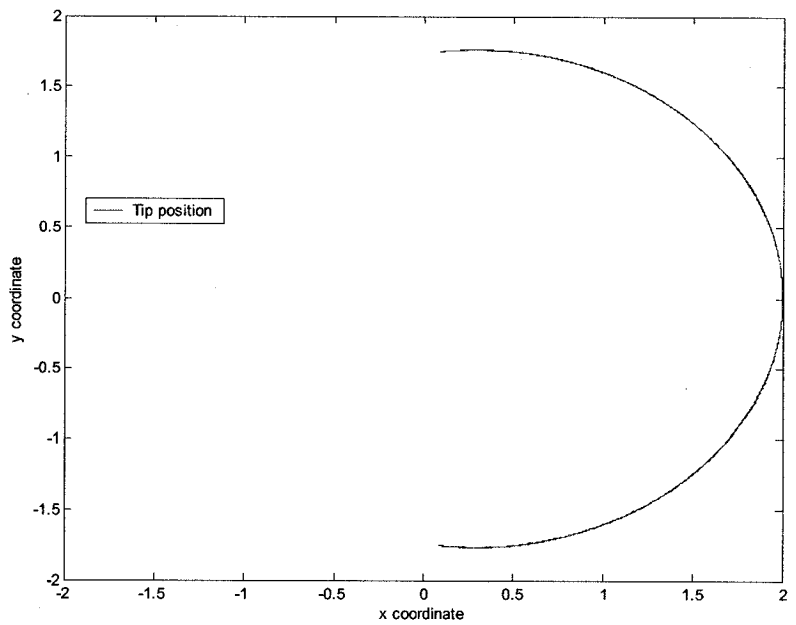

Figure 3-12 PD control scheme - tracking case - end-effector position

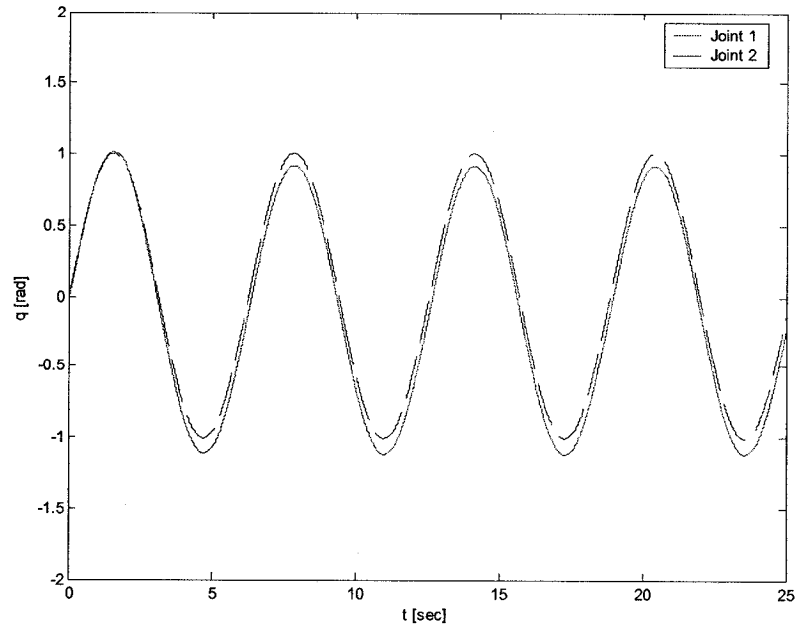

Figure 3-13 PD control scheme - tracking case -joint angles

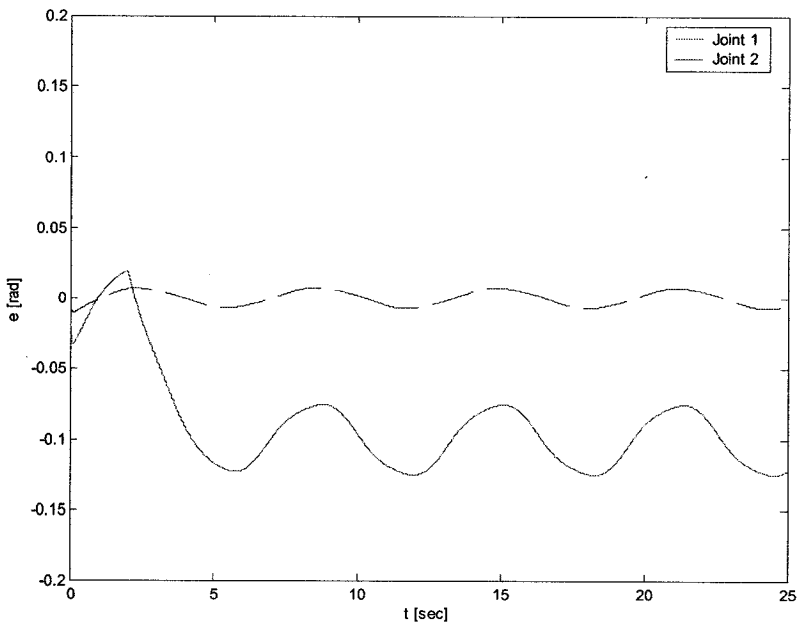

Figure 3-14 PD control scheme - tracking case - joint angles error

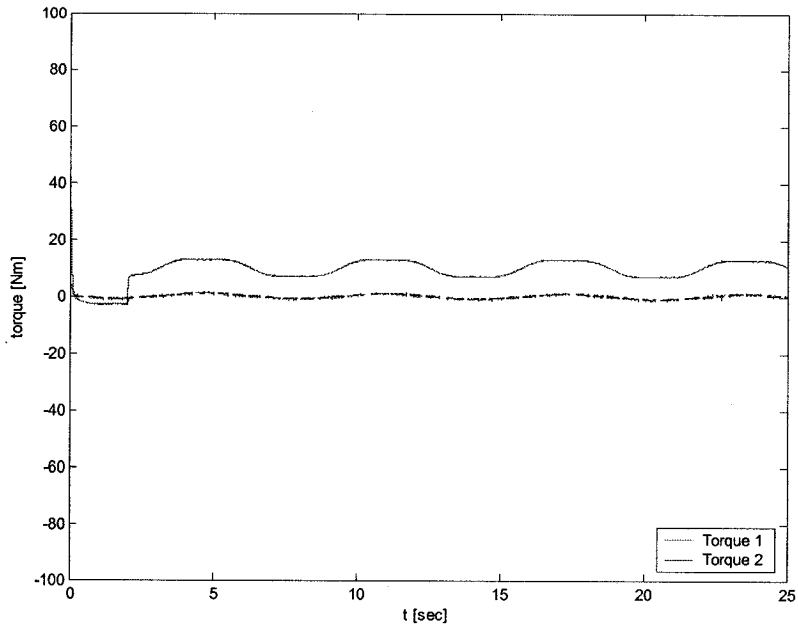

Figure 3-15 PD control scheme - tracking case -joint torques command

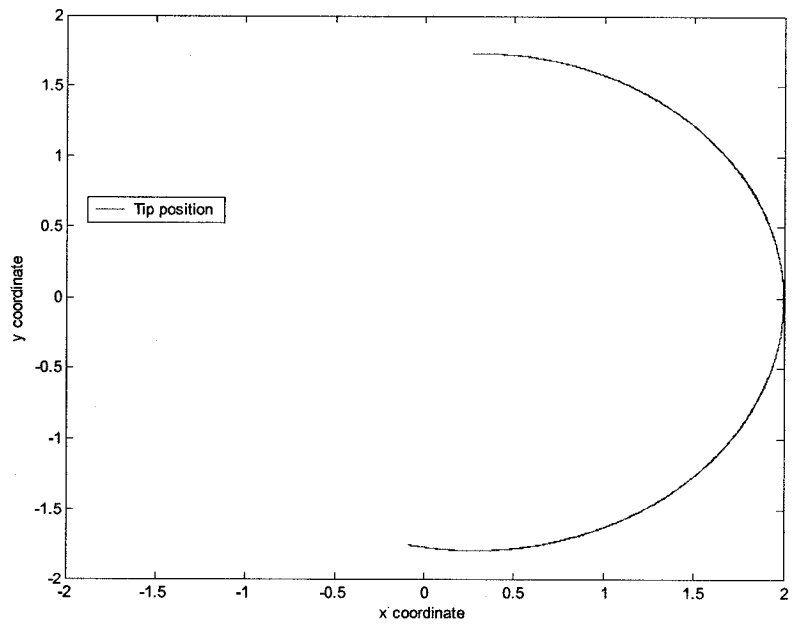

Figure 3-16 PD control scheme - tracking case - end-effector position

3.2 Computed torque method

Computed torque method, known in the literature also as inverse dynamics control, is an approach that uses the complete dynamic model of the manipulator in order to cancel the effects of the nonlinearities such as Coriolis and centrifugal forces, friction, as well as gravity terms. These terms are compensated by adding them to the control input.

The computed torque method is based on finding a control input as function of system state which can realize an input/output relationship of linear type.

Let us consider a planar, two-link, articulated manipulator. The dynamics of this two-rigid link manipulator can be written in the general form [48] as in the equation (3.1):

$$D(q)\ddot{q}+C(q,\dot{q})\dot{q}+g(q)=\tau$$

Let us define the following control law structure, taking τ as a function of the manipulator state namely:

$$\tau = Du + C\dot{q} + g \tag{3.10}$$

Substituting the above control law structure in the equations of the manipulator model leads to the system described by:

$$\ddot{q} = u \tag{3.11}$$

where u represents a new input vector. The nonlinear control law (3.11) is named computed torque control or inverse dynamics control because is based on the calculation of the inverse dynamics. The closed loop system using this control is linear and decoupled with respect to the new input u.Each component of the input vector u_i influences each joint variable q_i.

Next step is to find a stabilizing control law u. Let us define:

$$u = \ddot{q}_d - 2\xi\lambda\dot{\tilde{q}} - \lambda^2\tilde{q}, \tag{3.12}$$

where $\lambda, \xi > 0$, and $\tilde{q} = q - q_d$

This implies that:

$$\ddot{\tilde{q}} + 2\xi\lambda\dot{\tilde{q}} + \lambda^2\tilde{q} = 0 \tag{3.13}$$

The above equation represents the differential equation of the linearized closed loop system.

3.2.1 **Simulation results**

We present the results of the computed torque control method for two rigid links manipulator. In these simulations the following parameters are used: the masse of each link is $m = 1kg$ and the length of each link is $l = 1m$.

The simulations are conducted using three different sets of initial conditions for the manipulator: the equilibrium point, near the equilibrium point, and away from the equilibrium point. Furthermore, we can consider two different cases regarding the manipulator:

3. $g(q) = 0$ - in the absence of gravitational force
4. $g(q) = 0$ and $\begin{cases} \tau_{d1} = 10Nm \\ \tau_{d2} = 0 \end{cases}$ - in the absence of the gravitational force and in the presence of the external torque disturbance τ_{d1} at joint 1.

We can choose different values for the settling time and we will have different values for the parameters of the controller.

Trajectory calculus

$$T^2 \ddot{q}_{di} + 2Td\dot{q}_{di} + q_{di} = r \tag{3.14}$$

where r is the final position for the joints.

We can choose:

a) $\begin{cases} T = 0.125 \\ d = 0.9 \end{cases}$

b) $\begin{cases} T = 0.5 \\ d = 0.9 \end{cases}$

c) $\begin{cases} T = 1 \\ d = 0.9 \end{cases}$

The equation of the closed-loop system is given by:

$$\ddot{\tilde{q}} + 2\xi\lambda\dot{\tilde{q}} + \lambda^2\tilde{q} = 0 \tag{3.15}$$

We can set the time constant τ ten times faster then the time constant T for the trajectory calculus. In this case, we can set:

a) $\tau = \frac{T}{10} = 0.0125 = \frac{1}{\lambda}$, so that $\lambda = 80$. We can also choose $\xi = .7$.

b) $\tau = \frac{T}{10} = 0.05 = \frac{1}{\lambda}$, so that $\lambda = 20$. We can also choose $\xi = .7$.

c) $\tau = \frac{T}{10} = 0.1 = \frac{1}{\lambda}$, so that $\lambda = 10$. We can also choose $\xi = .7$.

We can rewrite the equation of the closed loop system as:

$$\ddot{\tilde{q}} + K_D\dot{\tilde{q}} + K_P\tilde{q} = 0 \tag{3.16}$$

In this case, the values for the gains used are as follows:

a) $\begin{cases} K_P = 6400 \\ K_D = 112 \end{cases}$

b) $\begin{cases} K_P = 400 \\ K_D = 28 \end{cases}$

c) $\begin{cases} K_P = 100 \\ K_D = 14 \end{cases}$

The simulations results are shown in figures 3.17-3.20. The same simulations are performed again but in the presence of a disturbance $\begin{cases} \tau_{d1} = 10 \\ \tau_{d2} = 0 \end{cases}$. The results are shown in figures 3.21-3.24. These simulations are conducted using the following scenario: the initial conditions are $\begin{cases} q_{i1} = -\pi/2 \\ q_{i2} = 0 \end{cases}$, and the desired final position is set to $\begin{cases} q_{d1} = -\pi \\ q_{d2} = \pi/2 \end{cases}$, and the gains used are $\begin{cases} k_D = 400 \\ k_P = 28 \end{cases}$.

For the tracking case, the results are shown in figures 3.25-3.28, and in figures 3.29-3.32 in the presence of a disturbance $\begin{cases} \tau_{d1} = 10 \\ \tau_{d2} = 0 \end{cases}$. For the tracking case, the trajectories to be followed are given by $y_{d1} = A\sin(\omega t)$ and $y_{d2} = A\sin(\omega t)$ where $A = 1$ and $\omega = 1$.

The results of the simulations are presented in the Tables 3.7-3.9, with the three sets of initial conditions given as:

I. Initial conditions are:

$$\begin{cases} q_{i1} = -\pi/2 \\ q_{i2} = 0 \end{cases} \qquad \begin{cases} q_{d1} = -\pi \\ q_{d2} = \pi/2 \end{cases} \qquad \begin{cases} \tau_{d1} = 10 \\ \tau_{d2} = 0 \end{cases}$$

Design Parameters		Disturbances	t_s	er_1	er_2	$\lvert\tau_1\rvert_{max}$	$\lvert\tau_2\rvert_{max}$
$T = 0.125$ $d = 0.9$ $\lambda = 80$ $\xi = 0.7$	$K_P = 6400$ $K_D = 112$	$\tau_{d1} = 0$ $\tau_{d2} = 0$	0.5	1.2e-5	9e-7	190	190
		$\tau_{d1} = 10$ $\tau_{d2} = 0$	0.5	0.0011	0.0011	190	190
$T = 0.5$ $d = 0.9$ $\lambda = 20$ $\xi = 0.7$	$K_P = 400$ $K_D = 28$	$\tau_{d1} = 0$ $\tau_{d2} = 0$	2	5e-6	-4e-6	13	13
		$\tau_{d1} = 10$ $\tau_{d2} = 0$	2	0.018	0.018	13	13
$T = 1$ $d = 0.9$ $\lambda = 10$ $\xi = 0.7$	$K_P = 100$ $K_D = 14$	$\tau_{d1} = 0$ $\tau_{d2} = 0$	4	-0.002	0.002	3	3
		$\tau_{d1} = 10$ $\tau_{d2} = 0$	4	0.07	0.06	3	3

Table 3-4 Summary of the results using the first set of initial conditions

II. Initial conditions are:

$$\begin{cases} q_{i1} = -\pi/2 + \pi/18 \\ q_{i2} = \pi/18 \end{cases} \qquad \begin{cases} q_{d1} = -\pi \\ q_{d2} = \pi/2 \end{cases} \qquad \begin{cases} \tau_{d1} = 10 \\ \tau_{d2} = 0 \end{cases}$$

Design Parameters		Disturbances	t_s	er_1	er_2	$\lvert\tau_1\rvert_{max}$	$\lvert\tau_2\rvert_{max}$
$T = 0.125$ $d = 0.9$ $\lambda = 80$ $\xi = 0.7$	$K_P = 6400$ $K_D = 112$	$\tau_{d1} = 0$ $\tau_{d2} = 0$	0.5	$5*10^{-5}$	$6*10^{-6}$	230	65
		$\tau_{d1} = 10$ $\tau_{d2} = 0$	0.5	-0.0011	0.0011	230	65
$T = 0.5$ $d = 0.9$ $\lambda = 20$ $\xi = 0.7$	$K_P = 400$ $K_D = 28$	$\tau_{d1} = 0$ $\tau_{d2} = 0$	2	$-2*10^{-6}$	$6*10^{-6}$	13	4
		$\tau_{d1} = 10$ $\tau_{d2} = 0$	2	-0.018	0.018	13	4
$T = 1$ $d = 0.9$ $\lambda = 10$ $\xi = 0.7$	$K_P = 100$ $K_D = 14$	$\tau_{d1} = 0$ $\tau_{d2} = 0$	4	0.0025	0.0020	4	1
		$\tau_{d1} = 10$ $\tau_{d2} = 0$	4	-0.076	0.069	13	1

Table 3-5 Summary of the results using the second set of initial conditions

III. Initial conditions are:

$$\begin{cases} q_{i1} = 0 \\ q_{i2} = 0 \end{cases} \qquad \begin{cases} q_{d1} = -\pi \\ q_{d2} = \pi/2 \end{cases} \qquad \begin{cases} \tau_{d1} = 10 \\ \tau_{d2} = 0 \end{cases}$$

Design Parameters		Disturbances	t_s	er_1	er_2	$\lvert\tau_1\rvert_{max}$	$\lvert\tau_2\rvert_{max}$
$T = 0.125$ $d = 0.9$ $\lambda = 80$ $\xi = 0.7$	$K_P = 6400$ $K_D = 112$	$\tau_{d1} = 0$ $\tau_{d2} = 0$	0.5	$-2*10^{-6}$	$7*10^{-7}$	470	140
		$\tau_{d1} = 10$ $\tau_{d2} = 0$	0.5	-0.0011	0.0012	470	140
$T = 0.5$ $d = 0.9$ $\lambda = 20$ $\xi = 0.7$	$K_P = 400$ $K_D = 28$	$\tau_{d1} = 0$ $\tau_{d2} = 0$	2	$2*10^{-6}$	$2*10^{-5}$	30	9
		$\tau_{d1} = 10$ $\tau_{d2} = 0$	2	-0.018	0.018	30	9
$T = 1$ $d = 0.9$ $\lambda = 10$ $\xi = 0.7$	$K_P = 100$ $K_D = 14$	$\tau_{d1} = 0$ $\tau_{d2} = 0$	4	-0.0046	0.0023	7	2.5
		$\tau_{d1} = 10$ $\tau_{d2} = 0$	4	0.078	0.069	14	2.5

Table 3-6 Summary of the results using the third set of initial conditions

3.2.2 Conclusions

As in the case of PD controller using higher gains can decrease the error for all the three different scenarios having different initial conditions. At the same time the estimated settling time is achieved. Using different values for the gains we can achieve settling times between 0.5 to 2 seconds.

Because of the high values for the gains used, the initial values for the input torque are very high, reaching to 230N or 470N. One solution would be to use the saturation limits used after the controller. As we discussed for the PD controller, we can choose the minimum and maximum values of +/- 50Nm.

In the case of tracking problem, the errors increase, but the system can track quite satisfactory the desired sinusoidal trajectory.

The method of computed torque control works quite well, and we can have better control than the PD control, but only if we have all necessary information about the dynamic model of the manipulator and the parameters of the robot. These are very hard to have in practice. At the same time, the dynamics of the robot can change during the process, and that can affect the results of the control, too. In this case, the performance of the computed torque method can decrease because of the inaccuracy of the dynamic model. As we have seen the performance of the computed torque control and PD controller is acceptable. We can achieve the desired settling time and we can achieve very small steady state tracking errors.

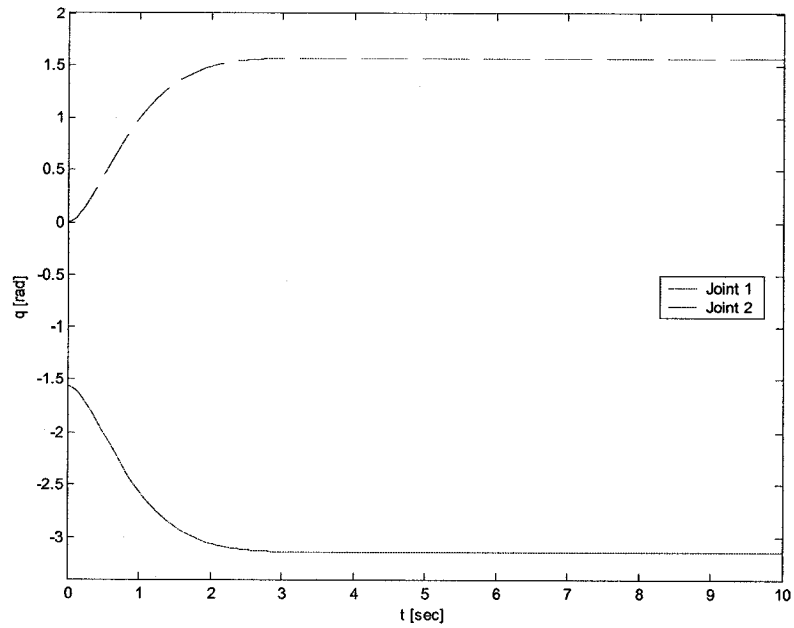

Figure 3-17 Computed torque scheme - joint angles

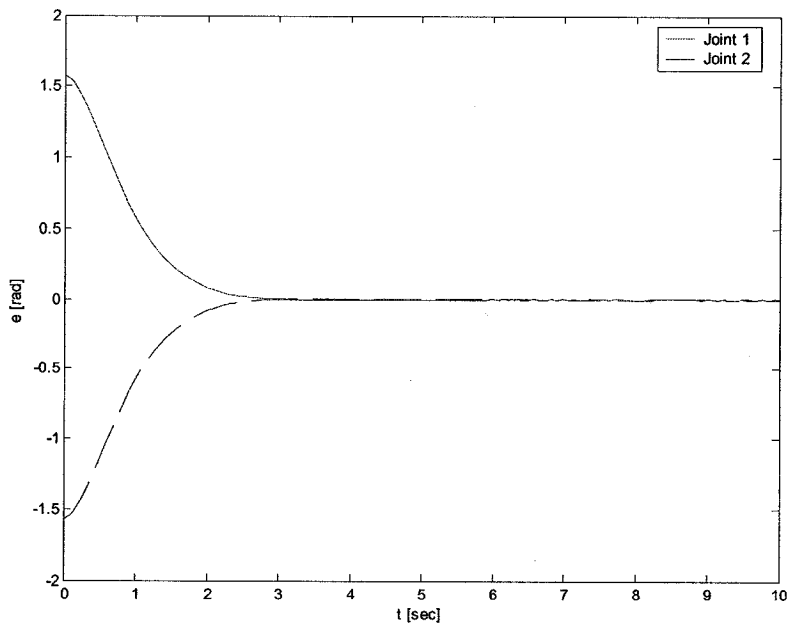

Figure 3-18 Computed torque scheme - joint angles error

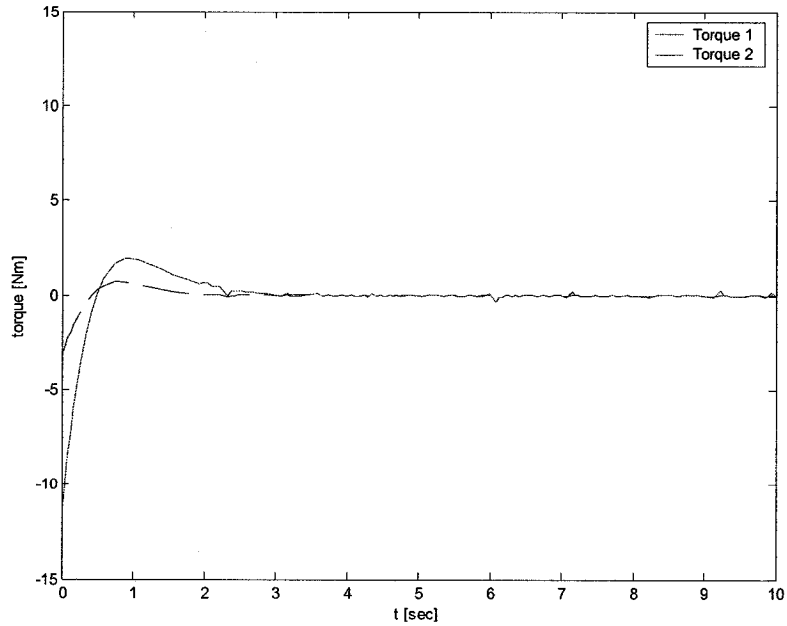

Figure 3-19 Computed torque scheme - joint torque commands

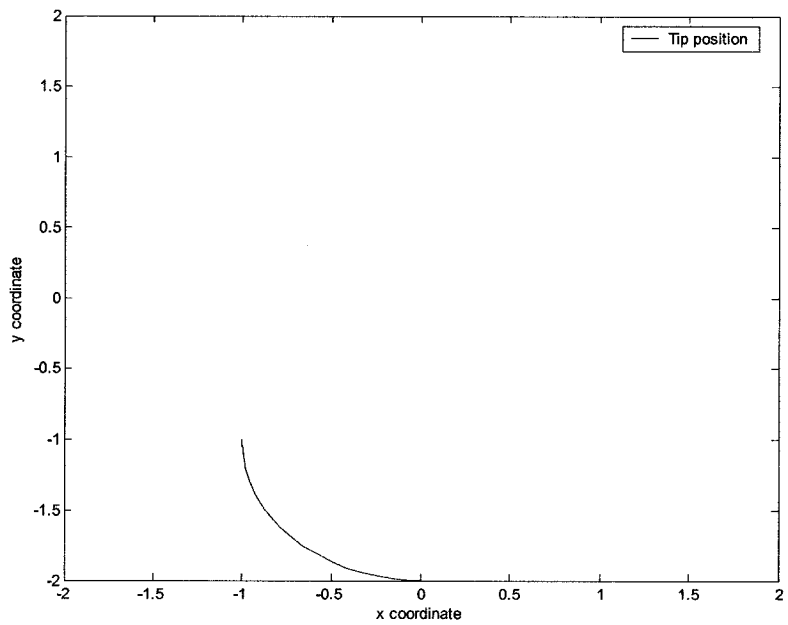

Figure 3-20 Computed torque scheme - end-effector position

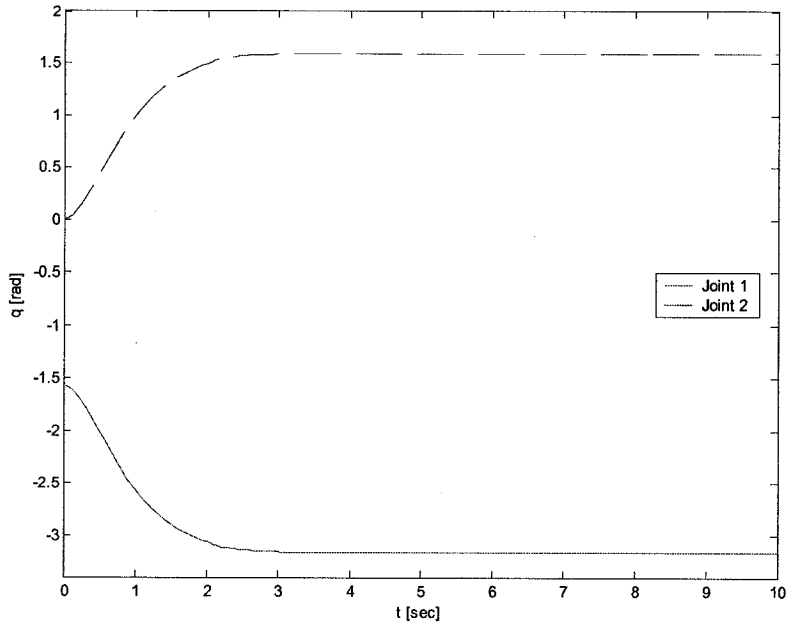

Figure 3-21Computed torque scheme - joint angles

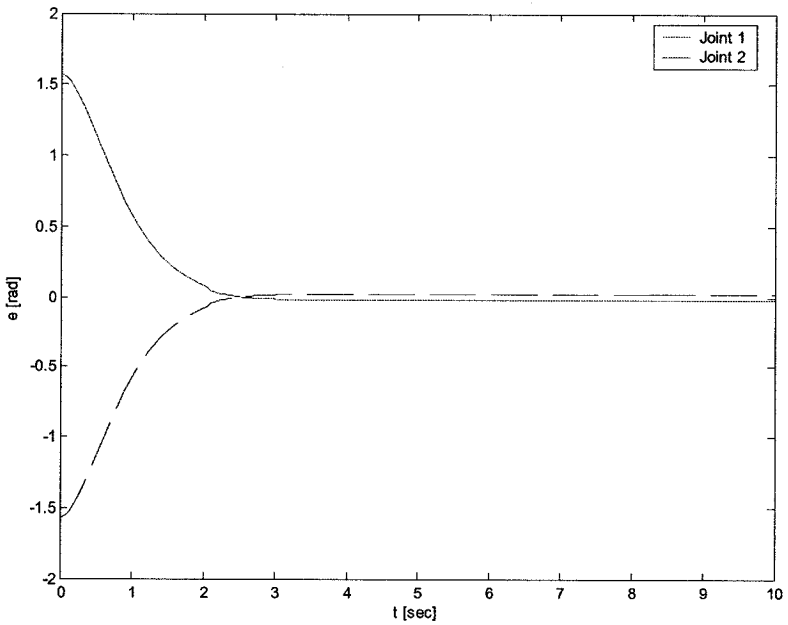

Figure 3-22 Computed torque scheme - joint angles error

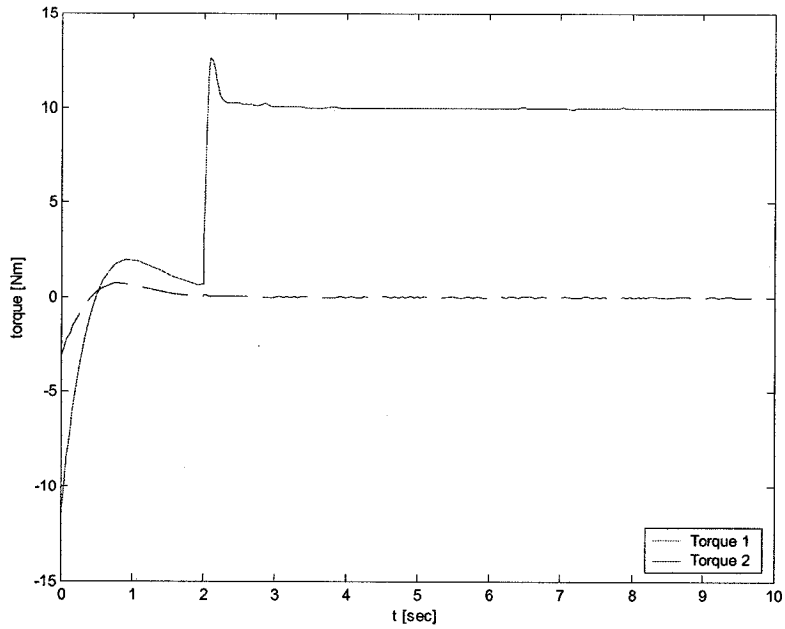

Figure 3-23 Computed torque scheme - torques command

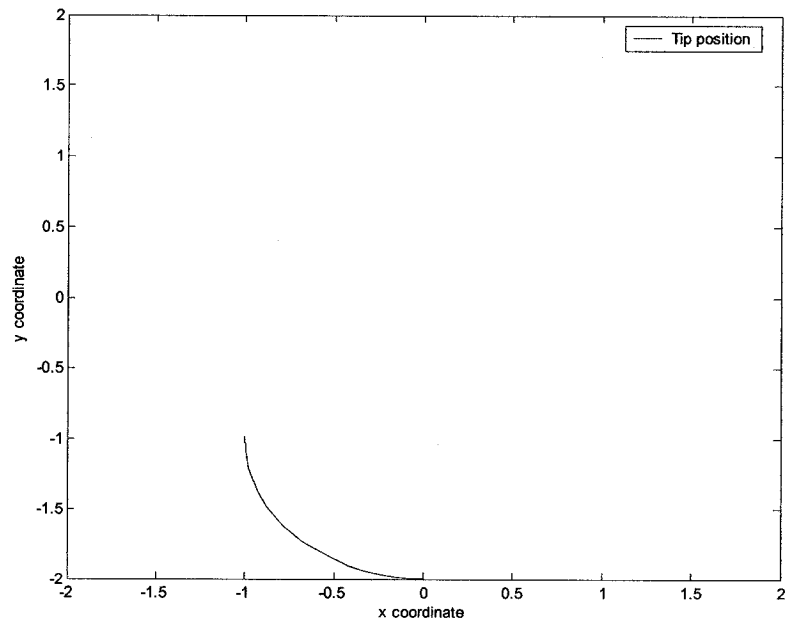

Figure 3-24 Computed torque scheme - tip position

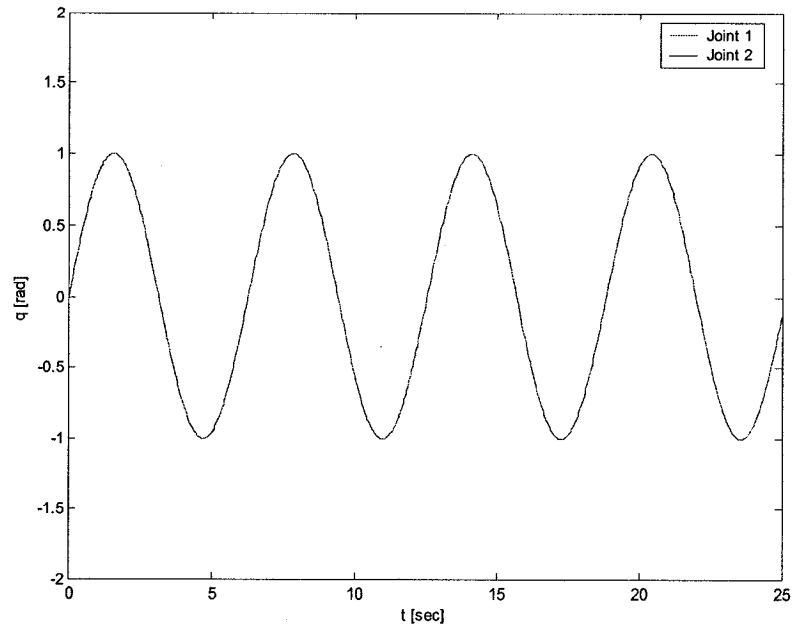

Figure 3-25 Computed torque scheme - tracking case - joint angles

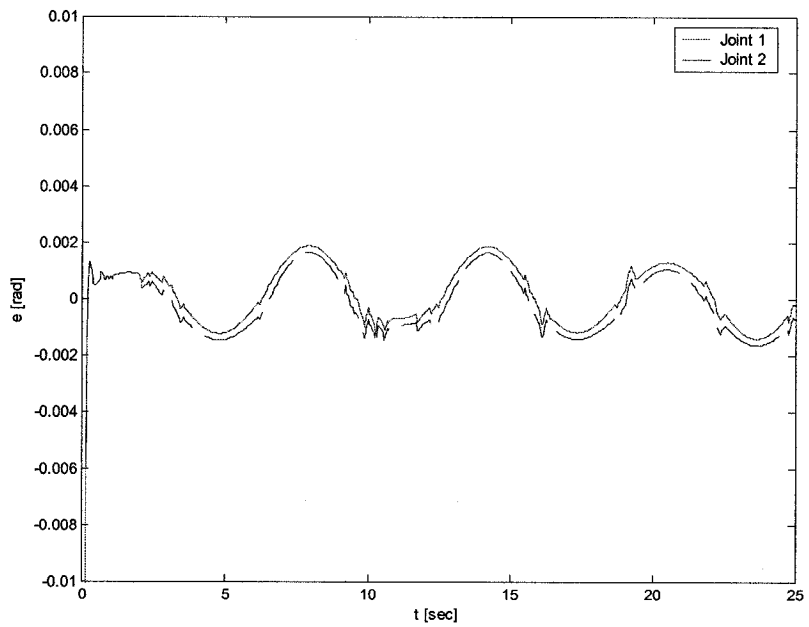

Figure 3-26 Computed torque scheme - tracking case - joint angles error

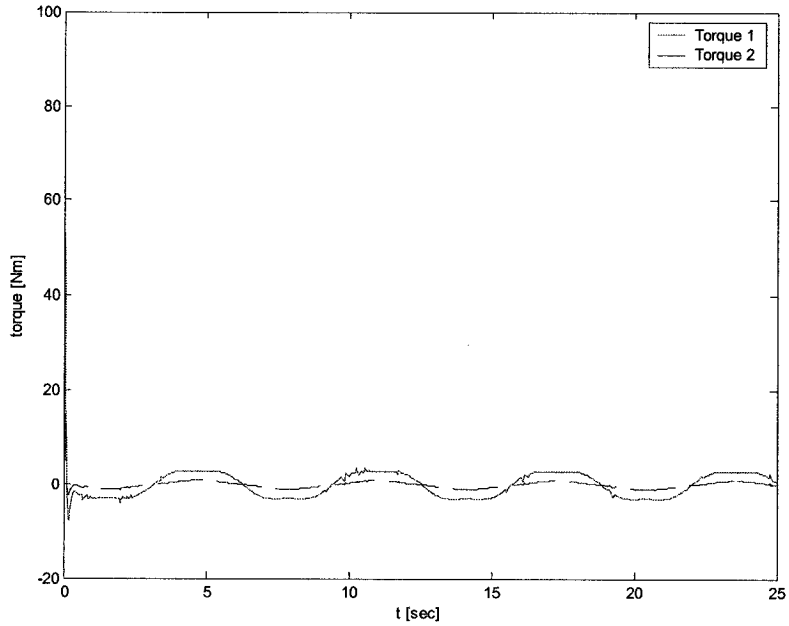

Figure 3-27 Computed torque scheme - tracking case -torques command

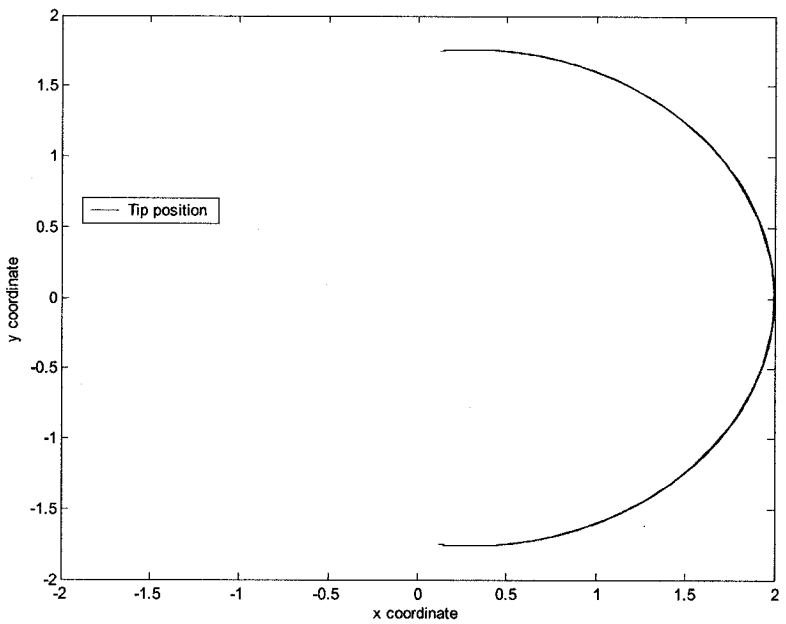

Figure 3-28 Computed torque scheme –tracking case - tip position

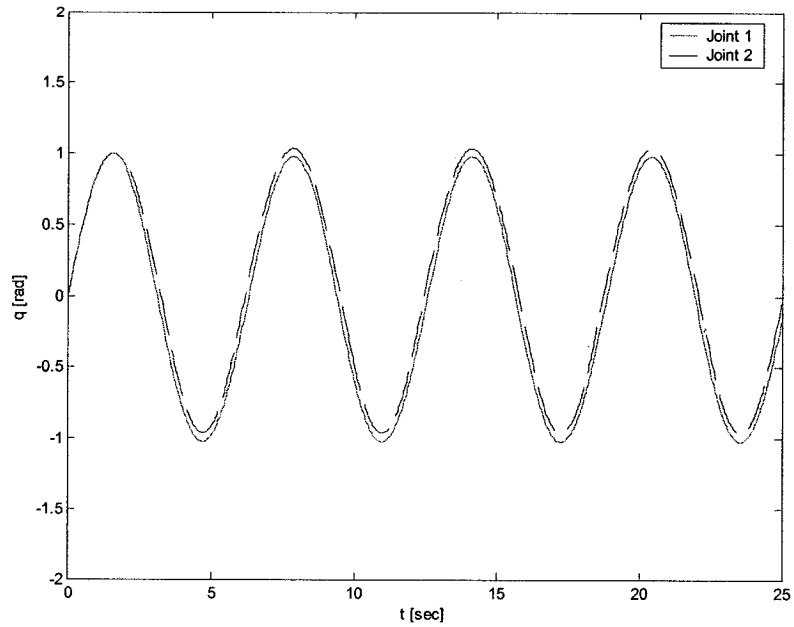

Figure 3-29 Computed torque scheme – tracking case - joint angles

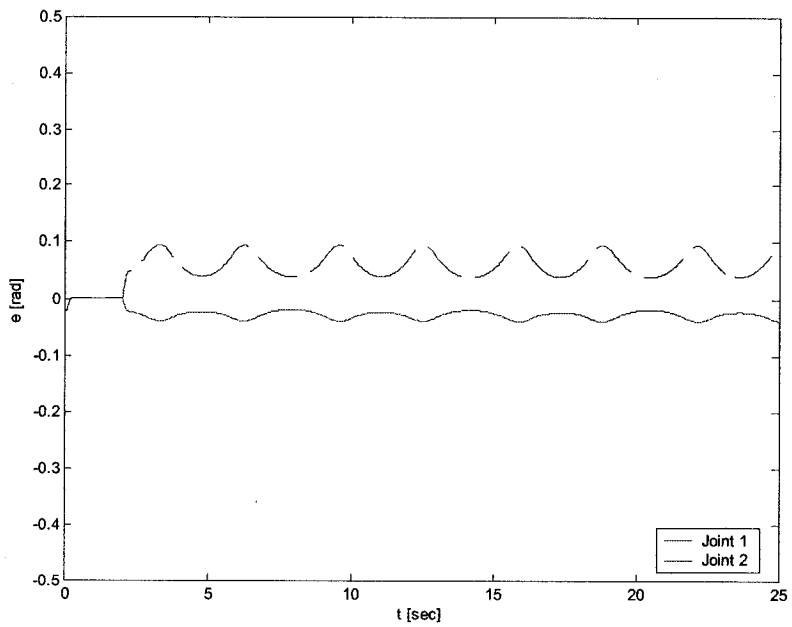

Figure 3-30 Computed torque scheme – tracking case - joint angles error

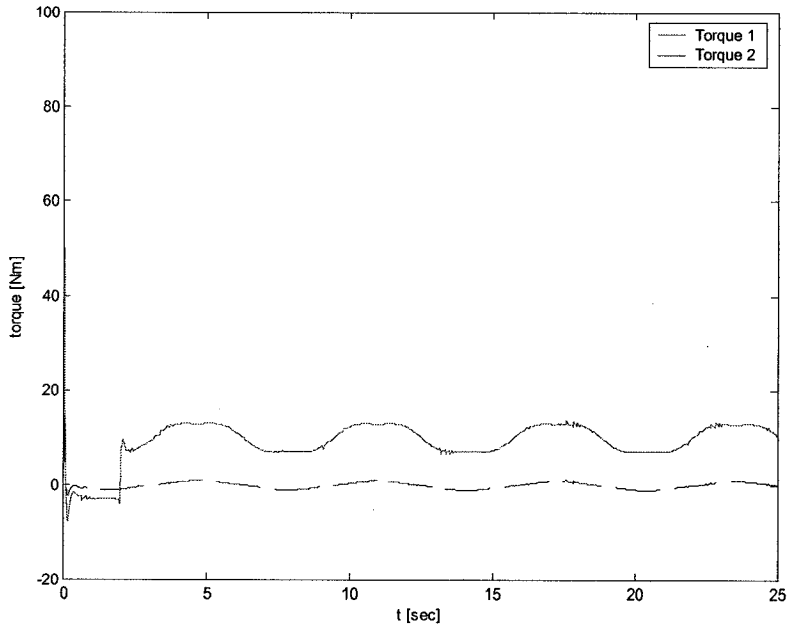

Figure 3-31 Computed torque scheme - joint torque commands

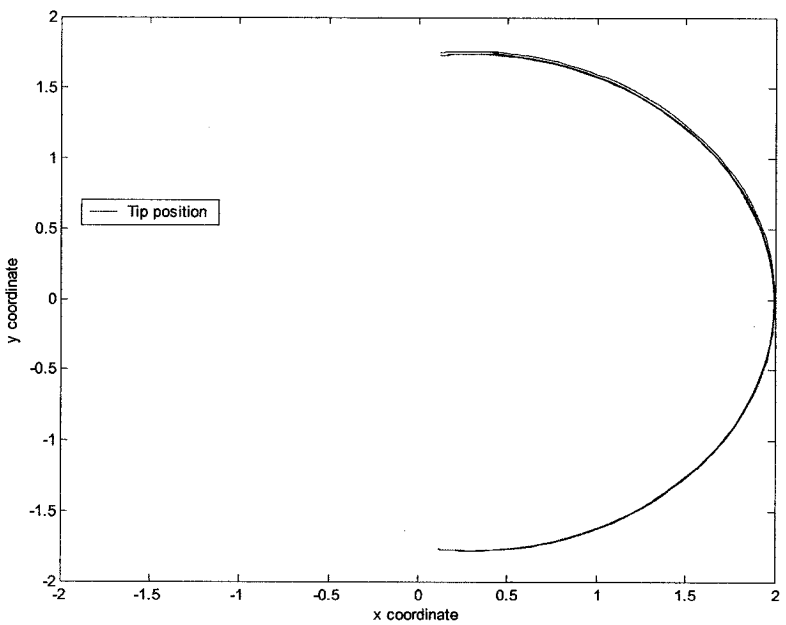

Figure 3-32 Computed torque scheme – tip position – tracking case

3.3 Localization method

The localisation is a method used for systems governed by partial differential equations. Using this method we can obtain the desired transients for the controlled system under the condition of incomplete information for finite-dimensional control systems. The localisation method is based on the use of state time derivatives as control law and high gain values in order to decrease the influence of disturbances and the uncertainty of model parameters on dynamic properties of the output trajectories.

Let us consider a planar, two-link, articulated manipulator. The dynamics of this two-rigid link manipulator can be written in the general form [48]:

$$D(q)\ddot{q} + C(q,\dot{q})\dot{q} + g(q) = \tau$$

We can rewrite the above equation in the following form:

$$\ddot{q} = f(q,\dot{q}) + B(q)u$$

where:

$$\begin{cases} f = -D^{-1}(q)[C(q,\dot{q}) + g(q)] \\ g = D^{-1}(q) \end{cases}$$

We assume that the information about the functions f and B is incomplete. Let us form the reference model for the output transients:

$$T_d^2\ddot{q} + 2\xi_d T_d\dot{q} + q = q_d \qquad (3.17)$$

Solving for the highest derivative we obtain:

$$\ddot{q} = \frac{1}{T_d^2}(-2\xi_d T_d\dot{q} - q + q_d) \qquad (3.18)$$

Let us denote:

$$F(q,\dot{q},q_d)=\frac{1}{T_d^2}(-2\xi_d T_d \dot{q}-q+q_d) \tag{3.19}$$

and

$$e^F = F(\dot{q},q,\dot{q}_d)-\ddot{q} \tag{3.20}$$

where

e^F is the realization error of the desired dynamics which is assigned by $F(\dot{q},q,q_d)$. Let us also assume that we have ideal differentiating filters and therefore we can consider the following structure:

$$u = Ke^F \Rightarrow u = k(F-\ddot{q}) \tag{3.21}$$

where k is the gain matrix, $k = k_0 k_1$, $k_0 \in R^1$ and k_1 is the "accordance matrix". The k_1 matrix can have the form $k_1 \approx D$. In order to calculate the control input u, it is necessary to calculate the instantaneous value of the inertia matrix D during the process dynamic changes.

The closed loop system is governed by:

$$\ddot{q} = f + Bu \Leftrightarrow f + Bk(F-\ddot{q}) = \ddot{q} \Leftrightarrow \ddot{q} = (1+Bk)^{-1} f + (1+Bk)^{-1} BkF \tag{3.22}$$

In this case it follows that, $\lim_{\substack{k\to\infty \\ t\to\infty}} \ddot{q} = F$, which ensures the desired transients are achieved.

In order to realise the control law it is necessary to obtain the derivatives of $q(t)$ and we can obtain them by means of a differentiating filter. It is possible to use a linear filter of the following form:

$$\mu^2 \hat{q}^{(2)} + 2\mu d \hat{q}^{(1)} + \hat{q} = q \tag{3.23}$$

where μ is a small parameter, $\mu, d > 0$, and $(\cdot)^i$ denotes i^{th} differentiation.

Using this differentiating filter, we can have the high derivative of the output namely:

$$\hat{q}^{(2)}(t) = \frac{1}{\mu^2}[q(t) - 2\mu d\,\hat{q}^{(1)}(t) - \hat{q}(t)] \tag{3.24}$$

3.3.1 Simulation results

We present the results of the localization control method for two rigid-links manipulator. In these simulations the following parameters are used: the masse of each link is $m = 1kg$ and the length of each link is $l = 1m$. For the simulation purposes the following parameters are used: for the desired high derivative: $\begin{cases} T_d = 1 \\ \xi = 1 \end{cases}$, and for the differentiating filter: $\begin{cases} \mu = 0.2 \\ d = 3 \end{cases}$.

The simulations are run using three different sets of initial conditions for the manipulator: the equilibrium point, near the equilibrium point, and away from the equilibrium point. Similarly, we can consider two different cases regarding the manipulator:

1. $g(q) = 0$ - in the absence of gravitational force
2. $g(q) = 0$ and $\begin{cases} \tau_{d1} = 10Nm \\ \tau_{d2} = 0 \end{cases}$ - in the absence of the gravitational force, and in the presence of the external torque disturbance τ_{d1} at joint 1.

The simulation results are shown in figures 4.33 - 4.36. The same simulations are conducted but in the presence of a disturbance $\begin{cases} \tau_{d1} = 10 \\ \tau_{d2} = 0 \end{cases}$. The results are shown in figures 4.37-4.40. These simulations are obtained using the following scenario: the initial

conditions are $\begin{cases} q_{i1} = -\pi/2 \\ q_{i2} = 0 \end{cases}$, and the desired final position is set to $\begin{cases} q_{d1} = -\pi \\ q_{d2} = \pi/2 \end{cases}$, and the gains used are $\begin{cases} k_1 = 100 \\ k_2 = 200 \end{cases}$.

The results of the simulations are presented in the Tables 3.11-3.13. The three sets of initial conditions are given as follows:

a) $\begin{cases} q_{i1} = -\pi/2 \\ q_{i2} = 0 \end{cases}$ $\begin{cases} q_{d1} = -\pi \\ q_{d2} = \pi/2 \end{cases}$ $\begin{cases} \tau_{d1} = 10 \\ \tau_{d2} = 0 \end{cases}$

Gain Parameters	Disturbances	t_s	er_1	er_2	$\lvert\tau_1\rvert_{max}$	$\lvert\tau_2\rvert_{max}$
$K_1 = 100$ $K_2 = 200$	$\tau_{d1} = 0$ $\tau_{d2} = 0$	3	-0.00004	0.0001	200	60
	$\tau_{d1} = 10$ $\tau_{d2} = 0$	3	-0.07	0.035	200	60
$K_1 = 200$ $K_2 = 400$	$\tau_{d1} = 0$ $\tau_{d2} = 0$	3	-0.00004	-0.00003	500	250
	$\tau_{d1} = 10$ $\tau_{d2} = 0$	3	-0.03	0.01	500	250
$K_1 = 400$ $K_2 = 800$	$\tau_{d1} = 0$ $\tau_{d2} = 0$	3	-0.00004	0.00006	1300	500
	$\tau_{d1} = 10$ $\tau_{d2} = 0$	3	-0.01	0.009	1300	500

Table 3-7 Summary of the results using the first set of initial conditions

b) $\begin{cases} q_{i1} = -\pi/2 + \pi/18 \\ q_{i2} = \pi/18 \end{cases}$ $\begin{cases} q_{d1} = -\pi \\ q_{d2} = \pi/2 \end{cases}$ $\begin{cases} \tau_{d1} = 10 \\ \tau_{d2} = 0 \end{cases}$

Gain Parameters	Disturbances	t_s	er_1	er_2	$\lvert\tau_1\rvert_{max}$	$\lvert\tau_2\rvert_{max}$
$K_1 = 100$ $K_2 = 200$	$\tau_{d1} = 0$ $\tau_{d2} = 0$	3	0.00005	0.0007	200	80
	$\tau_{d1} = 10$ $\tau_{d2} = 0$	3	-0.07	0.03	200	80
$K_1 = 200$ $K_2 = 400$	$\tau_{d1} = 0$ $\tau_{d2} = 0$	3	-0.00005	0.0002	500	200
	$\tau_{d1} = 10$ $\tau_{d2} = 0$	3	0.03	0.01	500	200
$K_1 = 400$ $K_2 = 800$	$\tau_{d1} = 0$ $\tau_{d2} = 0$	3	0.00005	0.0001	1200	500
	$\tau_{d1} = 10$ $\tau_{d2} = 0$	3	0.01	0.009	1200	500

Table 3-8 Summary of the results using the second set of initial conditions

c). $\begin{cases} q_{i1} = 0 \\ q_{i2} = 0 \end{cases}$ $\begin{cases} q_{d1} = -\pi \\ q_{d2} = \pi/2 \end{cases}$ $\begin{cases} \tau_{d1} = 10 \\ \tau_{d2} = 0 \end{cases}$

Gain Parameters	Disturbances	t_s	er_1	er_2	$\lvert\tau_1\rvert_{max}$	$\lvert\tau_2\rvert_{max}$
$K_1 = 100$ $K_2 = 200$	$\tau_{d1} = 0$ $\tau_{d2} = 0$	3	-0.00009	0.00001	350	100
	$\tau_{d1} = 10$ $\tau_{d2} = 0$	4	-0.07	0.03	350	100
$K_1 = 200$ $K_2 = 400$	$\tau_{d1} = 0$ $\tau_{d2} = 0$	3	-0.00009	-0.00009	900	250
	$\tau_{d1} = 10$ $\tau_{d2} = 0$	4	-0.03	0.01	900	250
$K_1 = 400$ $K_2 = 800$	$\tau_{d1} = 0$ $\tau_{d2} = 0$	3	-0.00008	0.00005	2000	800
	$\tau_{d1} = 10$ $\tau_{d2} = 0$	4	-0.01	0.009	2000	800
$K_1 = 1000$ $K_2 = 1000$	$\tau_{d1} = 0$ $\tau_{d2} = 0$	3	-0.0001	0.0001	5000	2000
	$\tau_{d1} = 10$ $\tau_{d2} = 0$	3	-0.007	0.007	5000	2000

Table 3-9 Summary of the results using the third set of initial conditions

3.3.2 **Conclusions**

First, we used as initial condition for the manipulator the equilibrium point, that is $\begin{cases} q_{i1} = -\pi/2 \\ q_{i2} = 0 \end{cases}$. Using different values for the gains used, we can see that the error is in the same neighbourhood for the first link (- 0.00004), while the error for the second link is decreasing (from 0.0001 to 0.00006). If we increase the gains we require higher torque, but the error remains still in the same range. In the case that there is a disturbance we can see that both errors are decreasing with increasing of the gains. For all the gain values the settling time is around 3 seconds.

Secondly, we change the initial conditions of the manipulator.The new set of initial conditions is given by a point near the equilibrium point such as: $\begin{cases} q_{i1} = -\pi/2 + \pi/18 \\ q_{i2} = \pi/18 \end{cases}$. In this case, we achieve the same results as reported above.

Thirdly, we change the initial conditions of the manipulator with a point away from the equilibrium point such as $\begin{cases} q_{i1} = 0 \\ q_{i2} = 0 \end{cases}$. In this case, the errors for both of the links are decreasing with the increasing of the gains used. In the case of disturbance, if we use a higher gain, we can achieve an acceptable error for both links (that is error = 0.007). As we have seen above, increasing the gains implies an increase in the torques used. The settling time is around 3 seconds or 4 seconds in the case of disturbance. Using higher gains, we can achieve the same settling time (3 seconds) even though there is a disturbance.

In order to use this method, we need to measure the acceleration for each joint $\ddot{q}$. Since generally this is difficult to measure, we should use a differentiating filter and estimate the position, velocity and acceleration for each joint. The most important advantage of this control method is that the desired transients are achieved under the conditions of incomplete information about disturbances.

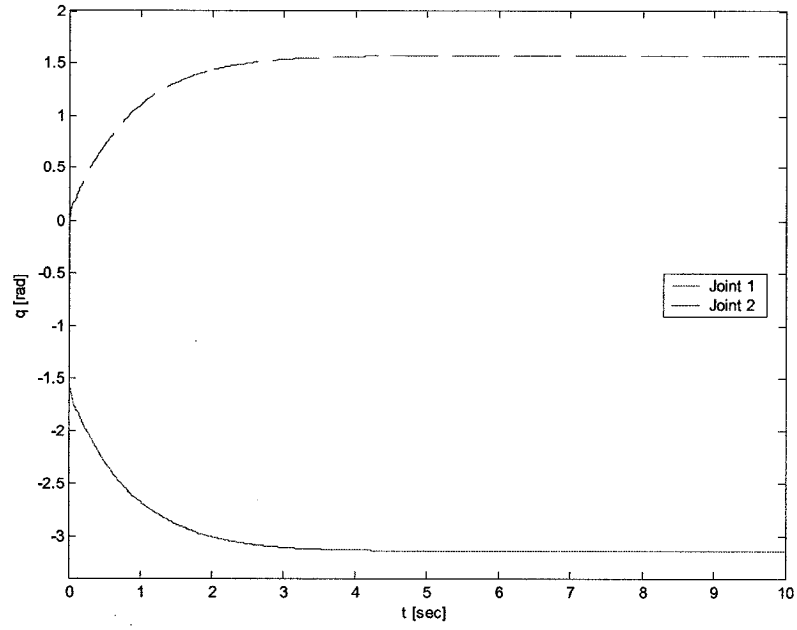

Figure 3-33 Localization method - joint angles

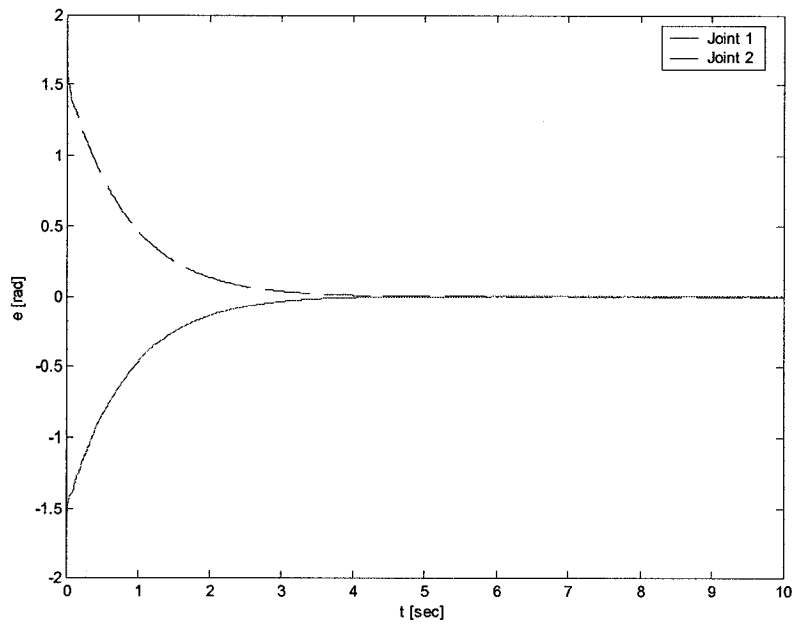

Figure 3-34 Localization method - joint angles error

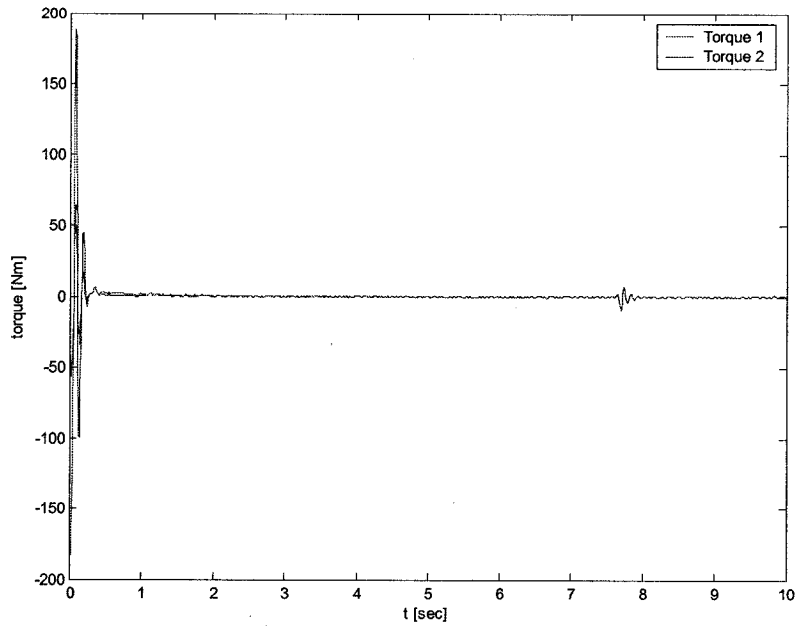

Figure 3-35 Localization method - torques commands

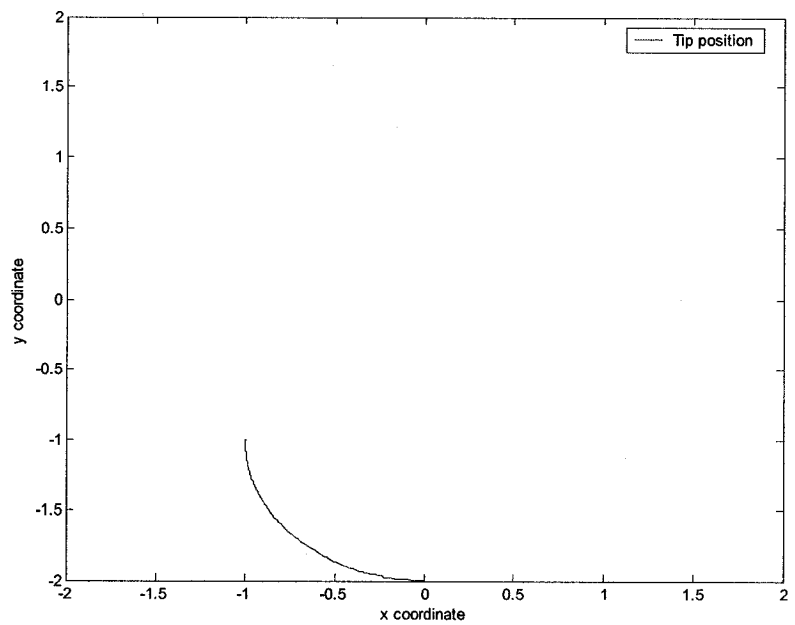

Figure 3-36 Localization method - tip position

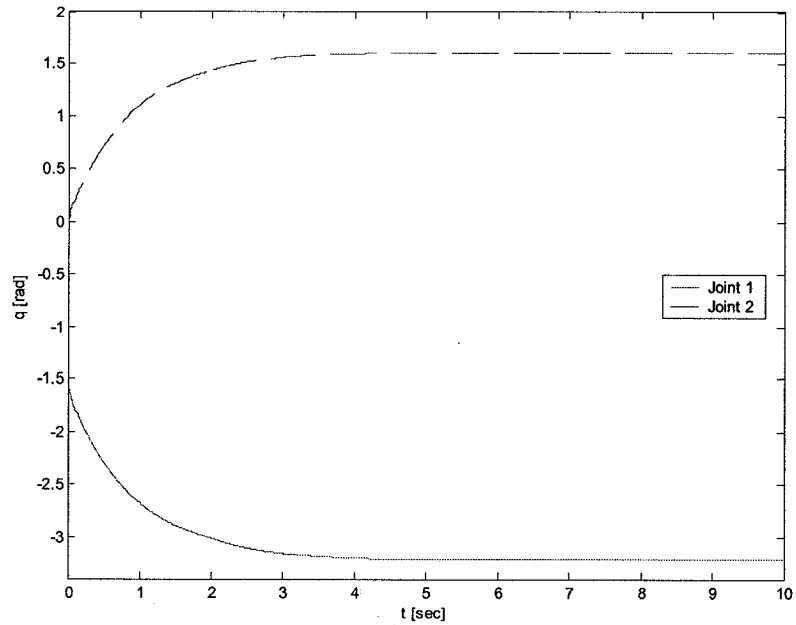

Figure 3-37 Localization method - joint angles

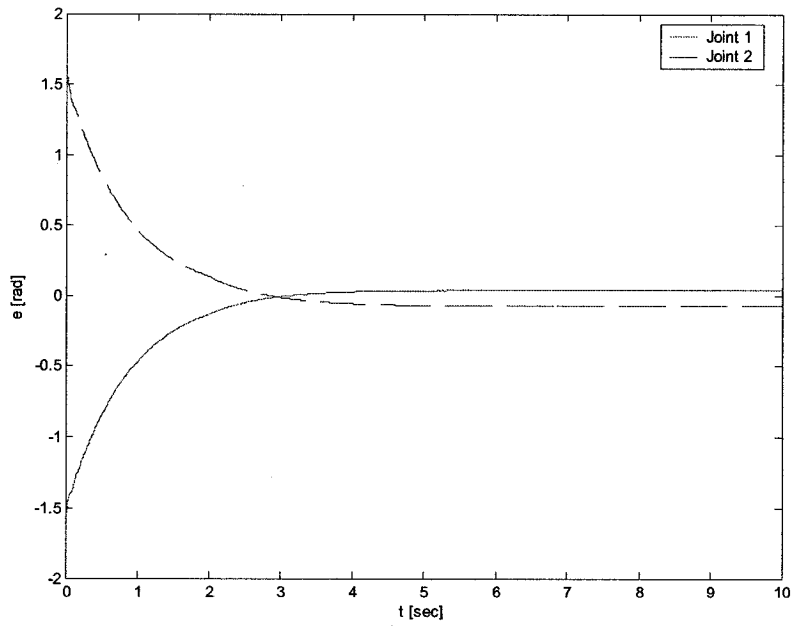

Figure 3-38 Localization method - joint angles error

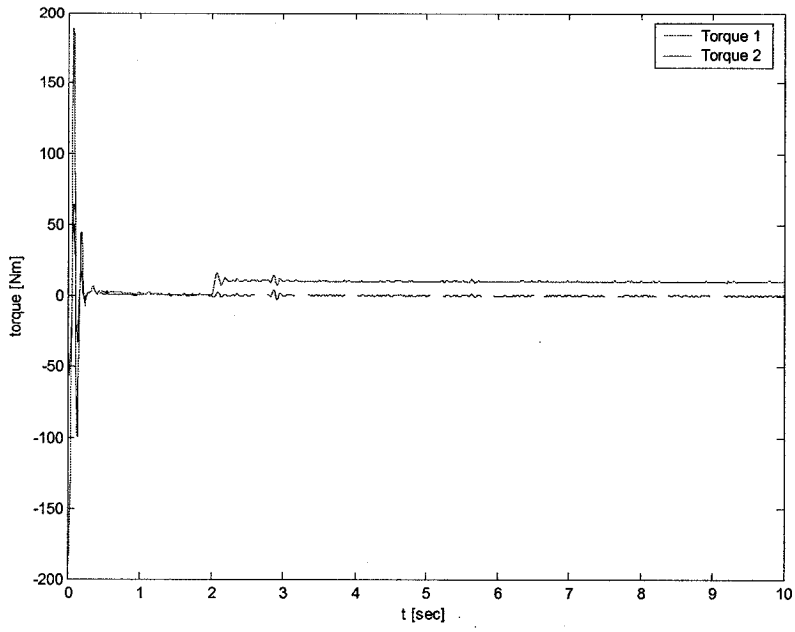

Figure 3-39 Localization method - torques commands

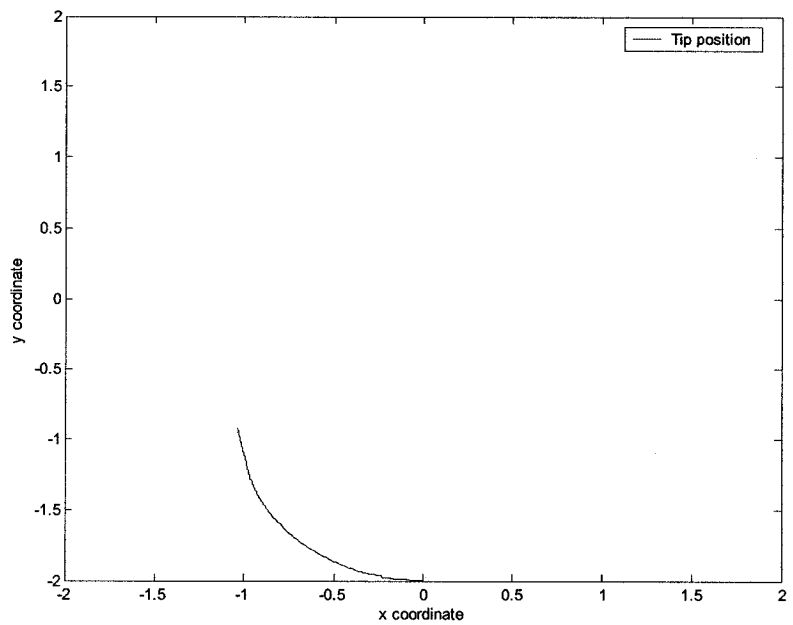

Figure 3-40 Localization method - tip position

3.4 Dynamic control method

In this section a novel dynamic control method for rigid-link manipulators is presented. This method allows us to obtain the desired transients under the incomplete information about the system. In order to decrease the influence of disturbances and model parameters uncertainty on dynamic properties of output trajectories, a high feedback gain is used. At the same time, a higher-order output derivative in the feedback loop is used. This method is a generalization and further development of results reported in [49], [50],[51].

3.4.1 Model of the rigid -link manipulator

Let us consider a planar, two-link, articulated manipulator. The dynamics of this two-rigid link manipulator can be written in the form [48]:

$$D(q)\ddot{q} + C(q,\dot{q})\dot{q} + g(q) = \tau \tag{3.25}$$

System (3.25) can be written in the state-space form:

$$\ddot{q} = f(q,\dot{q}) + B(q)u \tag{3.26}$$

where

$$f = -D^{-1}(q)[C(q,\dot{q}) + g(q)],\ B = D^{-1}(q)$$

Let us now denote:

$$e(t) = r(t) - y(t) \tag{3.27}$$

as the tracking error where $y(t)$ is the manipulator end-effector output and $r(t)$ is the reference input signal. The control system is being designed to provide the following:

$$\lim_{t\to\infty} e(t) = 0 \tag{3.28}$$

The output transient for $y(t)$ should have a desired behaviour which does not depend either on the external disturbances or on the possibly varying parameters of the rigid-link manipulator model.

3.4.2 Control problem reformulation

Let us form a reference model for the output transient of $y(t)$ according to the following vector differential equation:

$$\ddot{y} = F(\dot{y}, y, \dot{r}, r) \tag{3.29}$$

For example, (3.29) may have the form of a linear vector equation

$$\ddot{y} = -A_1^d \dot{y} - A_0^d y + B_1^d \dot{r} + B_0^d r \tag{3.30}$$

By selecting A_1^d, A_0^d and B_0^d as diagonal matrices, then we require the decoupling of the control channels.

Let us now denote

$$e^F = F(\dot{y}, y, \dot{r}, r) - \ddot{y} \tag{3.31}$$

where e^F is the realization error characteristics of the desired dynamics which is assigned by $F(\dot{y}, y, \dot{r}, r)$.

Accordingly, if the condition

$$e^F = 0 \tag{3.32}$$

is satisfied, then the desired behaviour of $y(t)$ with prescribed dynamics of (3.29) is achieved.

The expression (3.32) corresponds to the insensitivity condition of the output transient performance with respect to the external disturbances and varying parameters of the

flexible-link manipulator model. In other words, the control design problem (3.27) may be reformulated as the requirement (3.32).

To satisfy the (3.32) requirement let us construct the control law according to the following differential equation:

$$\mu^2 \ddot{\bar{v}} + \mu D_1 \dot{\bar{v}} + D_0 v = K_1 e^F, \ \bar{v}(0) = \bar{v}_0 \tag{3.33}$$

where

$$u = K_0 v \tag{3.34}$$

and $\bar{v} = \begin{bmatrix} \dot{v} & v \end{bmatrix}^T$

Assume that D_o, D_1, K_1 are diagonal matrices, μ is a sufficiently small positive parameter, and $K_1 = diag\{k_1,...,k_n\}$.

Consequently, when taken together, equations (3.31) and (3.33), the dynamic control law (3.33) may be re-written in the form:

$$\mu^2 \ddot{\bar{v}} + \mu D_1 \dot{\bar{v}} + D_0 v = K_1 \{-\ddot{y} - A_1^d \dot{y} - A_0^d y + B_1^d \dot{r} + B_0^d r\} \tag{3.35}$$

The analysis for the properties of the slow and fast motion dynamics properties will be provided later on for the case of flexible-link manipulators.

3.4.3 **Simulation results**

We present the results of the dynamic control method for two rigid links manipulator. In these simulations the following parameters are used: the masse of each link is $m = 1kg$ and the length of each link is $l = 1m$. Let us take the reference model according to the following differential equation:

$$T_d^2 \ddot{x} + 2\xi_d T_d \dot{x} + x = b_1 \dot{r} + b_0 r$$

For simulation purposes we can choose the following parameters

$$\begin{cases} b_1 = 2 \\ b_0 = 1 \end{cases} \text{ and } \begin{cases} T_d = 1 \\ \xi_d = 1 \end{cases}.$$

The simulations are conducted using three different sets of initial conditions for the manipulator: the equilibrium point, near the equilibrium point, and away from the equilibrium point. Similarly, we can consider two different cases regarding the manipulator:

1. $g(q) = 0$ - in the absence of gravitational force
2. $g(q) = 0$ and $\begin{cases} \tau_{d1} = 10Nm \\ \tau_{d2} = 0 \end{cases}$ - in the absence of the gravitational force, and in the presence of the external torque disturbance τ_{d1} at joint 1.

The simulations results are shown in figures 3.41 - 3.44. The same simulations are conducted again but in the presence of a disturbance $\begin{cases} \tau_{d1} = 10 \\ \tau_{d2} = 0 \end{cases}$. The results are shown in figures 3.45-3.48. These simulations are obtained using the following scenario: the initial conditions are $\begin{cases} q_{i1} = -\pi/2 \\ q_{i2} = 0 \end{cases}$, and the desired final position is set to $\begin{cases} q_{d1} = -\pi \\ q_{d2} = \pi/2 \end{cases}$, and the gains used are $K_1 = \begin{bmatrix} 40 & 0 \\ 0 & 40 \end{bmatrix}$.

For the tracking case, the results are shown in figures 3.49-3.52, and in figures 3.53-3.56 in the presence of a disturbance $\begin{cases}\tau_{d1}=10\\ \tau_{d2}=0\end{cases}$. For the tracking case, the trajectories to be followed are given by $y_{d1}=A\sin(\omega t)$ and $y_{d2}=A\sin(\omega t)$ where $A=1$ and $\omega=1$.

The simulation results are presented in Tables 3.14-3.16 for the following three sets of initial conditions.

I. $\begin{cases}q_{i1}=-pi/2\\ q_{i2}=0\end{cases}$ $\begin{cases}q_{d1}=-pi\\ q_{d2}=pi/2\end{cases}$ $\begin{cases}\tau_{d1}=10\\ \tau_{d2}=0\end{cases}$

Gain parameters	Disturbances	t_s	er_1	er_2	$\lvert\tau_1\rvert_{max}$	$\lvert\tau_2\rvert_{max}$
$K_1=\begin{bmatrix}40 & 0\\ 0 & 40\end{bmatrix}$	$\tau_{d1}=0$ $\tau_{d2}=0$	5	0.0008	0.0008	3.5	1
	$\tau_{d1}=10$ $\tau_{d2}=0$	5	0.0005	0.0021	15	1
$K_1=\begin{bmatrix}80 & 0\\ 0 & 80\end{bmatrix}$	$\tau_{d1}=0$ $\tau_{d2}=0$	5	0.0007	0.0007	5	1
	$\tau_{d1}=10$ $\tau_{d2}=0$	5	0.0007	0.0011	17	2
$K_1=\begin{bmatrix}200 & 0\\ 0 & 200\end{bmatrix}$	$\tau_{d1}=0$ $\tau_{d2}=0$	5	0.0008	0.0007	6	2
	$\tau_{d1}=10$ $\tau_{d2}=0$	5	0.0007	0.0011	17	2

Table 3-10 Summary of the results using the first set of initial conditions

II. Initial conditions are:

$$\begin{cases} q_{i1} = -pi/2 + pi/18 \\ q_{i2} = pi/18 \end{cases} \qquad \begin{cases} q_{d1} = -pi \\ q_{d2} = pi/2 \end{cases} \qquad \begin{cases} \tau_{d1} = 10 \\ \tau_{d2} = 0 \end{cases}$$

Gain parameters	Disturbances	t_s	er_1	er_2	$\lvert\tau_1\rvert_{max}$	$\lvert\tau_2\rvert_{max}$
$K_1 = \begin{bmatrix} 40 & 0 \\ 0 & 40 \end{bmatrix}$	$\tau_{d1} = 0$ $\tau_{d2} = 0$	5	0.0008	0.0008	600	200
	$\tau_{d1} = 10$ $\tau_{d2} = 0$	5	0.0005	0.0019	600	200
$K_1 = \begin{bmatrix} 80 & 0 \\ 0 & 80 \end{bmatrix}$	$\tau_{d1} = 0$ $\tau_{d2} = 0$	5	0.0007	0.0007	2000	1000
	$\tau_{d1} = 10$ $\tau_{d2} = 0$	5	0.0007	0.0011	2000	1000
$K_1 = \begin{bmatrix} 200 & 0 \\ 0 & 200 \end{bmatrix}$	$\tau_{d1} = 0$ $\tau_{d2} = 0$	5	0.0003	0.0002	2000	900
	$\tau_{d1} = 10$ $\tau_{d2} = 0$	5	0.0007	0.0011	2000	900

Table 3-11 Summary of the results using the second set of initial conditions

III. $\begin{cases} q_{i1} = 0 \\ q_{i2} = 0 \end{cases}$ $\begin{cases} q_{d1} = -pi \\ q_{d2} = pi/2 \end{cases}$ $\begin{cases} \tau_{d1} = 10 \\ \tau_{d2} = 0 \end{cases}$

Gain parameters	Disturbances	t_s	er_1	er_2	$\lvert\tau_1\rvert_{max}$	$\lvert\tau_2\rvert_{max}$
$K_1 = \begin{bmatrix} 40 & 0 \\ 0 & 40 \end{bmatrix}$	$\tau_{d1} = 0$ $\tau_{d2} = 0$	5	0.0017	0.0006	9	2
	$\tau_{d1} = 10$ $\tau_{d2} = 0$	5	0.0014	0.0019	15	3
$K_1 = \begin{bmatrix} 80 & 0 \\ 0 & 80 \end{bmatrix}$	$\tau_{d1} = 0$ $\tau_{d2} = 0$	5	0.0017	0.0006	10	3
	$\tau_{d1} = 10$ $\tau_{d2} = 0$	5	0.0014	0.0019	15	3
$K_1 = \begin{bmatrix} 200 & 0 \\ 0 & 200 \end{bmatrix}$	$\tau_{d1} = 0$ $\tau_{d2} = 0$	5	0.0016	0.0007	11	3
	$\tau_{d1} = 10$ $\tau_{d2} = 0$	5	0.0015	0.0010	17	3

Table 3-12 Summary of the results using the third set of initial conditions

3.4.4 Conclusions

First, we use as initial condition for the manipulator the equilibrium point, that is $\begin{cases} q_{i1} = -\pi/2 \\ q_{i2} = 0 \end{cases}$. Using different gain values we can see that the error values are in the same range for both links (that is - 0.0008). In the case of a disturbance, the error still remains around 0.0007, but for the second link the error increases to 0.002. Increasing the gains, we can achieve a smaller error for the second link by as much as 0.001.

Second, we change the initial conditions to a point near the equilibrium point as $\begin{cases} q_{i1} = -\pi/2 + \pi/18 \\ q_{i2} = \pi/18 \end{cases}$. In this case, the same results as reported above are also obtained.

Third, we change the initial conditions of the manipulator to a point away from the equilibrium point as $\begin{cases} q_{i1} = 0 \\ q_{i2} = 0 \end{cases}$. In this case, the error for the first link is higher that the one achieved in the previous two cases that is 0.0017. The error for the second link is around 0.0006.

As for the previous two cases, in the presence of a disturbance the error for the second link increases to 0.0019. In order to reduce it, we can increase the gains. For $K_1 = \begin{bmatrix} 200 & 0 \\ 0 & 200 \end{bmatrix}$, we can achieve an error of 0.0015 and 0.001, for the two links respectively.

In the case of tracking the errors increase, but the system can still track the desired sinusoidal trajectory satisfactorily.

3.5 Conclusions

In this chapter, the control of rigid-link manipulators is discussed. Using the mathematical model of a two rigid-link manipulator [48], four different control methods are investigated namely PD control, computed torque method, localization method, and a novel dynamic control method. For each case, different sets of initial conditions are used for simulations. For comparative purposes, different control gains are used for each controlling method. It was shown that in general acceptable performances are achieved

using the proposed techniques. The potential and utility of these techniques for flexible-link manipulators are shown in the next Chapters.

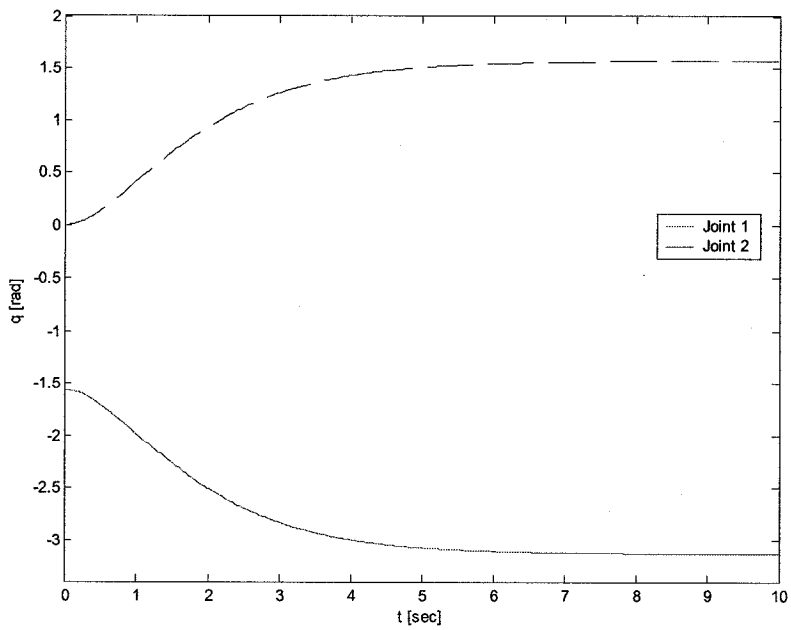

Figure 3-41 Dynamic control scheme - joint angles

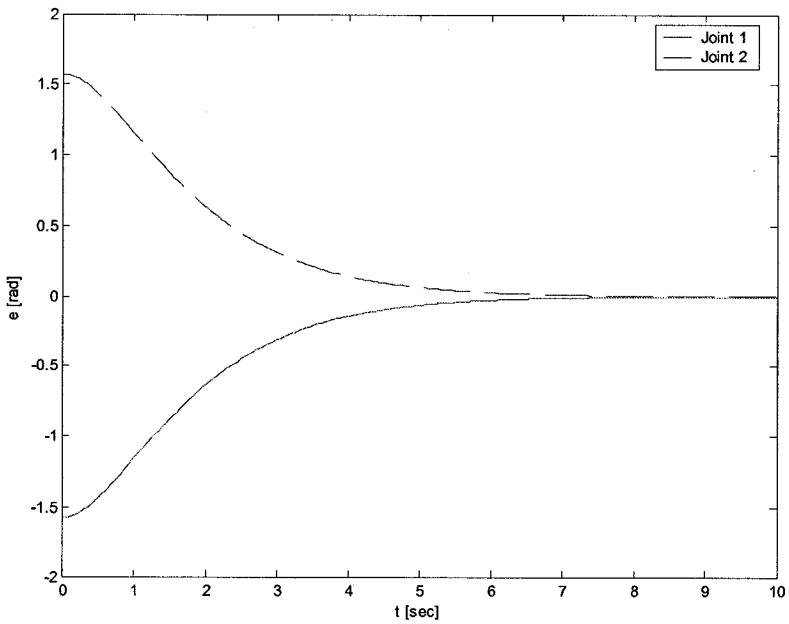

Figure 3-42 Dynamic control scheme - joint angles error

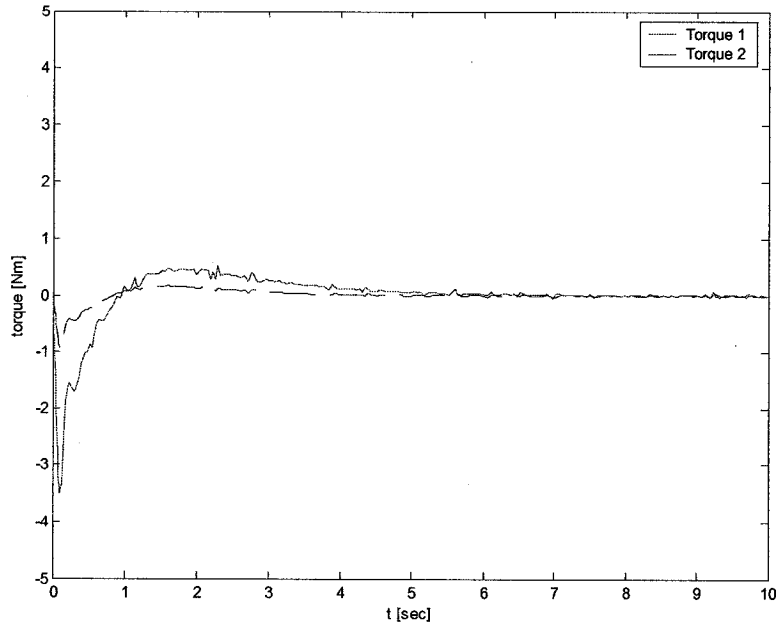

Figure 3-43 Dynamic control scheme - torques command

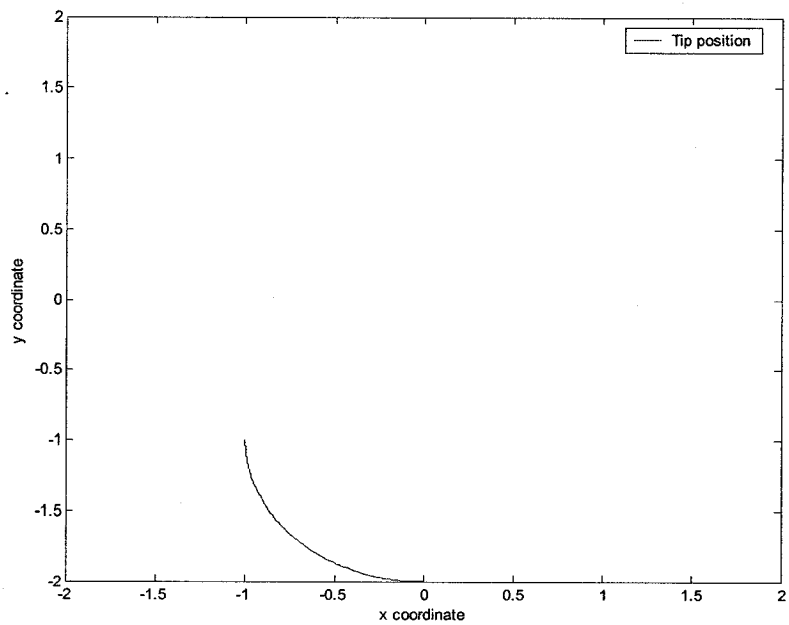

Figure 3-44 Dynamic control scheme - tip position

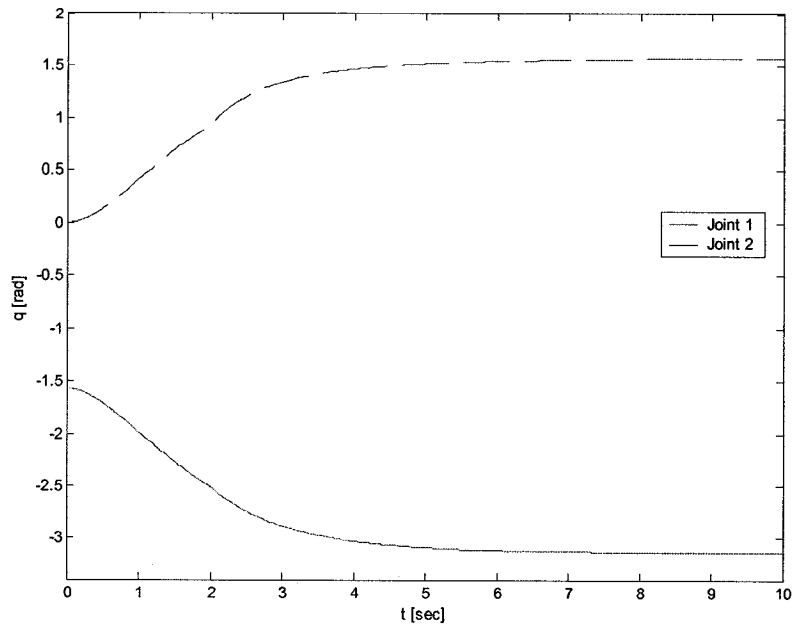

Figure 3-45 Dynamic control scheme - joint angles

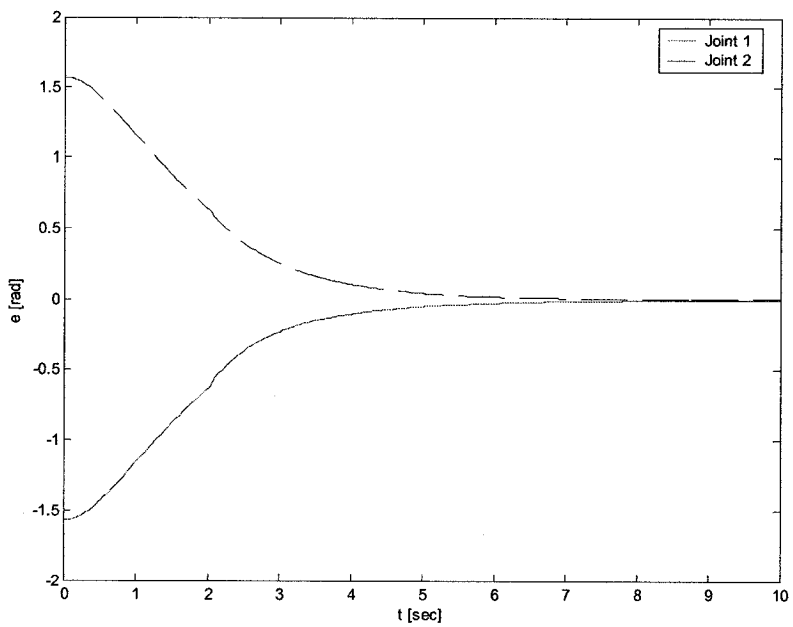

Figure 3-46 Dynamic control scheme - joint angles error

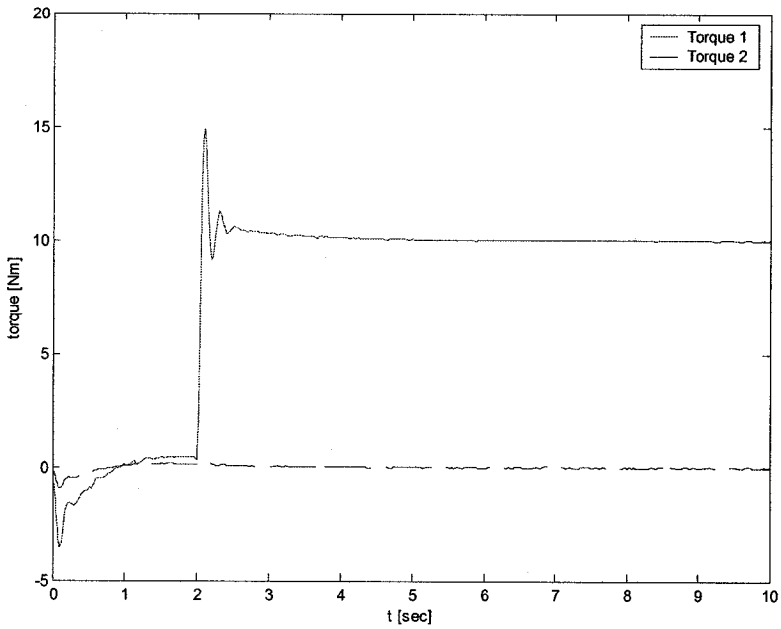

Figure 3-47 Dynamic control scheme - torques command

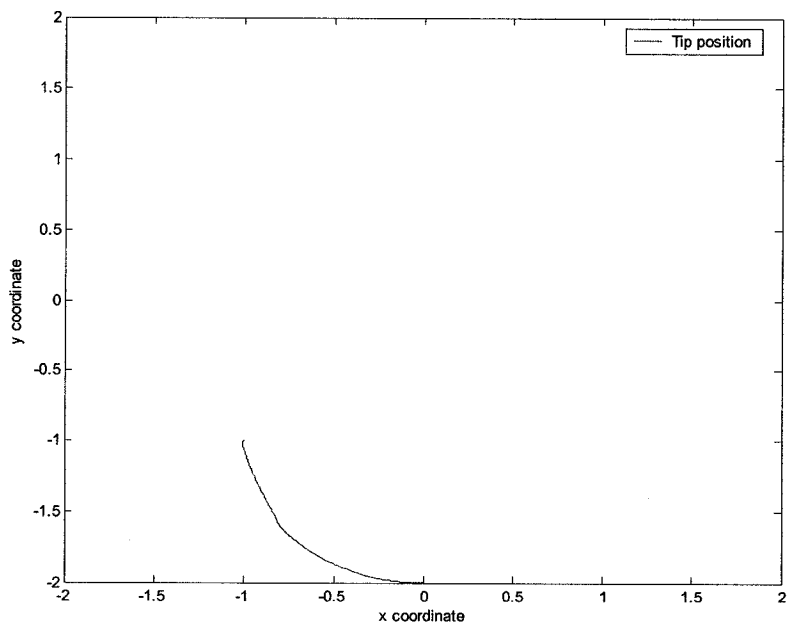

Figure 3-48 Dynamic control scheme - tip position

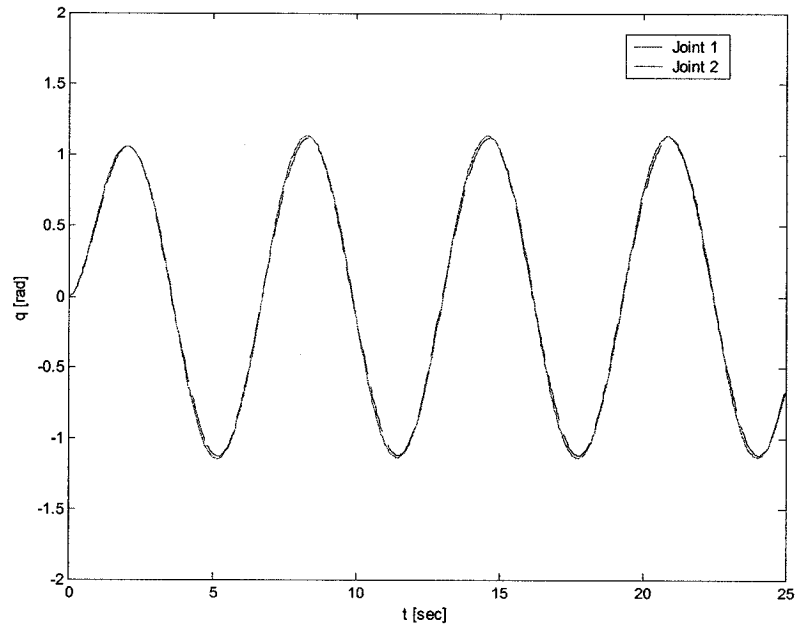

Figure 3-49 Dynamic control scheme – tracking case - joint angles

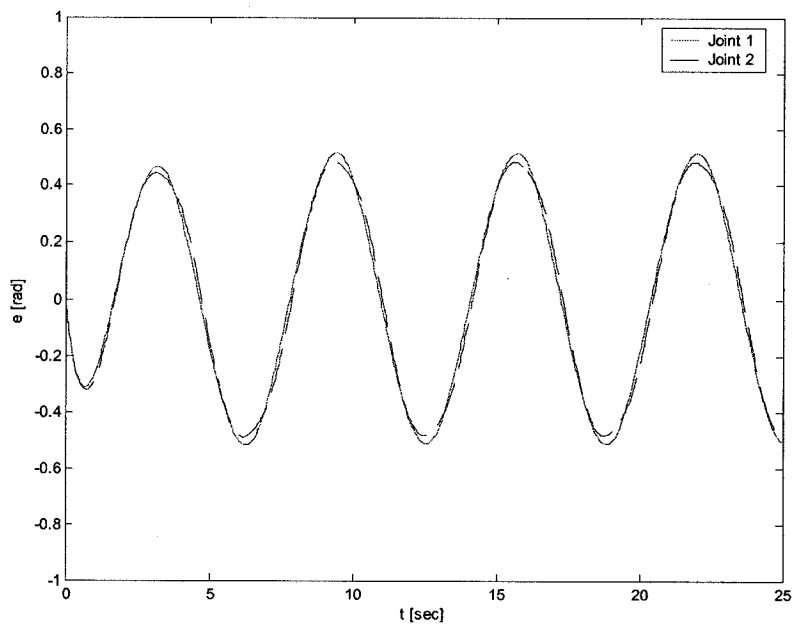

Figure 3-50 Dynamic control scheme – tracking case - joint angles error

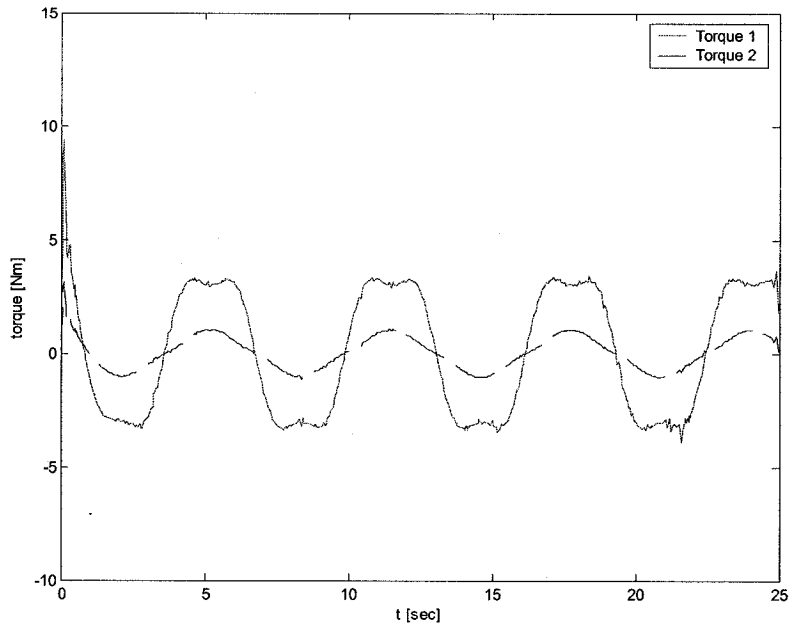

Figure 3-51 Dynamic control scheme – tracking case - torques command

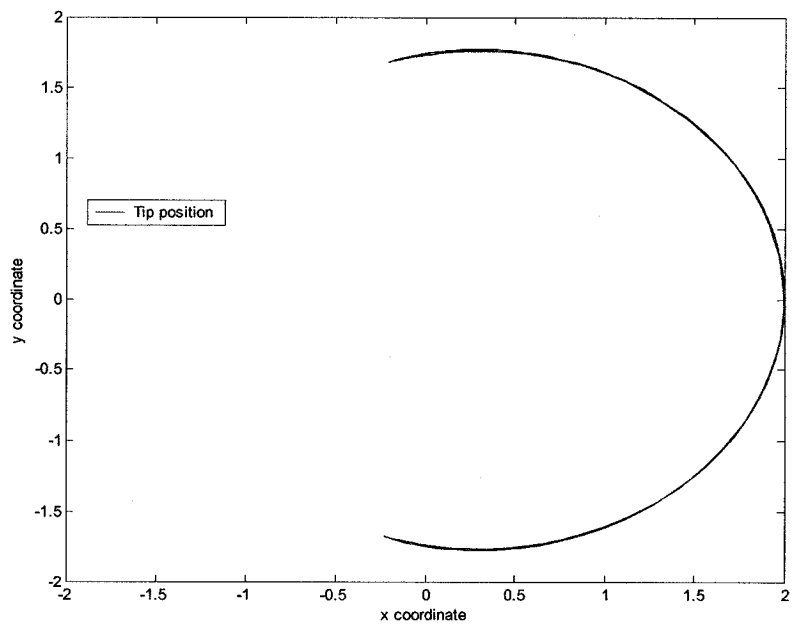

Figure 3-52 Dynamic control scheme – tracking case - tip position

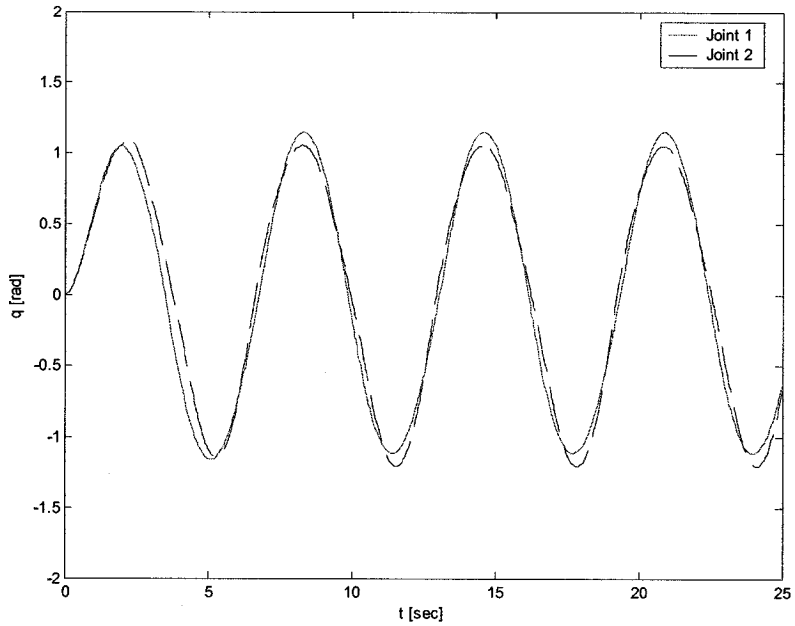

Figure 3-53 Dynamic control scheme – tracking case - joint angles

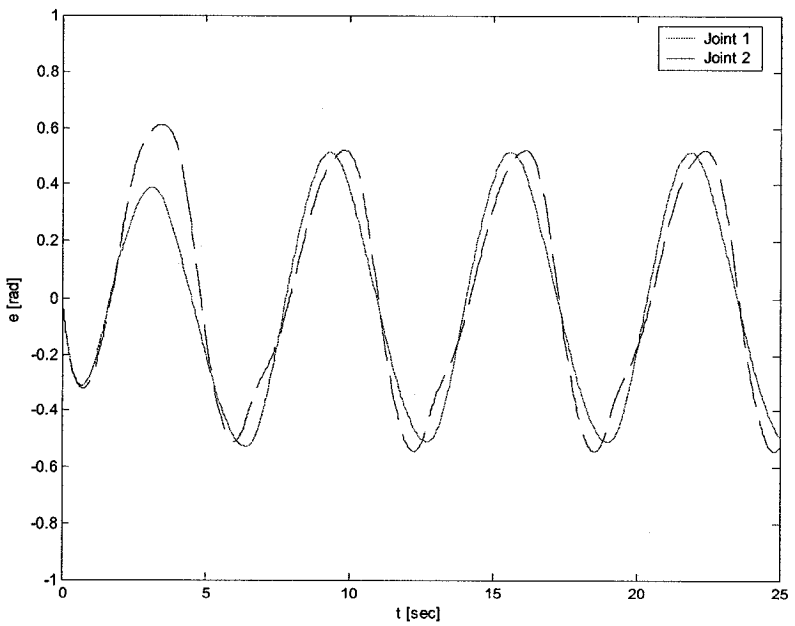

Figure 3-54 Dynamic control scheme – tracking case - joint angles error

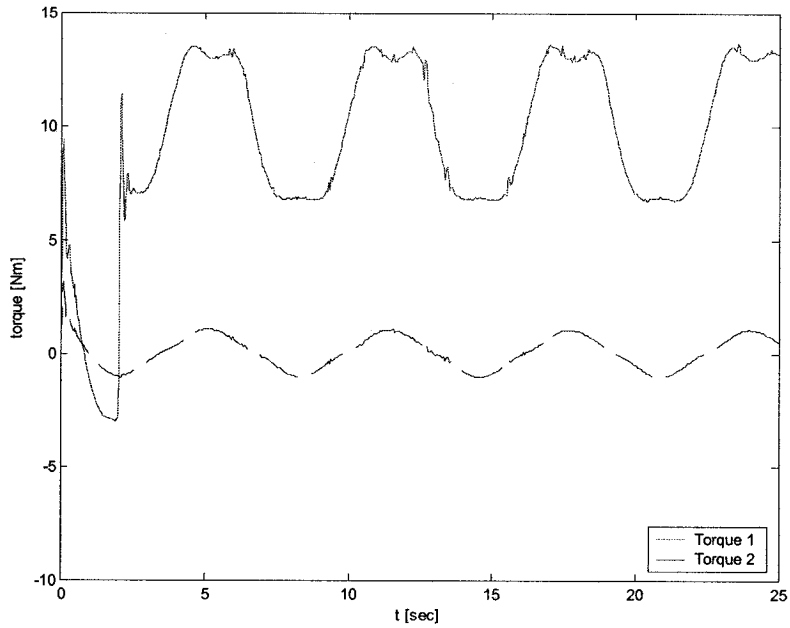

Figure 3-55 Dynamic control scheme – tracking case - torques command

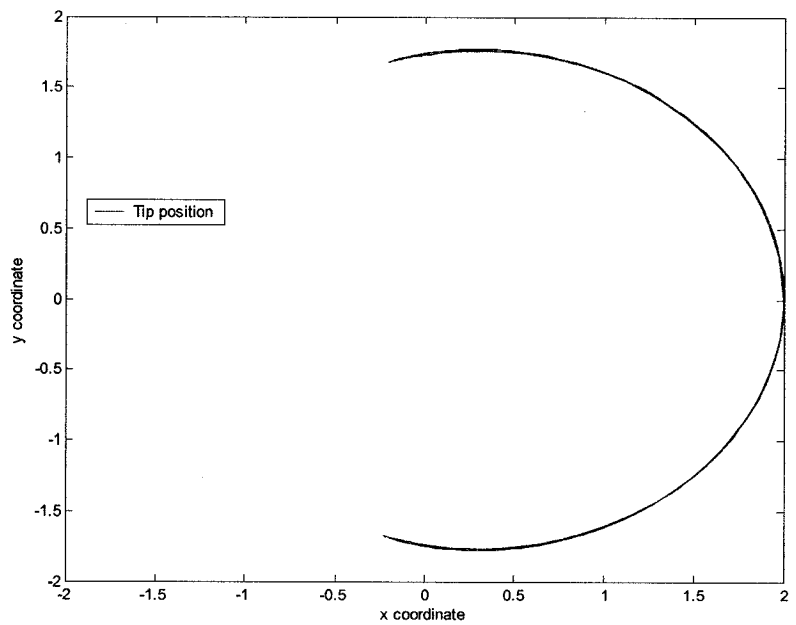

Figure 3-56 Dynamic control scheme – tracking case - tip position

Chapter 4 Control of Flexible-Link Manipulators

This chapter is dedicated to the control of a single flexible-link manipulator and a two-link manipulators for which the first link is rigid and the second link is flexible. One of the most important issues in controlling of the flexible link is that there are fewer number of inputs than the degrees of freedom. This yields to the difficulties in having different desired trajectories for each generalized coordinate.

In the previous chapter the dynamical model of one flexible-link was discussed. In this chapter issues such as output redefinition, input-output linearization, and non-minimum phase problems will be discussed. Furthermore, control techniques such as computed torque, and a novel dynamical control method will be presented.

4.1 Output redefinition

The objective of the control can be divided into two different categories: regulation and tracking. Regulation problem or the point-to-point control is when the desired trajectory of the end-effector is chosen to be constant by specifying the final point. Tracking problem consists of following a time-varying joint reference trajectory. A very important issue in the case of control of flexible-link manipulators is the stability. The problem of tip-trajectory tracking has been investigated by many researchers. As it was shown in [21] if the tip-position is the controlled output, and the joint-torque is chose as the input, the system is then non-minimum phase.

4.1.1 **Input-output feedback linearization**

Let consider the following system:

$$\begin{cases} \dot{x} = f(x,u) \\ y = h(x) \end{cases} \tag{4.1}$$

The control problem consists of designing u such that a desired trajectory $y_d(t)$ is tracked by the output $y(t)$, while the states remain bounded. Furthermore, $y(t)$ and its derivatives are assumed to be known. In this case, the output $y(t)$ is related to the inputs through the state variable x of the nonlinear state equations. This framework is difficult to design a controller to ensure the output tracks a desired signal. An easier way to design the control is to find a direct relationship between the output to be controlled and the inputs applied to the system.

By means of input-output linearization, an n^{th} order system could be divided into two parts: the external dynamics (input-output map), and the internal dynamics (the unobservable subsystem). The external dynamics is observed from the output and its derivatives with a relative degree of "r"; the internal dynamics could not be seen from the input-output relationship, and it has the order"$n-r$". In order to achieve the control objective, the internal dynamics should be stable, which means that the states remain bounded during tracking.

4.1.2 **The zero dynamics**

The stability of the internal dynamics for linear systems is based on the locations of the zeros. In the case of nonlinear systems, one approach to check the stability is using the zero-dynamics [52]:

Definition: The zero-dynamics is defined to be the internal dynamics of the system when the system output is kept at zero by the input.

It can be shown that local asymptotic stability of the zero-dynamics is enough to provide the local asymptotic stability of the internal dynamics. If the zero-dynamics is asymptotically stable then the original system is a minimum-phase, otherwise, the system is called non-minimum phase. The flexible link manipulator has a non-minimum phase characteristic due to the actuator-sensor non-collocated configuration. In the open-loop case, the transfer function from the joint-torque to the tip-position has zeros in the right half s-plane, and therefore, the closed-loop system using non-collocated control is conditionally stable.

4.1.3 **The output redefinition**

In order to achieve a minimum-phase characteristic, the concept of output redefinition is used in this thesis. The objective is to define a new output which provides a stable zero-dynamics. A new output can be defined using [53]:

$$y_{redefined\_i} = q_i + \alpha_i \frac{W(l_i,t)}{l_i} \tag{4.2}$$

where $-1 < \alpha_i < 1$.

In the equation (4.2), by setting $\alpha = -1$, the output becomes the reflected tip position, for $\alpha = 0$ the output becomes the joint angle, and for $\alpha = 1$ the output becomes the tip angular position.

Following [53], there exists a value $\alpha = \alpha_i^* < 1$, such that the zero-dynamics is stable if $\alpha < \alpha_i^*$, and the zero-dynamics becomes unstable for $\alpha > \alpha_i^*$. In this case, the controlled output will be a point close to the actual tip position.

In the following section, let us consider the dynamics of a multi-link flexible manipulator with a structural damping added and is given by:

$$M\begin{bmatrix} \ddot{q} \\ \ddot{\delta} \end{bmatrix} + \begin{bmatrix} f_1(q,\dot{q}) + g_1(q,\dot{q},\delta,\dot{\delta}) + E_1\dot{q} \\ f_2(q,\dot{q}) + g_2(q,\dot{q},\delta,\dot{\delta}) + E_2\dot{\delta} + K\delta \end{bmatrix} = \begin{bmatrix} \tau \\ 0 \end{bmatrix} \tag{4.3}$$

where

q is the $nx1$ vector of joint variables, δ is the $mx1$ vector of deflection variables, f_1, g_1, f_2, g_2 are the terms due to gravity, Coriolis, and centripetal forces, M is the positive definite mass matrix, u the $nx1$ vector of input torques.

Let us define

$$H = M^{-1}(q,\delta) = \begin{bmatrix} H_{11} & H_{12} \\ H_{21} & H_{22} \end{bmatrix} \tag{4.4}$$

Then, the above equation may be expressed in the state-space form:

$$\dot{x} = f(x) + g(x)u \tag{4.5}$$

where

$$x^T = \begin{bmatrix} q^T & \delta^T & \dot{q}^T & \dot{\delta}^T \end{bmatrix}$$

$$f(x)=\begin{bmatrix} \dot{q} \\ \dot{\delta} \\ -H_{11}(f_1+g_1+E_1\dot{q})-H_{12}(f_2+g_2+K\delta+E_2\dot{\delta}) \\ -H_{21}(f_1+g_1+E_1\dot{q})-H_{22}(f_2+g_2+K\delta+E_2\dot{\delta}) \end{bmatrix}$$

$$g(x)=\begin{bmatrix} O_{(m+n)xn} \\ H_{11}(q,\delta) \\ H_{21}(q,\delta) \end{bmatrix}$$

Assuming the beam deflection is small with respect to the length of the link, we can write:

$$y_i = q_i + \alpha_i d_{ie} / l_i, i = 1,2,...,n \tag{4.6}$$

The tip deflection can be written as:

$$d_{ie} = \sum_{j=1}^{n_i} \Phi_{ij}(l_i)\delta_{ij} \tag{4.7}$$

where Φ_{ij} id the j-th mode shape function of the i-th link and δ_{ij} is the j-th mode of the i-th link. The output vector can be expressed as:

$$y = q + \psi_{nxm}\delta \tag{4.8}$$

where

$$\psi_{nxm}=\begin{bmatrix} v_1^T & 0^T & ... \\ 0^T & ... & 0^T \\ ... & ... & ... \\ 0^T & 0^T & v_n^T \end{bmatrix}$$

$$v_i^T = \frac{\alpha_i}{l_i}\begin{bmatrix}\Phi_{i1}(l_i) & ... & \Phi_{in_i}(l_i)\end{bmatrix},\ i=1,...,n$$

$$y^T = \begin{bmatrix} y_1 & ... & y_n \end{bmatrix}$$

$\delta^T = \lfloor \Delta_{n1}^T \quad \Delta_{n2}^T \quad \ldots \quad \Delta_{nn}^T \rfloor$, where Δ_{ni} is the vector of the deflection variables of link i, defined as $\Delta_{ni}^T = \lfloor \delta_1 \quad \ldots \quad \delta_{in_i} \rfloor$.

Let us consider equation (4.5) and the new redefined output given by (4.8). In order to achieve input-output linearization, it is necessary to derive the output till the inputs appear. The state-space form can be rewritten as following:

$$\ddot{y} = a(\alpha, x) + B(\alpha, q, \delta)u \tag{4.9}$$

where

$\alpha^T = \lfloor \alpha_1 \quad \ldots \quad \alpha_n \rfloor, B(\alpha, q, \delta) = H_{11} + \psi_{nxm} H_{21}$,

$a(\alpha, x) = -(H_{11} + \psi H_{21})(f_1 + g_1 + E_1 \dot{q}) - (H_{11} + \psi H_{22})(f_2 + g_2 + K\delta + E_2 \dot{\delta})$.

By selecting specific values for α, the matrix $B(\alpha, q_d, 0)$ can be made non-singular. Let us express the input torque as:

$$u = B^{-1}(\alpha, q, \delta)(v - a(\alpha, x)) \tag{4.10}$$

This implies:

$$\ddot{y} = v \tag{4.11}$$

which describes the input-output linearized system with a new input vector v. Now, we can consider the state transformation:

$$z = T(x) = D_T x \tag{4.12}$$

where

$z := \lfloor z_o^T \quad z_u^T \rfloor, \; z_o^T = \lfloor z_{o1}^T \quad z_{o2}^T \rfloor, \; z_u^T = \lfloor z_{u1}^T \quad z_{u2}^T \rfloor$.

$$D_T = \begin{bmatrix} I_{nxn} & \psi_{nxm} & 0_{nxn} & 0_{nxm} \\ 0_{nxn} & 0_{nxm} & I_{nxn} & \psi_{nxm} \\ 0_{mxn} & I_{mxm} & 0_{mxn} & 0_{mxm} \\ 0_{mxn} & 0_{mxm} & 0_{mxn} & I_{mxm} \end{bmatrix}$$

The original space state form is rewritten as:

$$\begin{cases} \dot{z}_{01} = z_{02} \\ \dot{z}_{02} = a(\alpha, x) + B(\alpha, q, \delta)u \\ \dot{z}_u = C(x) + D(x)u \\ y = z_{01} \end{cases} \tag{4.13}$$

In order to find the zero dynamics, we have to set z_{01} and z_{02} identically to zero. We can find the following relationships for the zero dynamics:

$$\begin{cases} \dot{z}_{u1} = z_{u2} \\ \dot{z}_{u2} = [-H_{22} + H_{21}(H_{11} + \psi H_{21})^{-1}(H_{12} + \psi H_{22})]|_{(\omega 1, \omega 3)} \times \\ \qquad [f_2(\omega_1, \omega_2) + g(\omega_1, \omega_2, \omega_3, \omega_4) + Kz_{u1} + E_2 z_{u2}] \end{cases} \tag{4.14}$$

where $\omega_1 = -\psi z_{u1}$ $\omega_2 = -\psi z_{u2}$ $\omega_3 = z_{u1}$ $\omega_4 = z_{u2}$ .Linearizing the system given by (4.14) about the equilibrium point z_{u1} , $z_{u2} = 0$ we have:

$$\begin{cases} \dot{z}_{u1} = z_{u2} \\ \dot{z}_{u2} = [-H_{22} + H_{21}(H_{11} + \psi H_{21})^{-1}(H_{12} + \psi H_{22})]|_{z_{u1}, z_{u2}=0} [Kz_{u1} + E_2 z_{u2}] \end{cases} \tag{4.15}$$

In order to investigate the conditions for minimum phase property, let us consider the matrix A:

$$A(\alpha) = \begin{bmatrix} 0 & I \\ -P_0 K & -P_0 E_2 \end{bmatrix} \tag{4.16}$$

where

$P_0 = [-H_{22} + H_{21}(H_{11} + \psi H_{21})^{-1}(H_{12} + \psi H_{22})]|_{(0,0)}$.

If the matrix $A(\alpha)$ is a Hurwitz matrix, then the origin of system (3.15) is locally asymptotically stable and the original nonlinear system is locally minimum phase [48].

As discussed in [54], the parameter α_i^* depends on the payload. In order to achieve the exact values for α_i^*, the exact value of the payload should be known. The lowest value of the α_i^* is obtained when there is no payload. This guarantees the stability of the zero-dynamics when the payload is added.

Using Matlab, the value obtained for α_i^* is $\alpha_i^* = 0.84$. For values $\alpha_i \leq 0.84$ the stability of the zero dynamics system is achieved, while for values $\alpha_i > 0.84$ the zero-dynamics will become unstable.

4.2 Computed torque method

4.2.1 A single-flexible link manipulator

Taking into consideration a finite number of modes, the dynamic equations can be derived using the recursive Lagrange approach [13]. The dynamic equations for a planar single flexible-link manipulator are given by:

$$M\begin{bmatrix} \ddot{q} \\ \ddot{\delta} \end{bmatrix} + \begin{bmatrix} f_1(q,\dot{q}) + g_1(q,\dot{q},\delta,\dot{\delta}) + E_1\dot{q} \\ f_2(q,\dot{q}) + g_2(q,\dot{q},\delta,\dot{\delta}) + E_2\dot{\delta} + K\delta \end{bmatrix} = \begin{bmatrix} \tau \\ 0 \end{bmatrix} \tag{4.17}$$

The output of the system is defined as:

$$y = q + \psi_{nxm}\delta \tag{4.18}$$

where $\psi_{nxm}(\alpha)$ is the matrix depending on the modal shape functions and the vector $\alpha^T = [\alpha_1 \quad ... \quad \alpha_n]$ defines the physical output locations on the links for ensuring the stable zero-dynamics .

We present the results of the computed torque method for one flexible-link manipulator. In these simulations the following parameters are used: the masse of the link is $m = 1.356kg$ and the length of the link is $l = 1.2m$. The value $\alpha_i^* = 0.84$ was obtained using the approach discussed above. The initial condition is $y = 0$, and the desired final position is set to $y = 1$.

The simulations graphs for the set of gains $\begin{cases} k_P = 100 \\ k_D = 100 \end{cases}$ are shown in the figures 4.1-4.4.

The results of using the same control method for tracking purpose are shown in figures 4.5-4.8. The simulations results are presented in Table 4.1.

Design parameters	er_1	er_2	t_s [sec]	$\lvert\tau_1\rvert_{max}$ [Nm]
$k_1 = 50$ $k_2 = 50$	0.0037	7e-8	5	4
$k_1 = 100$ $k_2 = 100$	0.0038	4e-7	5	8
$k_1 = 400$ $k_2 = 400$	0.0038	2e-7	5	30

Table 4-1 Summary of the simulation results for one flexible link using the computed torque method

Analyzing the simulation results for the one flexible-link manipulator using the computed torque method, it can be stated that this method has acceptable results for both the regulation and the tracking cases. The regulation error between the desired tip position and the redefined position is about 4e-7, while the error between the desired tip position

and the real position is about 0.0038. The settling time is about 5 seconds. These results are comparable for the three different sets of gains used. The maximum torque used is increasing with the increasing of the gains.

In the case of tracking, the error between the desired position of the tip and the redefined position, and the error between the desired position of the tip and the real position have almost the same value about 0.0044. As in the case of regulation, the maximum torque used is about 8 Nm for $\begin{cases} k_1 = 100 \\ k_2 = 100 \end{cases}$.

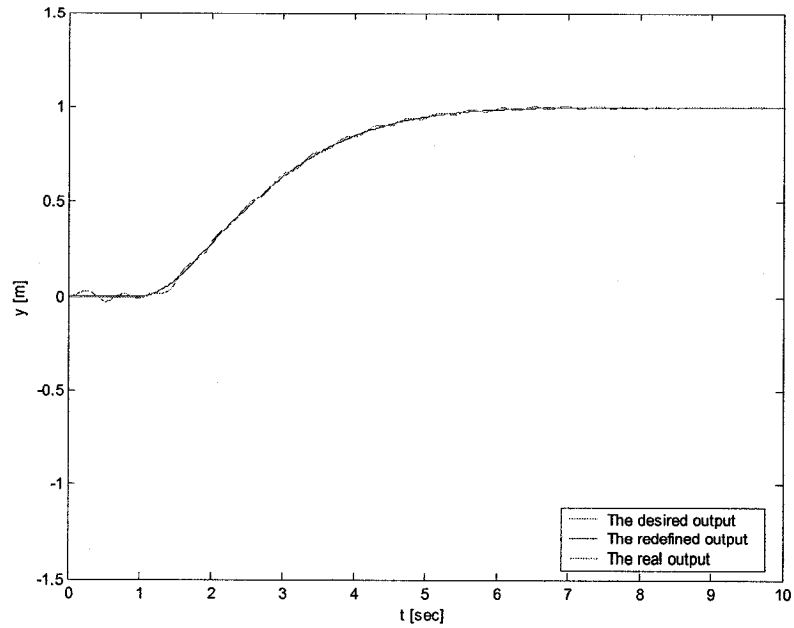

Figure 4-1 Computed torque method applied to a flexible link manipulator – redefined output

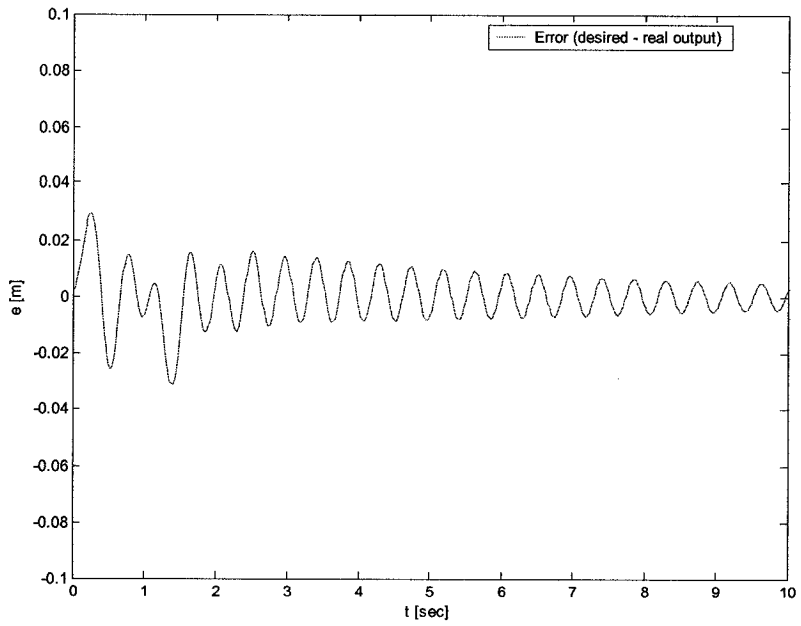

Figure 4-2 Computed torque method applied to a flexible link manipulator - error between the real and the desired output

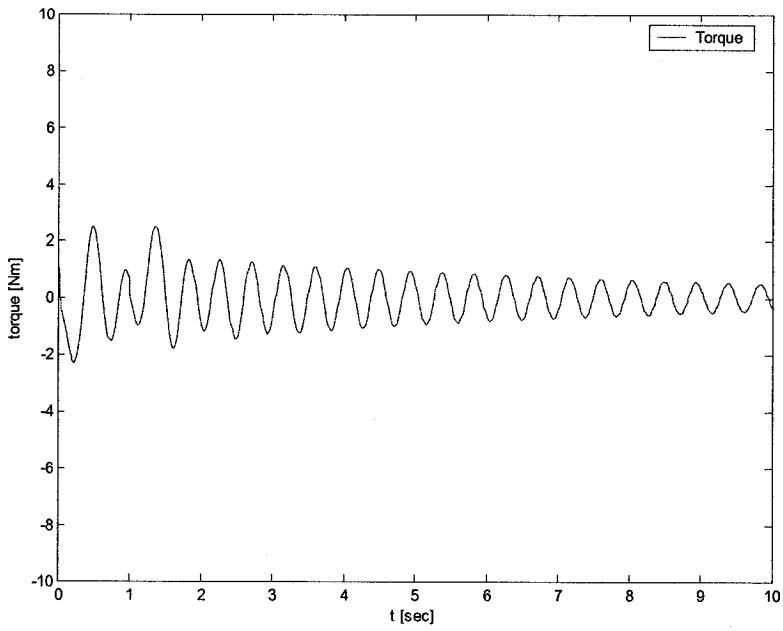

Figure 4-3 Computed torque method applied to a flexible link manipulator - torque command

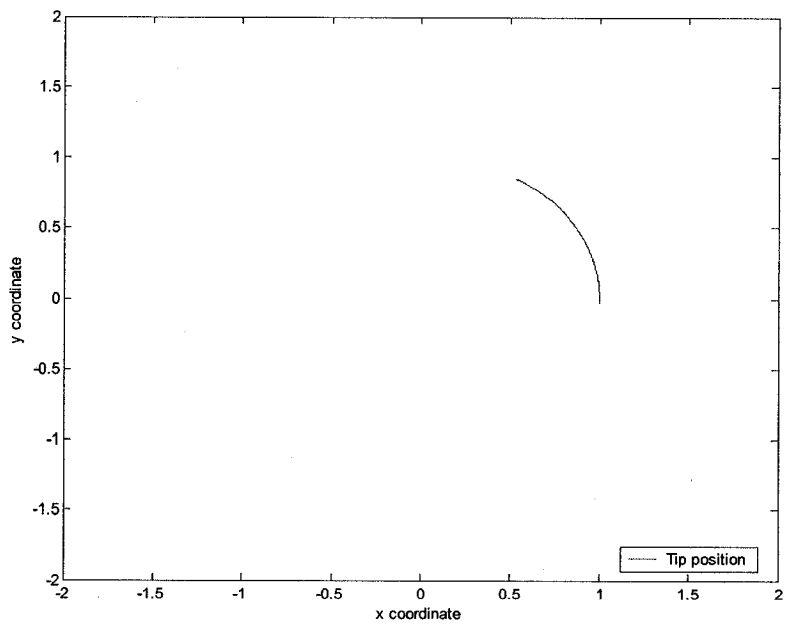

Figure 4-4 Computed torque method applied to a flexible link manipulator - tip position

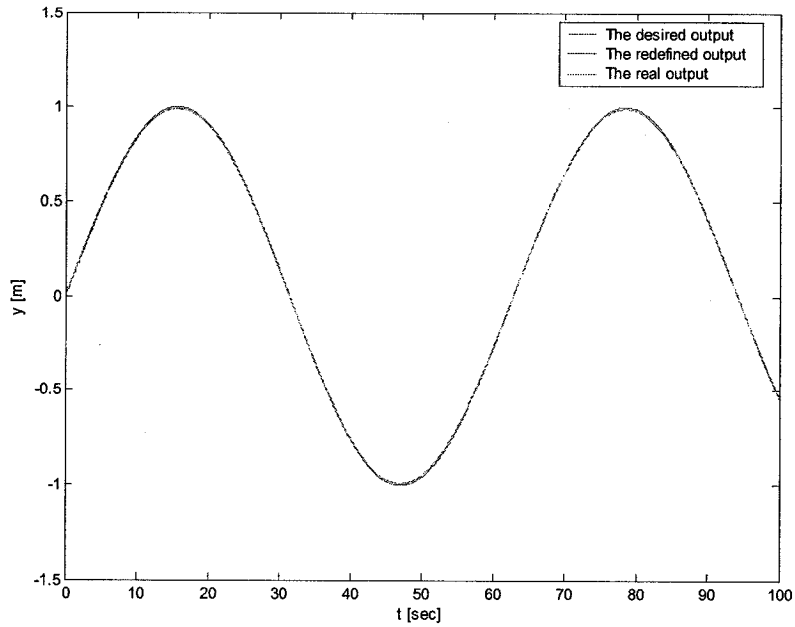

Figure 4-5 Computed torque method applied to a flexible link manipulator - tracking case - redefined output

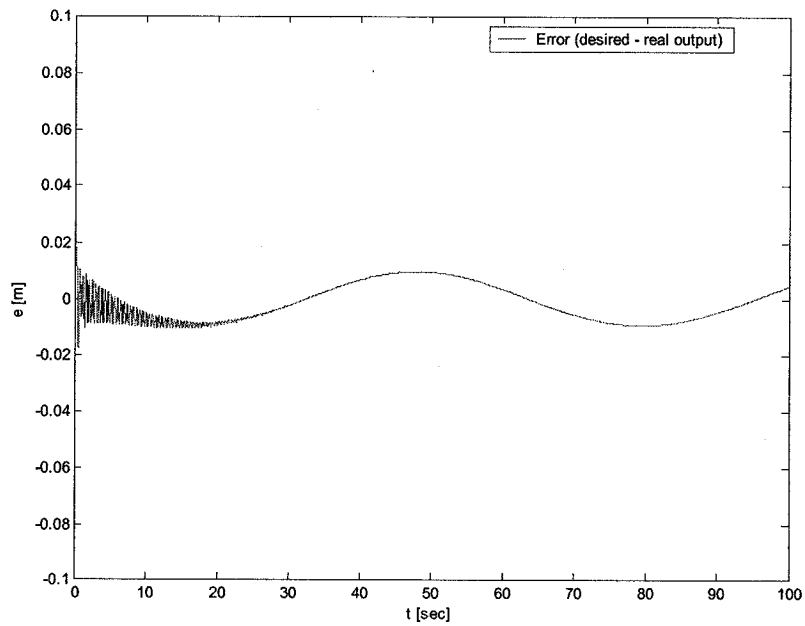

Figure 4-6 Computed torque method applied to a flexible link manipulator - tracking case - error between the real and the desired output

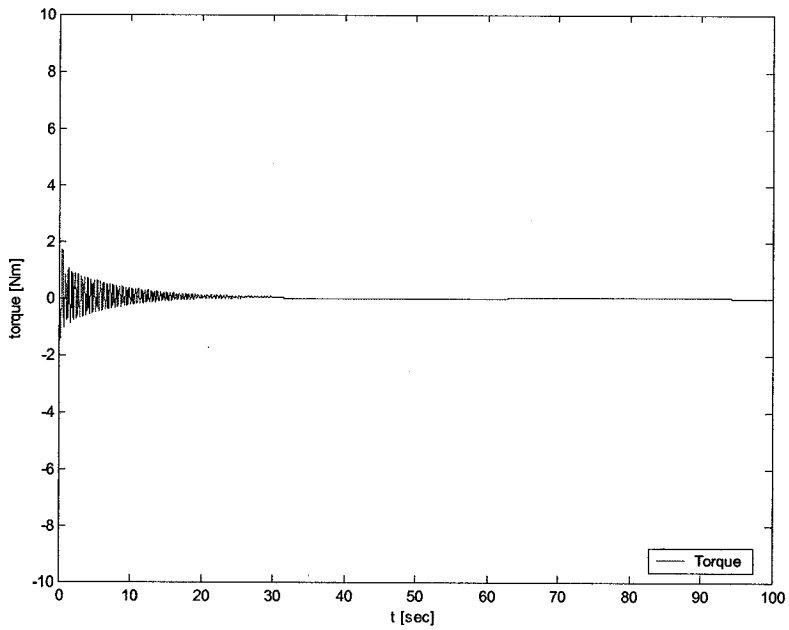

Figure 4-7 Computed torque method applied to a flexible link manipulator - tracking case - torque command

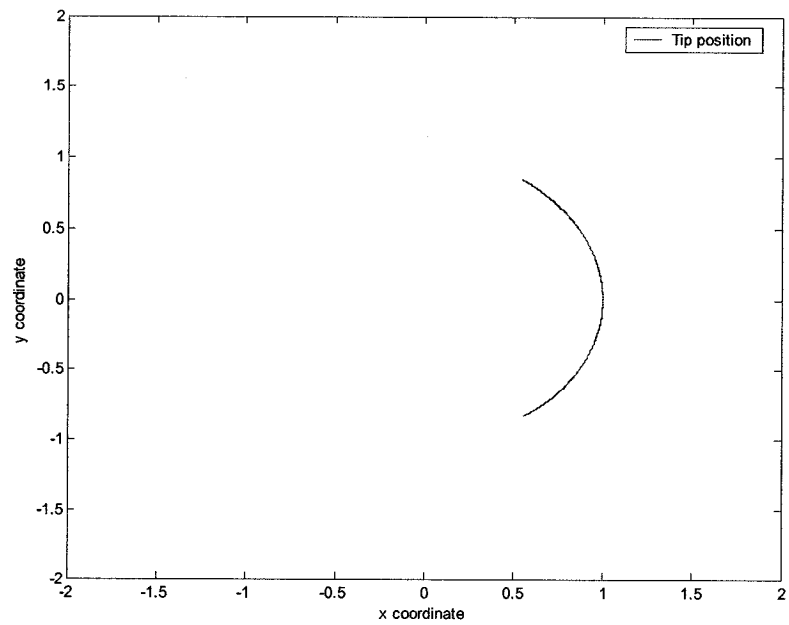

Figure 4-8 Computed torque method applied to a flexible link manipulator - tracking case - tip position

4.2.2 A two-link planar manipulator

Let us now consider a two-link manipulator having the first link rigid and the second link flexible. The parameters of the manipulator are as follows [55]:

$l_1 = 20cm, l_2 = 60cm, A_1 = 5cm \times 0.9mm, A_2 = 3.14cm \times 1.3cm$
$\rho_1 = 2700kg/m^3 (Al), \rho_2 = 7981(StainlessSteel),$
$M_1 = 1kg, M_l = 0.251kg, m_1 = 0.236kg, m_2 = 0.216kg$
$E = 194 \times 10^9 N/m^2, J_1 = 0.11 \times 10^{-3} kgm^2, J_l = 0.11 \times 10^{-4}, J_h = 3.8 \times 10^{-5}$

where l_1, l_2 are link lengths, A_1, A_2 are cross-sectional areas, E and ρ are modulus of elasticity and mass density, M_1, M_l, J_1, J_l are masses and mass moment of inertia at the end-points of the two links. In the previous section, the critical value of α^* was obtained to be $\alpha^* = 0.84$. In the case of two-link manipulator, $\alpha^* = 0.45$. The initial condition for both links is $y = 0$, and the desired final positions are set to $y = 1$. For the tracking case, the trajectory to be followed is given by $y_d = A\sin(\omega t)$, where $A = 1$ and $\omega = 0.1$.

Table 4.2 shows the results of using the computed torque method for a two-link manipulator. The simulations results are presented in figures 4.9-4.16.

Design parameters	er_1	er_2	t_s [sec]	$\lvert\tau_1, \tau_2\rvert_{max}$ [Nm]
$k_1 = 50$ $k_2 = 50$	0.0011	0.0006	5	2.5
$k_1 = 100$ $k_2 = 100$	0.0011	0.0004	5	2.5
$k_1 = 400$ $k_2 = 400$	0.0010	0.0006	5	2.5

Table 4-2 Summary of the simulation results for a two-link manipulator using computed torque method

where er_1 denotes the error between the desired position of the tip and the real position of the tip, and er_2 denotes the error between the desired position of the tip and the redefined position of the tip.

Analyzing the simulation results for the two-link manipulator using the computed torque method it can be stated that this method has acceptable results for both the regulation and the tracking cases. The regulation error between the desired position of the tip and the redefined position is about 0.0006, while the error between the desired position of the tip and the real position is about 0.0011. The settling time is about 5 seconds. These results are comparable for all the three different sets of gains used. The maximum of the torque used remains about 2.5 Nm with the increasing of the gains.

In the case of tracking, the error between the desired position of the tip and the redefined position and the error between the desired position of the tip and the real position are about 0.004. The maximum used torque is about 23 Nm while using $\begin{cases} k_1 = 100 \\ k_2 = 100 \end{cases}$.

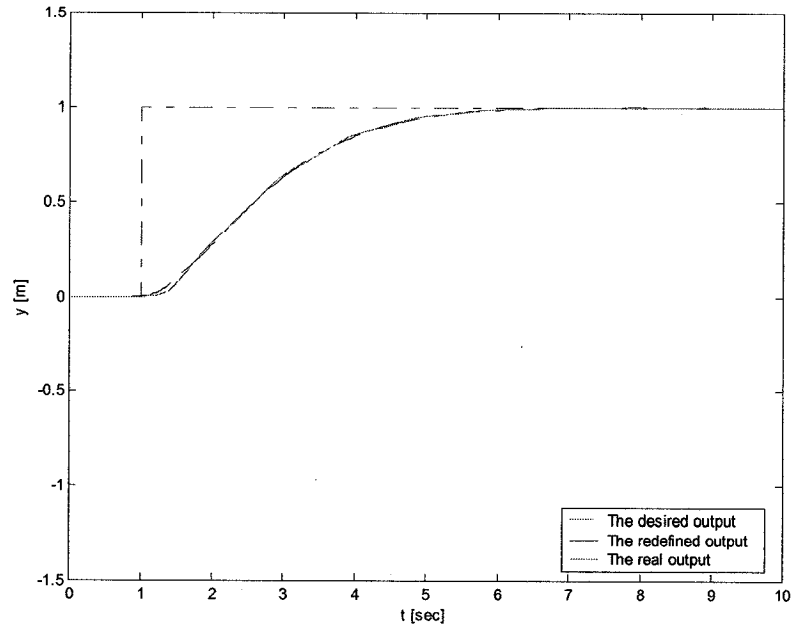

Figure 4-9 Computed torque method applied to a two-link manipulator – redefined output

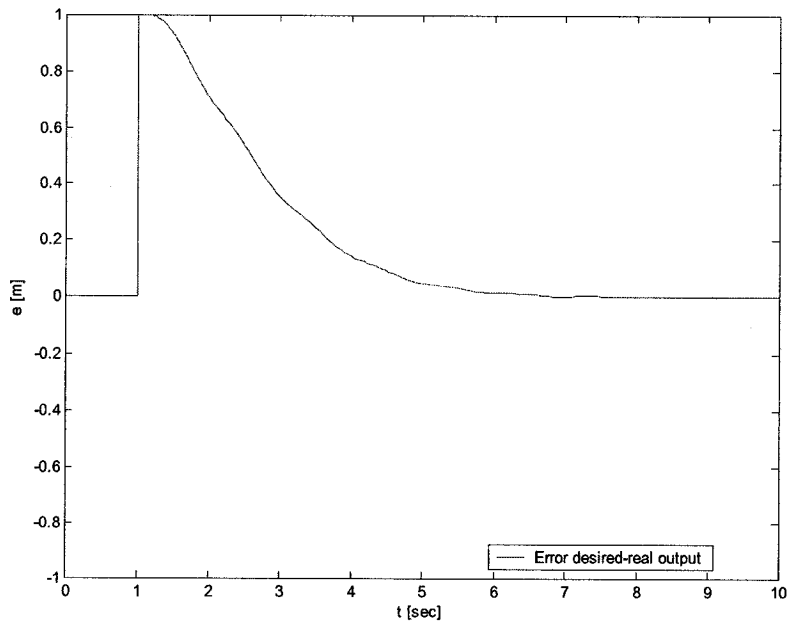

Figure 4-10 Computed torque method applied to a two-link manipulator - error between the real and the desired output

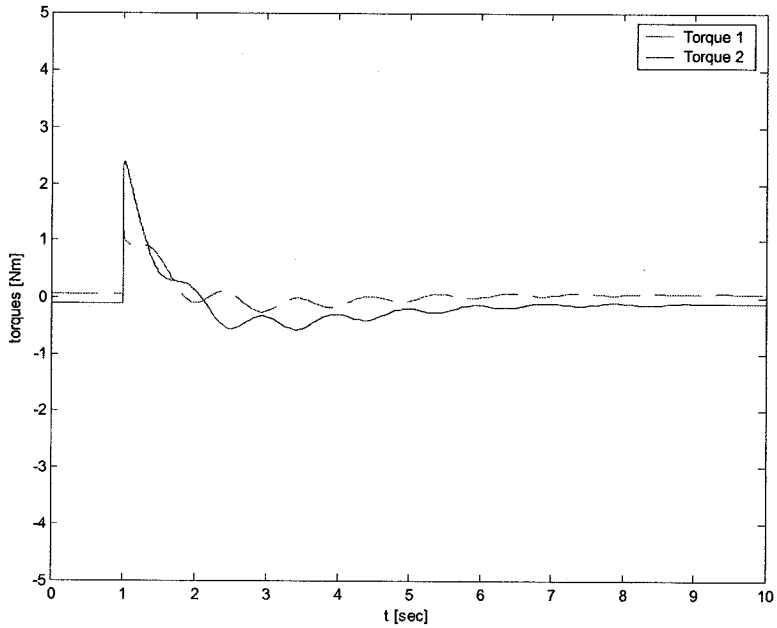

Figure 4-11 Computed torque method applied to a two-link manipulator -torques command

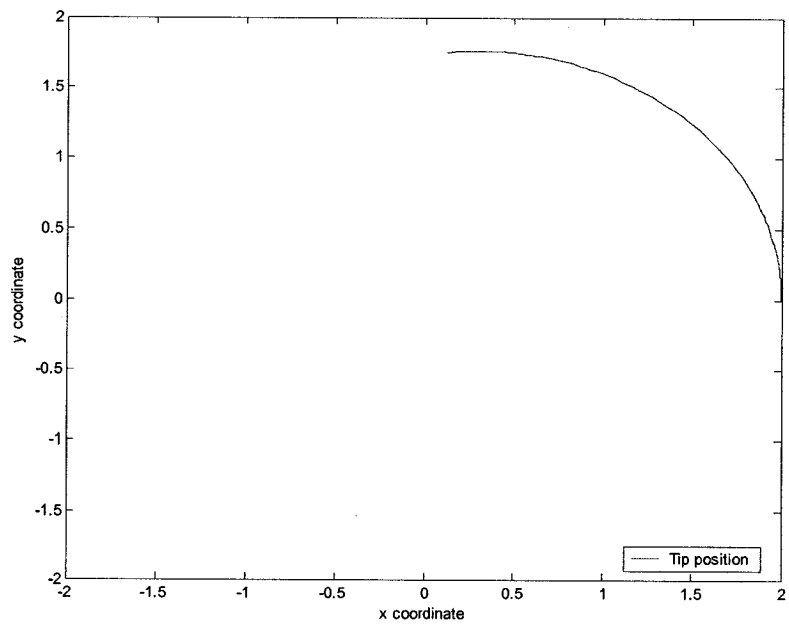

Figure 4-12 Computed torque method applied to a two-link manipulator - tip position

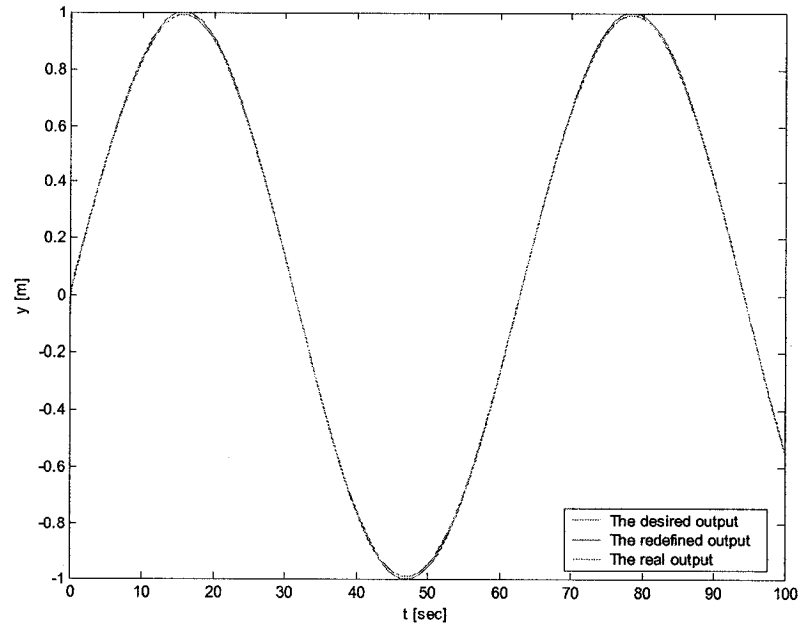

Figure 4-13 Computed torque method applied to a two-link manipulator - tracking case – redefined output

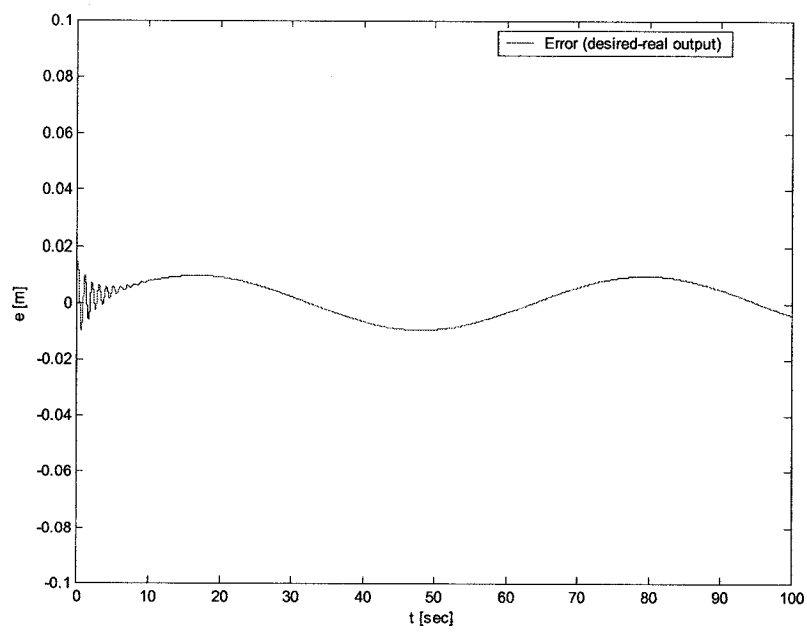

Figure 4-14 Computed torque method applied to a two-link manipulator - tracking case - error between the real and the desired output

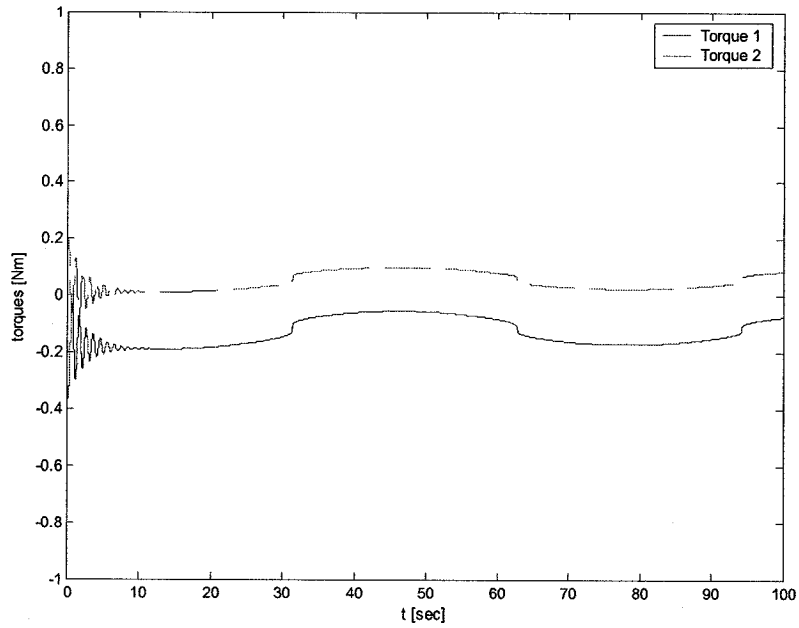

Figure 4-15 Computed torque method applied to a two-link manipulator - tracking case - torques command

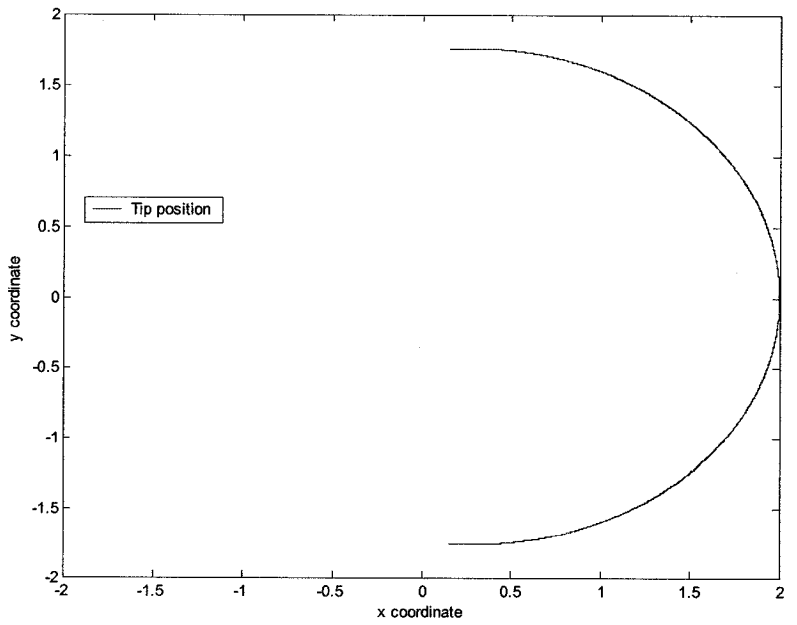

Figure 4-16 Computed torque method applied to a two-link manipulator - tracking case - tip position

4.3 Dynamic control method

In this section, a novel dynamic control method for a flexible-link manipulator is developed. This method allows us to obtain the desired transient behavior under the condition where there is incomplete information about the system. In order to decrease the influence of disturbances and the uncertainty of model parameters on dynamic properties of the output trajectories, a high feedback gain is used. Furthermore, a higher-order output derivative in the feedback loop is used. This method is a generalization and further development of results that are reported in [49], [50],[51].

In this section, we develop a control strategy based on input-output linearization of the flexible-link system. The output re-definition concept is employed to choose points near the tip outputs such that stable zero-dynamics are achieved. It is assumed that the vibrations are mainly lateral vibrations about the axis of each link. In other words, for each link it is assumed that a considerable amount of potential energy is stored in the direction of bending corresponding to the axis of rotation of that link, and that the potential energies due to deflections in other directions are negligible. This may be achieved by proper mechanical structure design. A planar manipulator with rectangular cross sections in which the height to thickness ratio of each cross section is large is an example of such a system.

A closed-loop stability analysis is performed and conditions for achieving stable closed-loop behavior are stated. The theoretical developments are further complemented by simulation studies for a flexible-link manipulator as well as for a two-link manipulator with the second link flexible to demonstrate the potential and capabilities of the proposed dynamic controller. In particular, stable closed-loop performance with small tip position

tracking errors is achieved with relatively large control gains, resulting in reduced closed-loop sensitivity that would otherwise not be achieved by conventional methods.

Model of the flexible-link manipulator

Let us rewrite again the dynamic equations for the planar single-link manipulator as

$$M\begin{bmatrix}\ddot{q}\\ \ddot{\delta}\end{bmatrix}+\begin{bmatrix} f_1(q,\dot{q})+g_1(q,\dot{q},\delta,\dot{\delta})+E_1\dot{q} \\ f_2(q,\dot{q})+g_2(q,\dot{q},\delta,\dot{\delta})+E_2\dot{\delta}+K\delta \end{bmatrix}=\begin{bmatrix}\tau\\ 0\end{bmatrix} \tag{4.19}$$

where as before q is the $nx1$ vector of joint variables, δ is the $mx1$ vector of deflection variables, f_1, g_1, f_2, g_2 are the terms due to Coriolis and centrifugal forces, K is the stiffness matrix, and τ is the vector of joint control torques.

Let us define $H = M^{-1}(q,\delta) = \begin{bmatrix} H_{11} & H_{12} \\ H_{21} & H_{22}\end{bmatrix}$. Consequently, (4.19) can be rewritten in the state-space form:

$$\dot{x} = f(x) + g(x)u \tag{4.20}$$

where $x^T = \begin{bmatrix} q^T & \delta^T & \dot{q}^T & \dot{\delta}^t \end{bmatrix}$ and

$$f(x) = \begin{bmatrix} \dot{q} \\ \dot{\delta} \\ -H_{11}(f_1+g_1+E_1\dot{q}) - H_{12}(f_2+g_2+K\delta+E_2\dot{\delta}) \\ -H_{21}(f_1+g_1+E_1\dot{q}) - H_{22}(f_2+g_2+K\delta+E_2\dot{\delta}) \end{bmatrix},\quad g(x) = \begin{bmatrix} O_{(m+n)xn} \\ H_{11}(q,\delta) \\ H_{21}(q,\delta) \end{bmatrix}$$

As it was previously discussed in section 4.1.3, since the beam deflection is usually small with respect to the link length, we have:

$$y_i = q_i + \alpha_i d_{ie} / l_i, i = 1,2,...,n \tag{4.21}$$

Defining the output vector as:

$$y = q + \psi_{nxm}(\alpha)\delta \tag{4.22}$$

where $\psi_{nxm}(\alpha)$ is the matrix depending on modal shape functions and the $\alpha^T = [\alpha_1 \quad ... \quad \alpha_n]$ is the vector defining the physical output locations on the links for ensuring stable zero-dynamics.

Input-output model of the flexible link manipulator

The input-output description of (4.19) with the output described by (4.22) is then obtained by differentiating the output vector y with respect to time until the input vector appears which is given by:

$$\ddot{y} = a(\alpha, x) + B(\alpha, q, \delta)u \tag{4.23}$$

where $y = [y_1 \quad ... \quad y_n]^T$ is the output available for measurement, and $u = [u_1 \quad ... \quad u_n]^T$ is the control vector

$$B(\alpha, q, \delta) = H_{11} + \psi_{nxm} H_{21} \tag{4.24}$$

$$a(\alpha, x) = -(H_{11} + \psi H_{21})(f_1 + g_1 + E_1 \dot{q}) - (H_{11} + \psi H_{22})(f_2 + g_2 + K\delta + E_2 \dot{\delta}) \tag{4.25}$$

Let us specify a finite region around the desired joint angles reference trajectories q_r and $\dot{q}_r$ that is given by:

$$\Omega_r = \left\{ x : | q - q_r | < k_1, | q - \dot{q} | < k_2, | \delta | < k_3, | \dot{\delta} | < k_4 \right\} \tag{4.26}$$

where k_i^s are some positive constants.

Assumption 4.1 Let $\det B(\alpha, q, \delta) \neq 0, \forall x \in \Omega_r$ where $x \in \Omega_r \subset R^{2(n+m)}$ and Ω_r is a bounded set of $R^{2(n+m)}$.

Assumption 4.2 Let the vector α, the matrices $H(0,0), K, E_2$ be such that the matrix:

$$A(\alpha) = \begin{bmatrix} 0 & I \\ -P_0 K & -P_0 E_2 \end{bmatrix} \tag{4.27}$$

with P_0 given by:

$$P_0 = [-H_{22} + H_{21}(H_{11} + \psi H_{21})^{-1}(H_{12} + \psi H_{22})]\,|_{(0,0)} \tag{4.28}$$

is a Hurwitz matrix.

Consequently, the origin of the manipulator model is locally asymptotically stable, and the original nonlinear model (4.20), (4.22) is locally minimum phase.

Assumption 4.1 is basically a controllability-like assumption [48] and is guaranteed to hold when for instance $\alpha = 0$. In this case, $B = H_{11}$ is positive-definite and therefore invertible. Thus in a neighborhood of $\alpha = 0$, B is guaranteed to be invertible since it is continuously dependent on α.

Output tracking control problem

Let us denote

$$e(t) = r(t) - y(t) \tag{4.29}$$

as the tracking error where $y(t)$ is the manipulator end-effector output and $r(t)$ is the reference input signal. The dynamic controller designed is to ensure and guarantee the following condition:

$$\lim_{t \to \infty} e(t) = 0 \tag{4.30}$$

Moreover, the output transients for $y(t)$ should have a desired behavior which does not depend either on the external disturbances or on the possibly varying parameters of the flexible-link manipulator model (4.20) and (4.22).

Control problem reformulation

A. Desired dynamic equations

Let us form a reference model for output transients of $y(t)$ according to the following differential equation:

$$\ddot{y} = F(\dot{y}, y, \dot{r}, r) \tag{4.31}$$

For example, (4.31) may have the form of a linear equation

$$\ddot{y} = -A_1^d \dot{y} - A_0^d y + B_1^d \dot{r} + B_0^d r \tag{4.32}$$

By selecting A_1^d, A_0^d and B_0^d as diagonal matrices, then we require the decoupling of the control channels. Let us denote

$$e^F = F(\dot{y}, y, \dot{r}, r) - \ddot{y} \tag{4.33}$$

where e^F is the realization error characteristics of the desired dynamics which is assigned by $F(\dot{y}, y, \dot{r}, r)$. Accordingly, if the condition

$$e^F = 0 \tag{4.34}$$

is satisfied, the desired behaviour of $y(t)$ with prescribed dynamics of (4.31) is achieved. The expression (4.34) corresponds to the insensitivity condition of the output transient performance with respect to the external disturbances and varying parameters of the flexible-link manipulator model. In other words, the control design problem (4.29) may be reformulated as the requirement (4.34).

To satisfy the requirement of (4.34) let us construct the control law according to the following differential equation:

$$\mu^2 \ddot{v} + \mu D_1 \dot{v} + D_0 v = K_1 e^F, \ \bar{v}(0) = \bar{v}_0 \tag{4.35}$$

where

$$u = K_0 v \tag{4.36}$$

and $\bar{v} = \begin{bmatrix} \dot{v} & v \end{bmatrix}^T$

Assume that D_o, D_1, K_1 are diagonal matrices, μ is a sufficiently small positive parameter, and $K_1 = diag\{k_1,...,k_n\}$. Consequently, when taken together, equations (4.33) and (4.35), the dynamic control law (4.35) may be rewritten in the form:

$$\mu^2 \ddot{v} + \mu D_1 \dot{v} + D_0 v = K_1\{-\ddot{y} - A_1^d \dot{y} - A_0^d y + B_1^d \dot{r} + B_0^d r\} \tag{4.37}$$

Analysis of the two-time scale dynamic motion

The analysis below for the properties of the slow and fast motion dynamics properties assumes that the states of the manipulator, namely, q and δ are bounded within an open set. This is also consistent with the assumption of internally stable dynamics of the flexible manipulator system.

A. Fast-motion subsystem

Theorem 4.1 Associated with the closed-loop system (4.23), (4.35) as $\mu \to 0$, the fast-motion subsystem is governed by the following equation:

$$\mu^2 \ddot{v} + \mu D_1 \dot{v} + \{D_0 + K_1 B(\alpha, q, \delta) K_0\} v = K_1\{F(\dot{y}, y, \dot{r}, r) - a(\alpha, x)\} \tag{4.38}$$

where it is assumed that $\dot{y} \approx 0$, $\dot{r} \approx const.$, $y \approx const.$ and $r \approx const.$ during the fast-time scale transient of the system.

Proof: The closed-loop input-output governing equations have the following form:

$$\ddot{y} = a(\alpha, x) + B(\alpha, q, \delta) K_0 v \tag{4.39}$$

$$\mu^2 \ddot{v} + \mu D_1 \dot{v} + D_0 v = K_1 e^F \tag{4.40}$$

From (4.31), (4.33) it follows that the closed loop system equations may be rewritten in the form:

$$\ddot{y} = a(\alpha, x) + B(\alpha, q, \delta) K_0 v \tag{4.41}$$

$$\mu^2 \ddot{v} + \mu D_1 \dot{v} + \{D_0 + K_1 B(\alpha, q, \delta) K_0\} v = K_1 \{F(\dot{y}, y, \dot{r}, r) - a(\alpha, x)\} \tag{4.42}$$

The equations (4.41), (4.42) may be rewritten in the following state-space representation:

$$\begin{cases} \dfrac{d}{dt}\eta_1 = \eta_2, \\ \dfrac{d}{dt}\eta_2 = a(\alpha, x) f + B(\alpha, q, \delta) K_0 v_1, \\ \dfrac{d}{dt} v_1 = v_2, \\ \mu \dfrac{d}{dt} v_2 = -\{D_0 + K_1 B(\alpha, q, \delta) K_0\} v_1 - D_1 v_2 + K_1 \{F(\eta_2, \eta_1, \dot{r}, r) - a(\alpha, x)\} \end{cases} \tag{4.43}$$

where $\eta_1 = y, \eta_2 = \dot{y}, v_1 = v, v_2 = \dot{v}$

Following the standard singular perturbation procedure, let us introduce the new fast time scale $t_0 = t / \mu$, where we now have:

$$\begin{cases} \dfrac{d}{dt_0}\eta_1 = \mu \eta_2, \\ \dfrac{d}{dt_0}\eta_2 = \mu \{a(\alpha, x) + B(\alpha, q, \delta) K_0 v_1\}, \\ \dfrac{d}{dt_0} v_1 = v_2, \\ \dfrac{d}{dt_0} v_2 = -\{D_0 + K_1 B(\alpha, q, \delta) K_0\} v_1 - D_1 v_2 + K_1 \{F(\eta_2, \eta_1, \dot{r}, r) - a(\alpha, x)\} \end{cases} \tag{4.44}$$

By setting $\mu \to 0$ in the above equations we get

$$\begin{cases} \dfrac{d}{dt_0}\eta_1 = 0, \\ \dfrac{d}{dt_0}\eta_2 = 0, \\ \dfrac{d}{dt_0} v_1 = v_2 \\ \dfrac{d}{dt_0} v_2 = -\{D_0 + K_1 B(\alpha, q, \delta) K_0\} v_1 - D_1 v_2 + K_1 \{F(\eta_2, \eta_1, \dot{r}, r) - a(\alpha, x)\}, \end{cases} \tag{4.45}$$

Expressing the above in the original time scale $t = \mu t_0$, we obtain the following fast-motion subsystem:

$$\begin{cases} \eta_i = const, \\ \mu \dfrac{d}{dt} v_1 = v_2, \\ \mu \dfrac{d}{dt} v_2 = -\{D_0 + K_1 B(\alpha, q, \delta) K_0\} v_1 - D_1 v_2 + K_1 \{F(\eta_2, \eta_1, \dot{r}, r) - a(\alpha, x)\} \end{cases} \tag{4.47}$$

The above fast-motion subsystem equations may be alternatively rewritten in the form (4.38).

Remark 4.1: The asymptotic stability, desired behaviour of transients and desired settling time of $v(t)$ can be achieved by a proper choice of the control law parameters.

Remark 4.2: In order to provide stability of the fast motion subsystem (4.38), the matrix K_0 should be nonsingular such that $K_0 B$ is positive definite (or e.g. if $K_0 \approx \{B^{-1}\}$.)

B. Slow-motion subsystem

Theorem 4.2: If $\mu \to 0$ and the fast-motion subsystem of (4.38) is asymptotically stable then

$$\ddot{y} = F(\dot{y}, y, \dot{r}, r) + K_1^{-1} D_0 \{K_1^{-1} D_0 + B K_0\}^{-1} \{a(\alpha, x) - F\} \tag{4.48}$$

represents the slow-motion subsystem.

Proof: If the fast-motion subsystem (4.38) is stable, by taking the limit $\mu \to 0$ in (4.41), (4.42) the slow-motion subsystem (4.48) may be obtained.

Remark 4.3: If $D_0 \neq 0$ and $k_i >> 1$, $\forall$ $i = 1,2$ then the slow-motion subsystem (4.48) approaches that of (4.31). If $D_0 = 0$ and $k_i >> 0$, $\forall$ $i = 1,2$ then the slow-motion subsystem (4.48) is the same as (4.31).

Remark 4.4: If $\mu \to 0$ then from (4.41), (4.42) it follows that the behaviour of $y(t)$ tends to the solution of the reference model and accordingly the controlled output transients in the closed loop system have desired performance specifications after the fast-motion subsystem transients.

4.3.1 A single-flexible link manipulator

Let us rewrite again the dynamic equations for the planar single link manipulator that are given by:

$$M\begin{bmatrix} \ddot{q} \\ \ddot{\delta} \end{bmatrix} + \begin{bmatrix} f_1(q,\dot{q}) + g_1(q,\dot{q},\delta,\dot{\delta}) + E_1\dot{q} \\ f_2(q,\dot{q}) + g_2(q,\dot{q},\delta,\dot{\delta}) + E_2\dot{\delta} + K\delta \end{bmatrix} = \begin{bmatrix} \tau \\ 0 \end{bmatrix}$$

The output of the system is defined as

$$y = q + \psi_{nxm}\delta$$

where $\psi_{nxm}(\alpha)$ is the matrix depending on modal shape functions and the vector $\alpha^T = [\alpha_1 \quad \ldots \quad \alpha_n]$ defines the physical output locations on the links for ensuring the stable zero-dynamics.

We present the simulation results of the dynamic control for one flexible-link manipulator. In these simulations the following parameters are used: the masse of the link is $m = 1.356kg$, and the length of the link is $l = 1.2m$. The value $\alpha_i^* = 0.84$ was obtained using the approach discussed previously. The initial condition is set to $y = 0$, and the desired final position is set to $y = 1$.

The simulations graphs for the set of gains $K_1 = 100$ are shown in the figures 4.17-4.20. The simulation results for the dynamic control method for tracking problem are shown in figures 4.21-4.24. The simulations results are summarized in Table 4.3.

Design parameters	er_1	er_2	t_s [sec]	$\lvert\tau_1\rvert_{max}$ [Nm]
$k_1 = 50$	0.0018	0.0016	5	1.25
$k_1 = 100$	0.0017	0.0014	5	1.25
$k_1 = 400$	0.0012	0.0010	5	1.25

Table 4-3 Summary of the simulation results for one-flexible link using dynamical control method

Analyzing the simulation results for one-flexible link manipulator using the dynamical control scheme, it can be stated that this method performs better than the computed torque method. The regulation error between the desired position of the tip and the redefined position is about 0.0016, while the error between the desired position of the tip and the real position is about 0.0018. The settling time is around 5 seconds, which is the same with the one achieved using computed torque method. The error between the desired position of the tip and the real position of the tip has decreased using this control method from 0.0038 to 0.0016. At the same time, the maximum torque command has decreased from about 8 Nm in the case of computed torque method to 1.25 Nm for the dynamic control. Increasing the gain, the error between the desired tip position and the real tip position, and the error between the desired tip position and the redefined tip

position can be decreased. However, the settling time and the maximum torque command remain in the same range.

For the problem of tracking, the error between the desired position of the tip and the redefined position, and the error between the desired position of the tip and the real position have almost the same value about 0.18. The maximum torque used is about 8 Nm while using $\begin{cases} k_1 = 100 \\ k_2 = 100 \end{cases}$ as in the case of computed torque method.

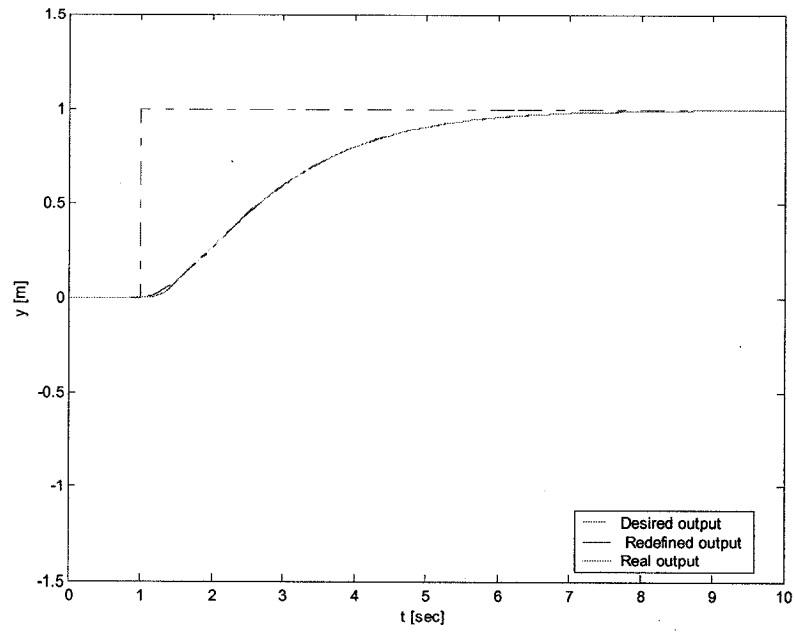

Figure 4-17 Dynamical control method applied to a flexible link manipulator – redefined output

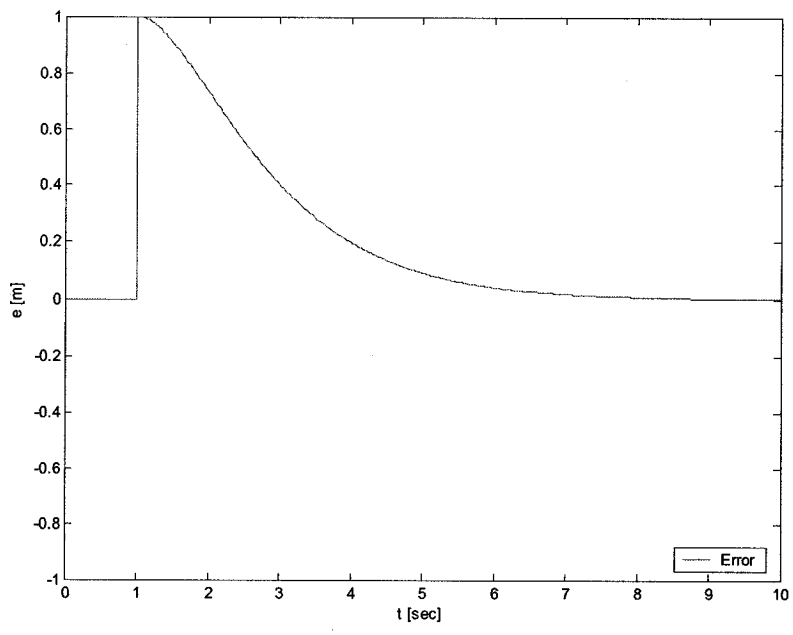

Figure 4-18 Dynamical control method applied to a flexible link manipulator - error between the real and the desired output

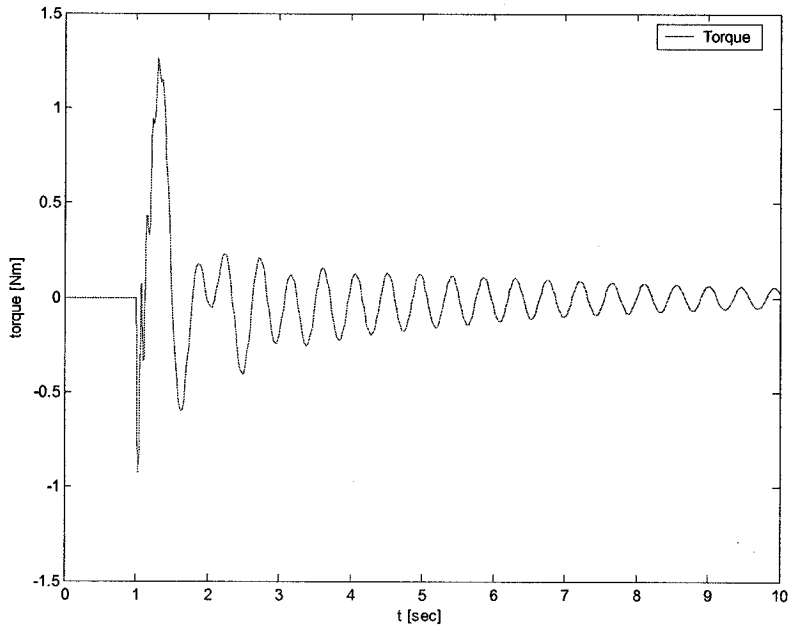

Figure 4-19 Dynamical control method applied to a flexible link manipulator - torque command

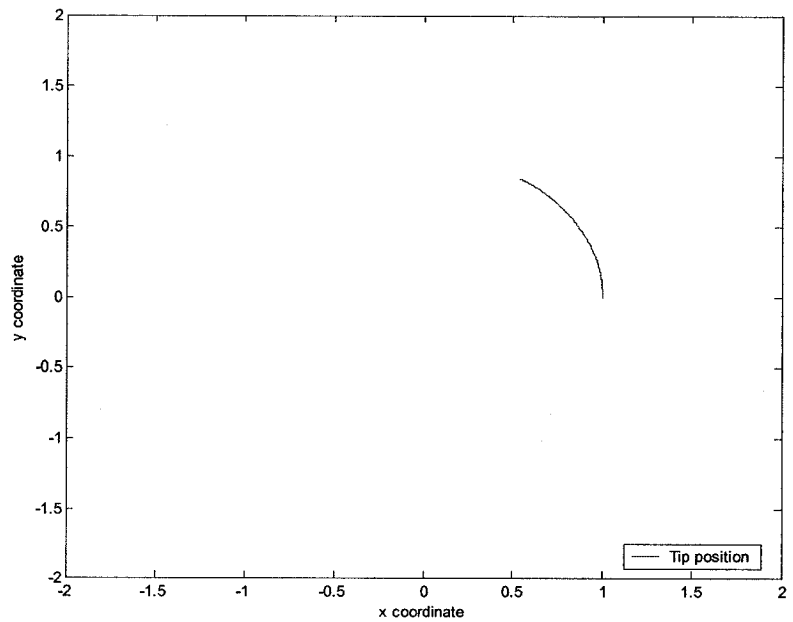

Figure 4-20 Dynamical control method applied to a flexible link manipulator - tip position

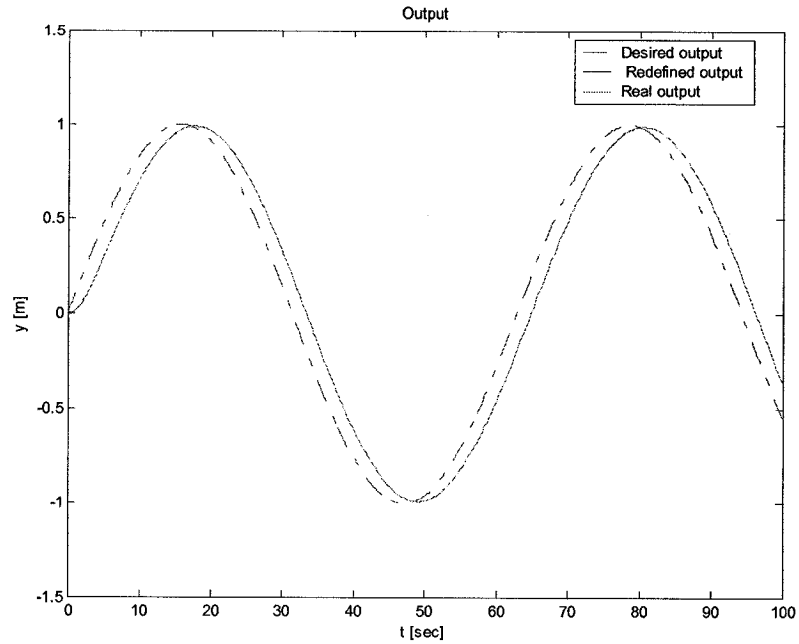

Figure 4-21 Dynamical control method applied to a flexible link manipulator - tracking case – redefined output

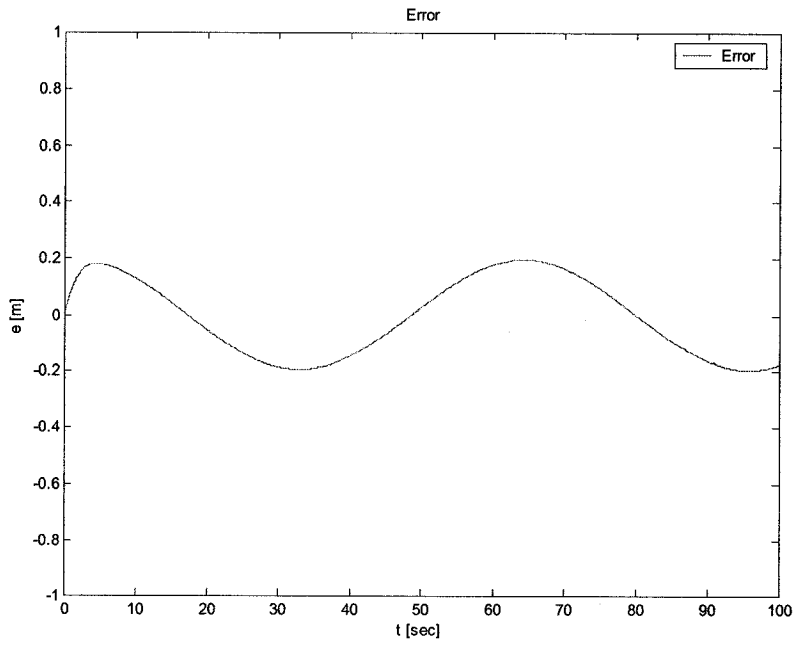

Figure 4-22 Dynamical control method applied to a flexible link manipulator - tracking case - error between the real and the desired output

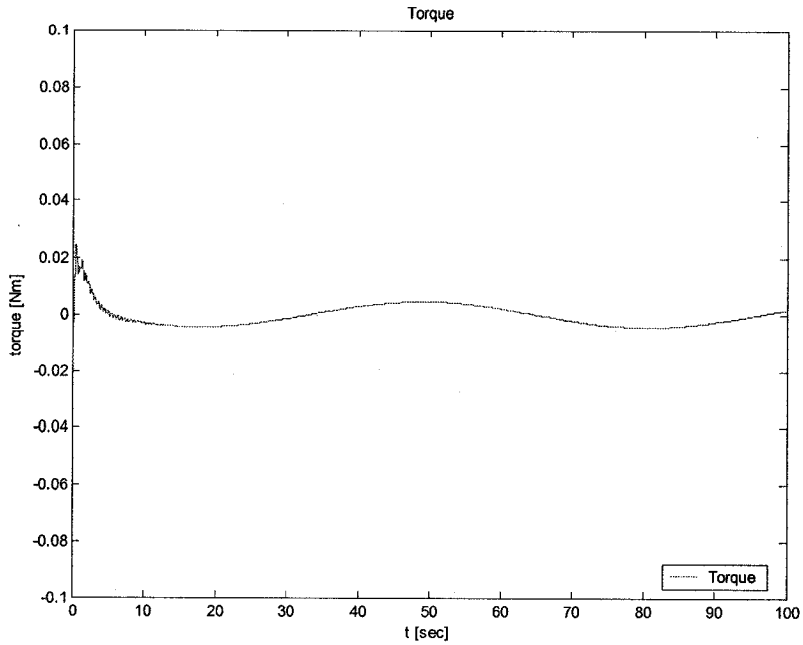

Figure 4-23 Dynamical control method applied to a flexible link manipulator - tracking case - torque command

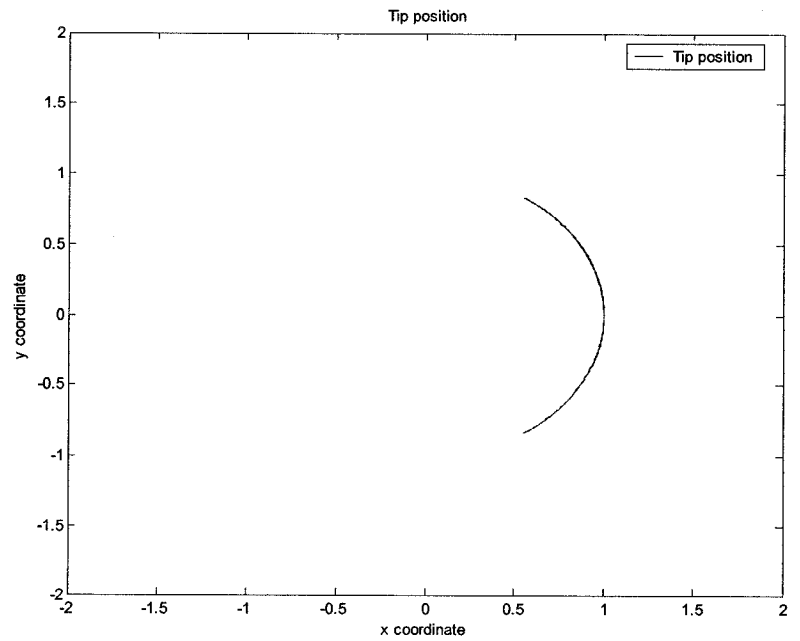

Figure 4-24 Dynamical control method applied to a flexible link manipulator - tracking case - tip position

4.3.2 A two-link planar manipulator

Let us now consider a two-link manipulator having the first link rigid and the second link flexible. The parameters of the manipulator are as follows [55]:

$l_1 = 20cm, l_2 = 60cm, A_1 = 5cm \times 0.9mm, A_2 = 3.14cm \times 1.3cm$
$\rho_1 = 2700kg/m^3 (Al), \rho_2 = 7981(StainlessSteel),$
$M_1 = 1kg, M_l = 0.251kg, m_1 = 0.236kg, m_2 = 0.216kg$
$E = 194 \times 10^9 N/m^2, J_1 = 0.11 \times 10^{-3} kgm^2, J_l = 0.11 \times 10^{-4}, J_h = 3.8 \times 10^{-5}$

where l_1, l_2 are link lengths, A_1, A_2 are cross-sectional areas, E and ρ are modulus of elasticity and mass density, M_1, M_l, J_1, J_l are masses and mass moment of inertia at the end-points of the two links. In the previous section, the critical value of α^* was obtained to be $\alpha^* = 0.84$. In the case of a two-link manipulator, $\alpha^* = 0.45$. The initial condition for both links is $y = 0$ and the desired final positions are set to $y = 1$. For the tracking case, the trajectory to be followed is given by $y_d = A\sin(\omega t)$ where $A = 1$ and $\omega = 0.1$.

Table 4.4 shows the results of using the dynamical control method for the two-link manipulator. The simulations results are shown in figures 4.25-4.32.

Design parameters	er_1	er_2	t_s [sec]	$\lvert\tau_1, \tau_2\rvert_{max}$ [Nm]
$K_1 = \begin{bmatrix} 50 & 0 \\ 0 & 50 \end{bmatrix}$	0.0058	0.0053	5	3.9
$K_1 = \begin{bmatrix} 100 & 0 \\ 0 & 100 \end{bmatrix}$	0.0025	0.002	5	4.2
$K_1 = \begin{bmatrix} 400 & 0 \\ 0 & 400 \end{bmatrix}$	0.0004	0.0004	5	4.9

Table 4-4 Simulations results for a two-link manipulator using dynamical control method

where er_1 represents the error between the desired position of the tip and the real position of the tip, and er_2 represents the error between the desired position of the tip and the redefined position of the tip.

Analyzing the simulations results for the two-link manipulator using the dynamical control method, it can be stated that this method has acceptable results for both regulation and tracking problems. The results are not much better than the results when compared to the computed torque method for gains less than 100. For higher gains, the dynamic control method performs better than the computed torque method. For example, the regulation error between the desired position of the tip and the redefined position and the error between the desired position of the tip and the real position is 0.0004 in case of using $K_1 = \begin{bmatrix} 400 & 0 \\ 0 & 400 \end{bmatrix}$. For a smaller gain $K_1 = \begin{bmatrix} 100 & 0 \\ 0 & 100 \end{bmatrix}$, the errors are about 0.002. The settling time is about 5 seconds. The maximum of the torque used is increasing with the increasing of the gains but remains about 4 Nm.

In the case of tracking problem, the error between the desired position of the tip and the redefined position and the error between the desired position of the tip and the real position are about 0.17 and they do not depend on the gain used. The maximum value of torque used is about 0.2 Nm.

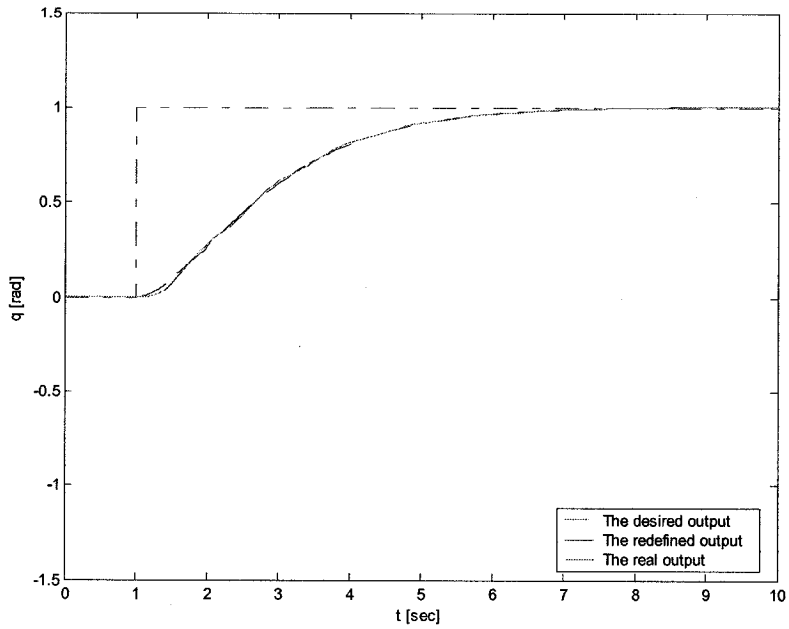

Figure 4-25 Dynamic control method applied to a two-link manipulator - redefined output

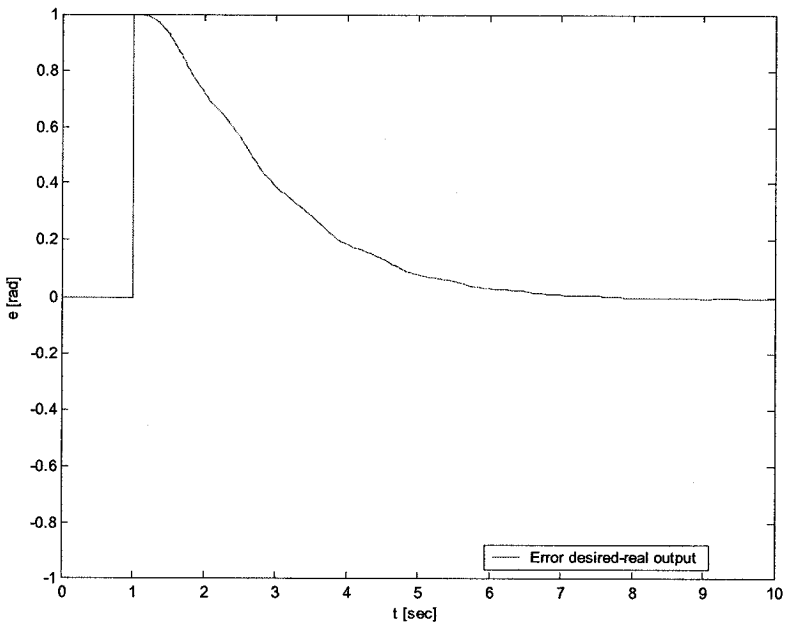

Figure 4-26 Dynamic control method applied to a two-link manipulator - error between the real and desired output

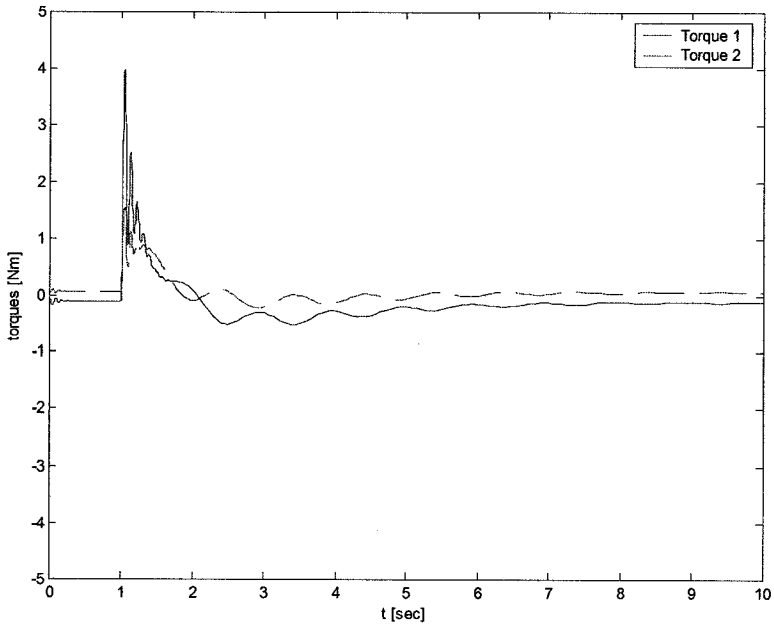

Figure 4-27 Dynamic control method applied to a two-link manipulator - torques command

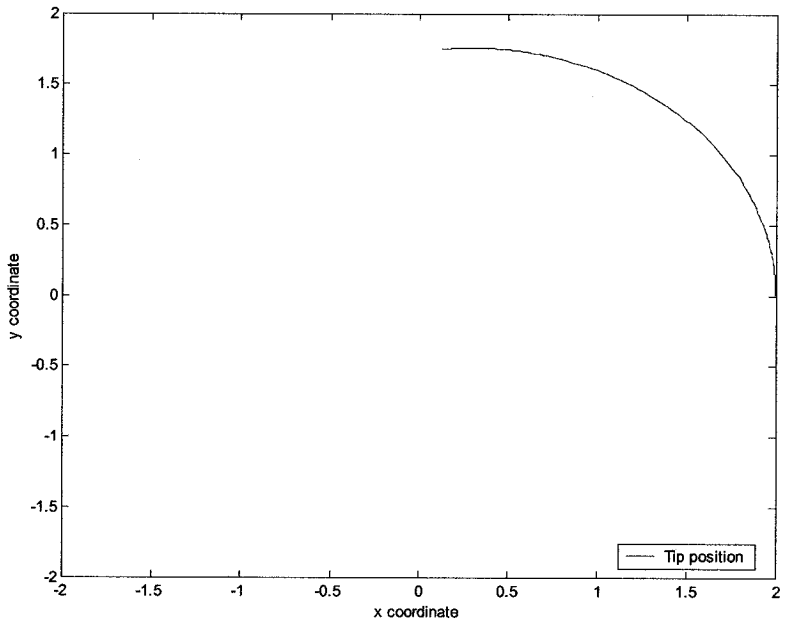

Figure 4-28 Dynamic control method applied to a two-link manipulator - tip position

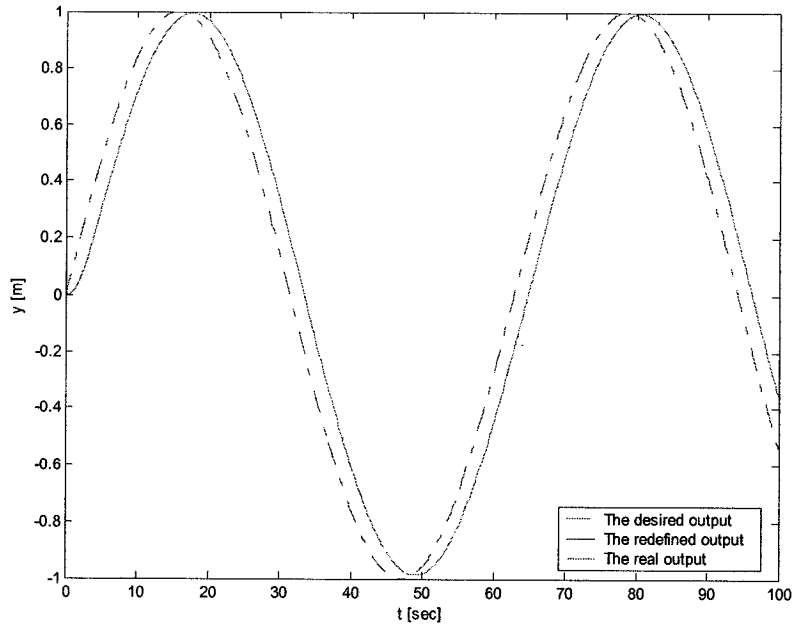

Figure 4-29 Dynamic control method applied to a two-link manipulator - tracking case - redefined output

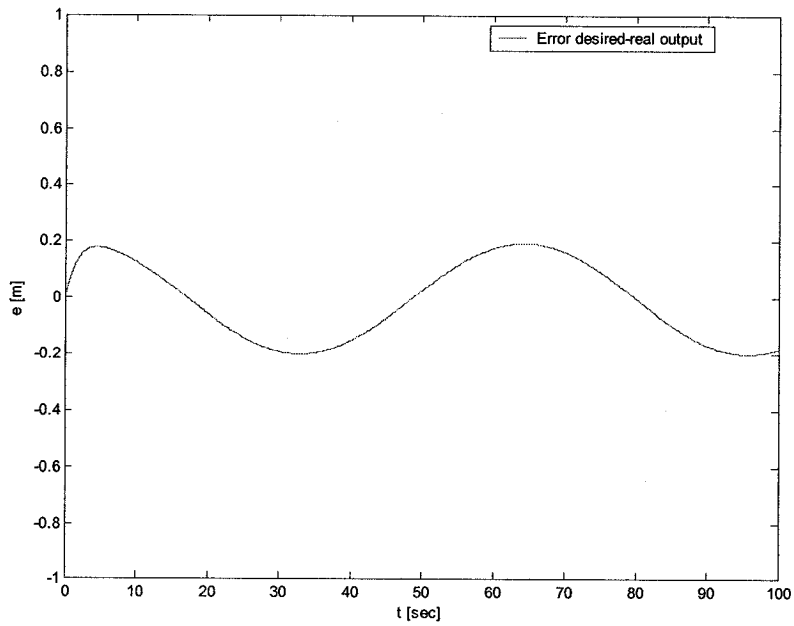

Figure 4-30 Dynamic control method applied to a two-link manipulator - tracking case - error between the real and desired output

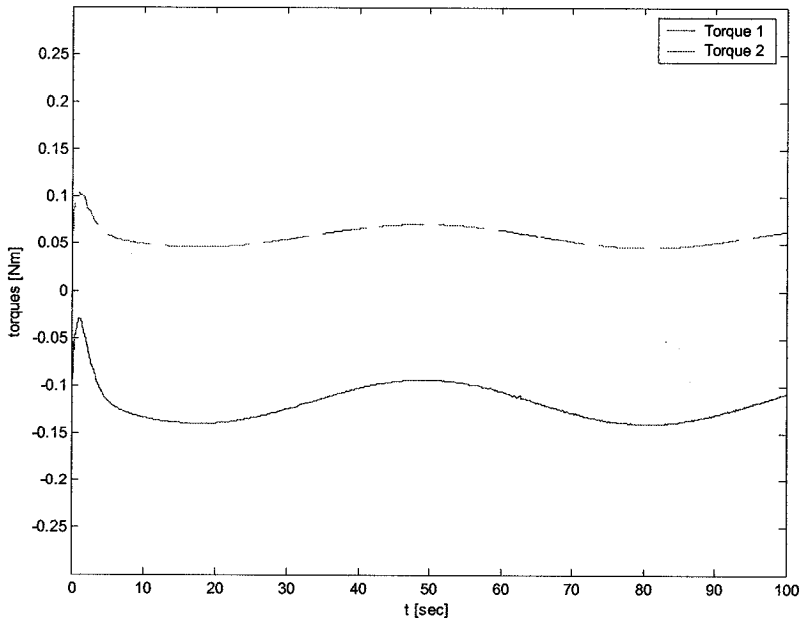

Figure 4-31 Dynamic control method applied to a two-link manipulator - tracking case - torques command

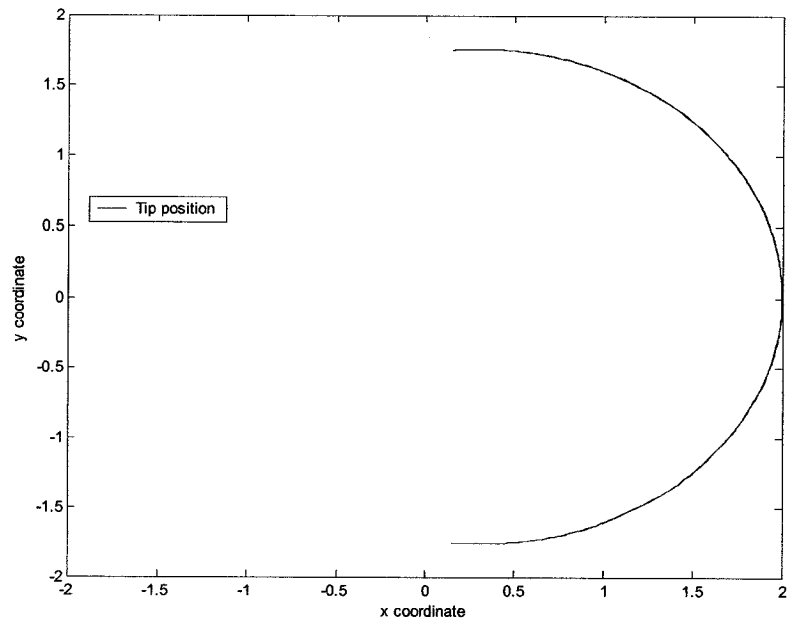

Figure 4-32 Dynamic control method applied to a two-link manipulator - tracking case - tip position

4.4 Performance comparison between rigid and flexible link manipulators control methods

In Chapter 3, the control of rigid link manipulators is discussed. In this chapter the control of a flexible-link manipulator, and a two-link manipulator having the first link rigid and the second one flexible are presented. In this section, the control of a flexible-link manipulator by using the rigid control methodology is investigated.

Let us consider the dynamic equations for a planar single link manipulator given by:

$$M\begin{bmatrix}\ddot{q}\\ \ddot{\delta}\end{bmatrix}+\begin{bmatrix} f_1(q,\dot{q})+g_1(q,\dot{q},\delta,\dot{\delta})+E_1\dot{q} \\ f_2(q,\dot{q})+g_2(q,\dot{q},\delta,\dot{\delta})+E_2\dot{\delta}+K\delta \end{bmatrix}=\begin{bmatrix}\tau\\ 0\end{bmatrix}$$

The controlled output of the system is defined as $y = q$. The dynamic control method that is designed based on the rigid model assumptions is now applied to the above flexible system.

In these simulations the following parameters are used: the masse of the link is $m = 1.356kg$ and the length of the link is $l = 1.2m$. The initial condition is set to $y = 0$, and the desired final position is set to $y = 1$.

When the controller that is based on rigid model assumptions is applied to the actual flexible system the closed-loop system is unstable. The controlled output in the rigid case is the joint angle q, whereas the controlled output in the flexible case is the redefined output $y = q + \Psi\delta$. The simulation results are shown in figures 4.33-4.36.

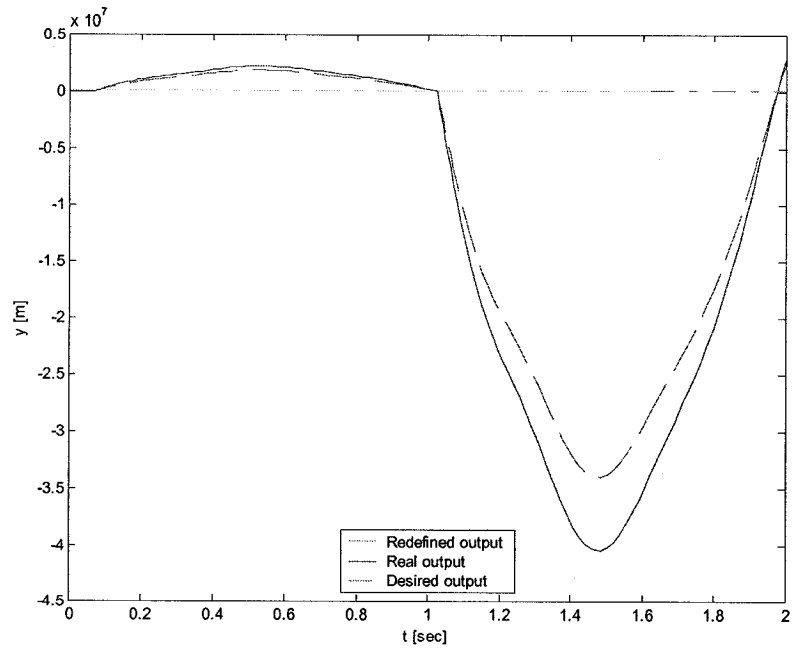

Figure 4-33 Dynamic control applied to a flexible manipulator designed based on the rigid model - redefined output

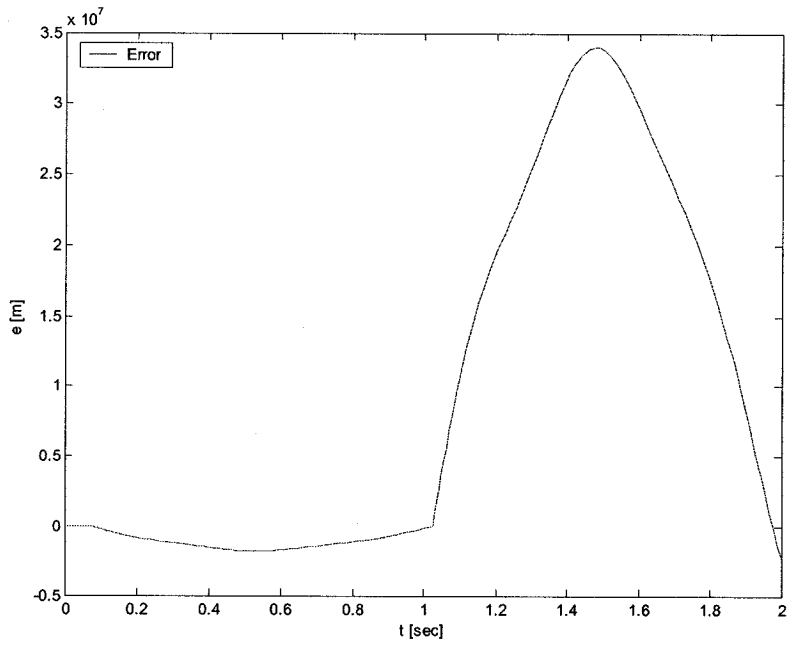

Figure 4-34 Dynamic control applied to a flexible manipulator designed based on the rigid model - redefined output error

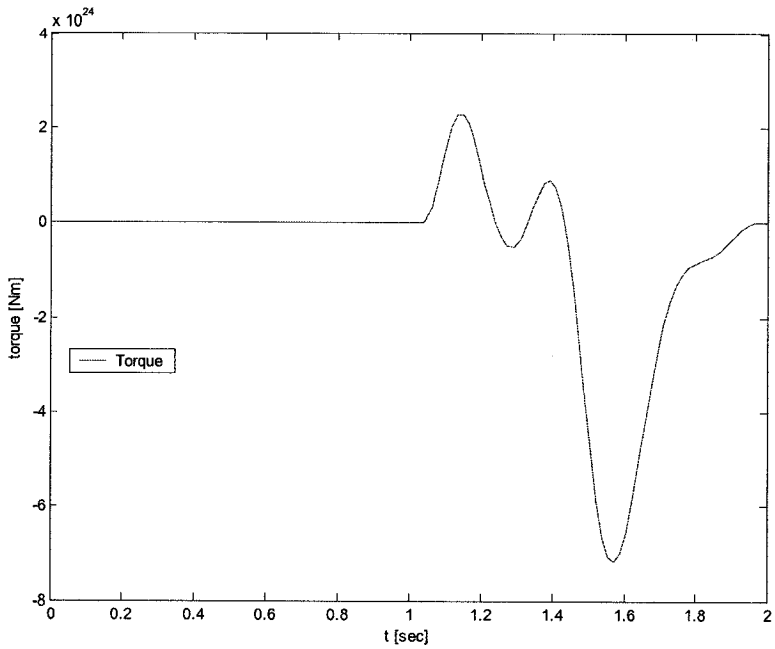

Figure 4-35 Dynamic control applied to a flexible manipulator designed based on the rigid model - torque command

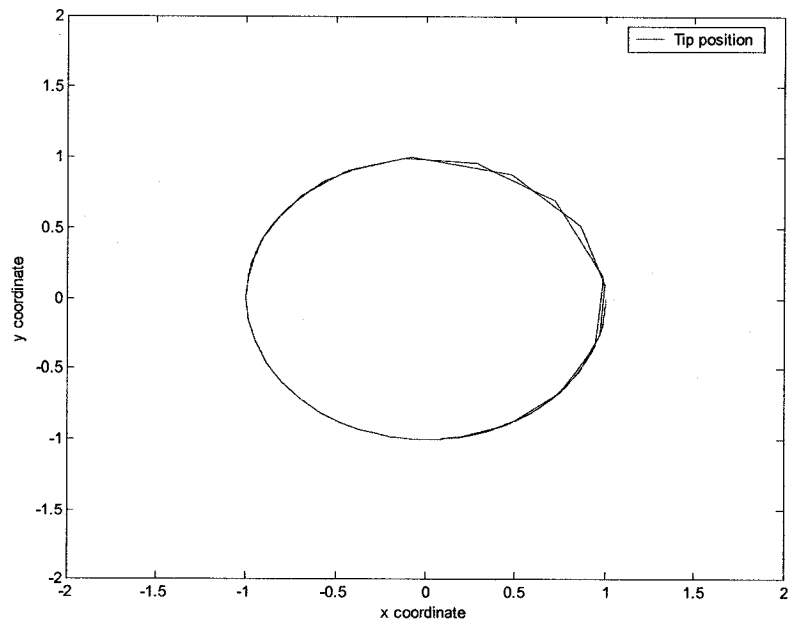

Figure 4-36 Dynamic control applied to a flexible manipulator designed based on the rigid model - tip position

4.5 Conclusions

In this chapter the control problem of flexible-link manipulators is discussed. Issues such as input-output linearization, zero dynamics, and output redefinition are introduced. Because of the non-minimum phase characteristic of the flexible manipulators, a new re-defined output is used instead of the joint angle. Based on this new output, two control methods are used for controlling a single flexible-link and a two-link manipulator for which the first link is rigid and the second one is flexible. Furthermore, it is shown that the dynamic control method designed based on the rigid model assumptions when applied to the actual flexible system results in an unstable system. This justifies and rationalizes the reasons for development of flexible-based control techniques as done in this chapter.

Chapter 5 **Conclusions and Future Work**

5.1 Conclusions

In this thesis, we develop robust dynamical controllers for solving the problem of tracking and regulation for rigid link manipulators and flexible link manipulators. The design of the dynamic controller is based on construction of a two-time scale dynamical motion of the closed-loop system. Stability conditions imposed on the fast and slow subsystems can then ensure that the full-order closed-loop system achieves the desired properties provided that the singular perturbation parameter is selected sufficiently small [37]. The output performance can then be made insensitive to disturbances.

The objective of the control is divided into two different categories: regulation and tracking. Regulation problem or the point-to-point control is concerned when the desired trajectory of the end-effector is chosen to be constant by specifying the final point. Tracking problem on the other hand is concerned with following a time-varying joint reference trajectory.

In the first part of the thesis, the modelling of the rigid and flexible-link manipulators is reviewed. Issues such as kinematics and dynamics of the manipulators are discussed. The properties of the dynamic models for rigid and flexible manipulators are presented. Based on Euler-Bernoulli beam equations of motion and using the assumed modes method and

taking into consideration a finite number of modes the dynamic equations for flexible-link manipulator are derived.

In Chapter 3, the control of rigid link manipulators is presented. Using the mathematical model of a two-rigid link manipulator [48], four different control methods are investigated: PD control, computed torque method, localization method, and a novel dynamic control method. Simulations are provided for each control method using different sets of initial conditions and their relative performance capabilities studied.

The PD control method is a simple and linear controller. In order to achieve smaller errors, larger gains have to be selected. The drawback is that system could become unstable if gains are not properly selected and/or the initial conditions deviate from the equilibrium points significantly. Another disadvantage is that the control torque could generally lead to large values. This could be an impediment when this method is implemented on a real manipulator. When there are disturbances in the system, the PD controller is generally not capable of overcoming their effects.

The manipulators are known as highly nonlinear systems. This is one reason that linear control theory is not generally suitable. One control method commonly used in robotics is the computed-torque technique. This approach works well and gives better control than a simple PD controller when an accurate dynamic model of the manipulator is available. However, in practical situations, it is very difficult for the parameters and nonlinearities associated with the robot model to be exactly determined. In addition, during the operation the dynamics of a robot may change significantly and rapidly. In this case, the trajectory tracking performance when using the computed-torque control method

significantly degrades due to the inaccuracy of the dynamic model for computing the control torques.

Taking into account the above discussion, two other control methods are investigated in this thesis.

The localization method uses state time derivatives and higher gains in order to decrease the influence of disturbances and model parameters uncertainties on dynamic properties of the output trajectories. In order to realise the control law, it is necessary to obtain the values of the derivatives of $q(t)$ and they are obtained by means of a linear differentiating filter. As was shown by simulations, it can be stated that this method performs better than the PD controller or the computed torque method. For both the regulation and tracking cases, in the presence and absence of a disturbance in the system, the localization controller is capable of achieving small errors. One drawback is that the initial input torques could have large values.

In Chapter 4, the control problem of flexible-link manipulators is presented. It is known that flexible manipulators are non-minimum phase systems. In order to achieve minimum-phase characteristic, a new re-defined output is used instead of the joint angle or the tip position. Based on this new output, two control methods are used for controlling a single flexible link and a two-link manipulator for which the first link is rigid and the second one is flexible. For both flexible-link manipulators, the proposed dynamic control approach performs better than the computed torque method as summarized in the following tables.

	Parameters Gains	er_1	er_2	t_s [sec]	$\|\tau_1\|_{max}$ [Nm]
computed torque	$k_P = 100$ $k_D = 100$	0.0038	4e-7	5	8
dynamic control	$k_1 = 100$	0.0017	0.0014	5	1.25

Table 5-1 Comparison between the computed torque and dynamic control for a single link flexible manipulator

	Parameters Gains	er_1	er_2	t_s [sec]	$\|\tau_1\|_{max}$ [Nm]
computed torque	$k_P = 400$ $k_D = 400$	0.0010	0.0006	5	2.5
dynamic control	$K_1 = \begin{bmatrix} 400 & 0 \\ 0 & 400 \end{bmatrix}$	0.0004	0.0004	5	4.9

Table 5-2 Comparison between the computed torque and dynamic control for a two link flexible manipulator

In the Tables 5.1 and 5.2 er_1 is the error between the desired position of the tip and the real position and er_2 is the error between the desired position of the tip and the redefined position. Furthermore, the dynamical control method designed based on the rigid model assumptions is also applied to the actual flexible system. In this case, the closed loop system is unstable justifying the need for development of flexible-based control methodologies.

5.2 Contributions of the thesis

In this thesis, we develop a robust dynamical controller for solving the problem of tracking and regulation for both rigid-link and flexible-link manipulators. The design of the controller is based on construction of a two-time scale dynamical motion of the closed-loop system. Stability conditions imposed on the fast and slow subsystems can

then ensure that the full-order closed-loop system achieves the desired properties. The output performance is insensitive to disturbances.

Furthermore, other control methods such as the PD control, computed torque and the localization methods are investigated for comparative purposes. The main control objective is to achieve sufficiently small tip-position tracking. It is known that flexible manipulators are systems characterized by non-minimum phase behavior. In order to achieve the minimum phase behavior, a new redefined output is proposed. Instead of using the joint angles as for the rigid link manipulator case, a new output is chosen which will provide the stability of the system.

Using a sufficiently small perturbation parameter and high-order derivatives of the output, a two time-scale separation of the fast and slow modes are induced in the closed-loop system. In order to decrease the influence of disturbances on dynamic properties of the output trajectories, a high feedback gain, and a higher-order output derivatives in the feedback loop are used.

It has been shown that if a sufficient time-scale separation between fast and slow modes in the corresponding closed loop system and stability of the fast motion subsystem are guaranteed, then the slow motion equations have the desired form and thus after rapid damping of the fast transients the output transient performance indices become insensitive to external disturbances.

By simulations it was shown that the dynamic control method yields better results than the previously presented methods. For all of the gains used the error remains in the same range. In the presence of disturbances the dynamic controller can achieve an error bound of $e = 0.0007$. The issue regarding the initial large values for the input torques has

disappeared. Using this control method, the input torque value is about $\tau = 2$ to 3 Nm. This is a clear advantage when a method is going to be physically implemented, because the torque availability and energy consumption are important issues in the implementation of any control method.

5.3 Future work

New dynamic control approaches proposed in this thesis were applied to a two-rigid link manipulator, to a single-link flexible manipulator and to a two-link manipulator for which the first link is rigid and the second link is flexible. One could naturally extend the results of this thesis to a multi-link flexible manipulator.

In the modelling of flexible-link manipulators, a finite number of modes were considered for the approximated model of the deflections. Specifically, only two modes were used. Derivation of an analytical model of the deflections using a larger number of modes could be studied. Furthermore, the elastic deformations are assumed to be small in order to have a linear relationship between the elastic deformation and the strain. In some applications, this assumption cannot be applied, so that analyzing the effects of the nonlinear relationships between the elastic deformation and strain could be examined.

In this thesis the effects of a varying payload was not addressed. A time-varying payload makes the design of the control for rigid and flexible manipulators more challenging. This issue could be investigated as part of our future work.

The modelling and control methods used in this thesis are illustrated by simulation using Matlab and Simulink. To realistically and actually demonstrate the effectiveness of these methods, experimental work should be done.

References:

[1] L. Sciavico and B. Siciliano, *Modelling and Control of Robot Manipulators*: The McGraw-Hill Companies Inc., 1996.

[2] A. Luca and B. Siciliano, "Closed-Form Dynamic Model of Planar Multilink Lightweight Robots," *IEEE Transactions on Systems, Man, and Cybernetics*, vol. 21, pp. 826-839, 1991.

[3] D. Wang and M. Vidyasagar, "Modelling a Class of Multilink Manipulators with the Last Link Flexible," *IEEE Trans. Robotics and Automatic*, vol. 8, pp. 33-41, 1992.

[4] D. S. Kwon and W. J. Book, "An Inverse Dynamics Method Yielding Flexible Manipulator State Trajectories," *Proceedings of American Control Conference*, pp. 186-193, 1990.

[5] D. Wang and M. Vidyasagar, "Transfer Functions for a Single Flexible Link," *Proceedings of the 28th IEEE Conference on Decision and Control*, 1989.

[6] G. Hastings and W. Book, "Verification of a Linear Dynamic Model for Fexible Robotic Manipulators," *Robotics and Automation. Proceedings. 1986 IEEE International Conference on*, vol. 3, pp. 1024 - 1029, 1986.

[7] Cannon Robert H. and Schmitz Jr. Eric, "Initial Experiments on the End-Point Control of a Flexible One-Link Robot," *The International Journal of Robotics Research*, vol. 3, pp. 62-75, 1984.

[8] F. Belleza, L. Lanari, and G. Ulivi, "Exact Modelling of the Slewing Flexible Link," *Proceedings 1990 IEEE Int. Conf. Robotics Automat.*, pp. 734-739, 1990.

[9] E. Barbieri and U. Ozguner, "Unconstrained and Constrained mode Expansion for a Flexible Link," *ASME J. Dynamic System, Measurement, Contr.*, vol. 110, pp. 416-421, 1988.

[10] P. Sooraska and G. Chen, "Mathematical Modelling for a Flexible Link Manipulator," *Proceedings of the 1996 IEEE International Conference on Control Applications*, pp. 960-964, 1996.

[11] R. P. Judd and D. R. Falkenburg, "Dynamics of Non-rigid Articulated Robot Linkage," *IEEE Trans. Automatic Control*, vol. AC-30, pp. 499-502, 1985.

[12] M. Benati and A. Moro, "Dynamics of Chain of Flexible Links," *ASME J. Dynamic System, Measurement, Contr.*, vol. 110, pp. 410-415, 1988.

[13] W. J. Book, "Recursive Lagrangian Formulation of Flexible Manipulator Arms," *The International Journal of Robotics Research"*, vol. 3, 1984.

[14] Y. Sakawa, F. Matsumo, and S. Fukushima, "Modelling and Feedback Control of a Flexible arm," *Journal of Robotic Systems*, vol. 2, pp. 453-472, 1985.

[15] A. Luca and B. Siciliano, "Regulation of Flexible Arms Under Gravity," *IEEE Transactions on Robotics and Automation*, vol. 9, pp. 436-467, 1993.

[16] a. B. S. A. De Luca, *Relevance of Dynamic Models in Analysis and Synthesis of Control Laws for Flexible Manipulators*. Amsterdam: S.G. Tzafestas and J.C. Gentina (Eds.), 1992.

[17] L. Lanari and J. T. Wen, "Asymptotically Stable Set Point Control Laws for Flexible Robots," *Systems and Control Lett.*, vol. 19, pp. 119-129, 1992.

[18] H. G. Lee, S. Arimoto, and F. Miyazaki, "Lyapunov Stability Analysis for PDS Control of Flexible Multi-link Manipulators," *Proceedings 27th IEEE Conf. Decision and Control*, pp. 75-80, 1988.

[19] a. B. S. Marco A. Arteaga, "On Tracking Control of Flexible Robot Arms," *IEEE TRANSACTIONS ON AUTOMATIC CONTROL*, vol. 45, pp. 520-527, 2000.

[20] M. W. Spong and M. Vidyasagar, *Robot dynamics and control*. New York: Wiley, 1989.

[21] D. Wang and M. Vidyasagar, "Feedback Linearizability of Multi-link Manipulators with One Flexible Link," *Proceedings of the 28th IEEE Conference on Decision and Control*, pp. 2072-2077, 1989.

[22] A. a. L. L. De Luca, "Achieving Minimum Phase Behavior in a One-Link Flexible Arm," *Proceedings of the Int. Symp. on Intelligent Robotics*, pp. 224-235, 1991.

[23] E. Bayo, "A Finite Element Approach to Control the End-Point Motion of a Single-Link Flexible Robot," *Journal of Robotic Systems*, pp. 63-75, 1987.

[24] M. Moallem, R. V. Patel, and K. Khorasani, "An Observer-Based Inverse Dynamics Control Strategy for Tip-Position Tracking of Flexible Multi-Link Manipulators," *Proceedings of the International Federation of Automatic Control 13th World Congress*, pp. 85-90, 1996.

[25] K. Khorasani, M. Moallem, and R. V. Patel, "An Observer-Based Inverse Dynamics Control Strategy for Tip-Position Tracking of Flexible Multi-Link Manipulators," *Proceedings of the 35th IEEE Conference on Decision and Control*, 1996.

[26] M. Moallem, R. V. Patel, and K. Khorasani, "Inverse Dynamics Sliding Control of Flexible Multi-Link manipulators," *Proceedings of the American Control conference*, vol. 4, 1997.

[27] K. L. Hillsley and S. Yurkovich, "Vibration Control of a Two-Link Flexible Robot Arm," *Proc. IEEE Int. Conference on Robotics and Automation*, vol. 3, pp. 2121-2126, 1991.

[28] A. Tzes and S. Yurkovich, "An Adaptive Input Shaping Control Scheme for Suppression in Slewing Flexible Structures," *IEEE Trans. on Contr. Systems Technology*, vol. 1, pp. 114-121, 1993.

[29] R. V. Patel and P. Misra, "Transmission Zero Assignment in Linear Multivariable Systems, Part II: The General Case," *Proceedings of American Control Conference*, pp. 644-648, 1992.

[30] H. Geniele, R. V. Patel, and K. Khorasani, "End-Point Control of a Flexible-Link Manipulator: Theory and Experiments," *IEEE Transactions on Control Systems Technology*, vol. 5, pp. 556-570, 1997.

[31] K. Khorasani and M. W. Spong, "Invariant Manifolds and Their Application to Robot Manipulators with Flexible Joints," *IEEE International Conference on Robotics and Automation*, pp. 978-983, 1985.

[32] B. Siciliano and W. J. Book, "A singular Perturbation Approach to Control of Lightweight Flexible Manipulators," *International Journal of Robotics Research*, vol. 7, pp. 79-90, 1989.

[33] D. A. Schoenwald and U. Ozguner, "On Combining Slewing and Vibration Control in Flexible Manipulator Via Singular Perturbations," *Proceedings of the 29th IEEE Conference on Decision and Control*, pp. 533-538, 1990.

[34] B. Siciliano, J. V. R. Prasad, and A. Calise, "Design of a Composite Controller for a Two-Link Flexible Manipulator," *Proceedings of the Int. Symp. on Intelligent Robotics*, pp. 126-137, 1991.

[35] F. L. Lewis and M. Vandergrift, "Flexible Robot Arm Control by a Feedback Linearization/Singular Perturbation Approach," *Proceedings of the IEEE Int. Conf. on Robotics and Automation*, pp. 729-736, 1993.

[36] Y. Aoustin, C. Chevallereau, A. Glumineau, and C.H. Moog, "Experimental Results for the End-Effector Control of a Single Flexible Robotic Arm," *IEEE Trans. on Control System Technology*, vol. 2, pp. 371-381, 1994.

[37] K. Khorasani, "Adaptive Control of Flexible-Joints Robots," *IEEE Trans. on Robotics and Automation*, pp. 250-267, 1992.

[38] M. W. Spong, K. Khorasani, and P.V. Kokotovic, "An Integral Manifold Approach to the Feedback Control of Flexible Joint Robots," *IEEE Journal of Robotics and Automation*, pp. 291-300, 1987.

[39] K. a. K. K. Hastrudi Zaad, "Control of Nonminimum Phase Singularly Perturbed Systems with Applications to Flexible-Link Manipulators," *Proceedings of the Workshop on Advances in Control and its Applications*, pp. 234-265, 1995.

[40] M. Moallem, R. V. Patel, and K. Khorasani, "Tip Position Tracking of Flexible Multi-Link Manipulators: An Integral Manifold Approach," *Proceedings of the*

IEEE International Conference on Robotics and Automation, pp. 2432-2437, 1996.

[41] B. Siciliano, W.J. Book, and G. de Marcia, "An Integral Manifold Approach to Control of a One-Link Flexible Arm," *Proceedings of the 25th IEEE Conference on Decision and Control*, 1986.

[42] S. Zhihong and K. Khorasani, "A Neural-Network-Based Controller for a Single-Link Flexible Manipulator Using the Inverse Dynamics Approach," *IEEE Transactions on Industrial Electronics*, vol. 48, pp. 1074-1086, 2001.

[43] E. Kubica and D. Wang, "A Fuzzy Control Strategy for a Flexible-Link Robot," *Proceedings of IEEE Int. Conference on Robotics and Automation*, pp. 236-241, 1993.

[44] F. L. Lewis, C. T. Abdallah, and D. M. Dawson, *Control of Robot Manipulators*. New York: Macmillan Publishing Company, 1993.

[45] M. V. Mark W. Spong, *Robot dynamics and control*. New York: Wiley, 1989.

[46] B. S. Carlos Canudas de Wit, and G. Bastin, *Theory of Robot Control*: Springer-Verlag, 1996.

[47] E. Volterra and E. C. Zachmanoglou, *Dynamics of vibrations*. Columbus, Ohio, 1965.

[48] J.-J. E. Slotine and L. Weiping, *Applied Nonlinear Control*. Englewood Cliffs, New Jersey: Prentice Hall, 1991.

[49] A. S. Vostrikov, "On the Synthesis of Control Units of Dynamic Systems," vol. 3, pp. 195-205, 1977.

[50] A. S. Vostrikov and V. D. Yurkevich, "Decoupling of Multi-Channel Non-Linear Time-Varying Systems by derivative Feedback," *Journal of Systems Science*, vol. 17, pp. 21-33, 1991.

[51] A. S. Vostrikov and V. D. Yurkevich, "Design of Control Systems by Means of Localization Method," *Preprints of 12th IFAC World Congress*, vol. 8, pp. 47-50, 1993.

[52] E. Slotine and L. Weiping, *Applied Nonlinear Control*. Englewood Cliffs, New Jersey: Prentice Hall, 1991.

[53] S. K. Madhavan and S. N. Singh, "Inverse Trajectory Control and Zero Dynamic Sensitivity of an Elastic Manipulator," *Int. Journal of Robotics and Automation*, pp. 179-191, 1991.

[54] H. A. Talebi, "Neural Network-Based Control of Flexible-Link Manipulator," vol. PhD. Montreal, Canada: Concordia University, 1997.

[55] M. Moallem, "Control and Design of Flexible-Link Manipulators," vol. PhD. Montreal,Canada: Concordia University, 1996.